DEVELOPMENT OF DETERMINATION METHOD AND FORMULATION OF POLYPLEX FOR NUCLEIC ACID DELIVERY

By

Miss Samarwadee Plianwong

A Thesis Submitted in Partial Fulfillment of the Requirements for the Degree

Doctor of Philosophy Program in Pharmaceutical chemistry and Natural products

Graduate School, Silpakorn University

Academic Year 2015

DEVELOPMENT OF DETERMINATION METHOD AND FORMULATION OF POLYPLEX FOR NUCLEIC ACID DELIVERY

By

Miss Samarwadee Plianwong

A Thesis Submitted in Partial Fulfillment of the Requirements for the Degree

Doctor of Philosophy Program in Pharmaceutical chemistry and Natural products

Graduate School, Silpakorn University

Academic Year 2015

การพัฒนาวิธีตรวจสอบและการตั้งตำรับพอลิเพล็กซ์สำหรับนำส่งกรดนิวคลีอิก

โดย

นางสาวสมาวดี เปลี่ยนวงษ์

วิทยานิพนธ์นี้เป็นส่วนหนึ่งของการศึกษาตามหลักสูตรปริญญาเภสัชศาสตรดุษฎีบัณฑิต

สาขาวิชาเภสัชเคมีและผลิตภัณฑ์ธรรมชาติ

บัณฑิตวิทยาลัย มหาวิทยาลัยศิลปากร

ปีการศึกษา 2558

The Graduate School, Silpakorn University has approved and accredited the thesis title of "Development of determination method and formulation of polyplex for nucleic acid delivery" submitted by Miss Samarwadee Plianwong as a partial fulfillment of the requirements for the degree of Doctor of Philosophy in Pharmaceutical chemistry and Natural products.

……..

(Associate Professor Panjai Tantatsanawong, Ph.D.)

Dean of Graduate School

...../...../.....

The Thesis Advisors

1. Associate Professor Theerasak Rojanarata, Ph.D.
2. Associate Professor Praneet Opanasopit, Ph.D.

The Thesis Examination Committee

…….. Chairman

(Associate Professor Tanasait Ngawhirunpat, Ph.D.)

...../...../.....

..... Member

(Assistant Professor Warisada Sila-on, Ph.D.)

...../...../.....

..... Member

(Associate Professor Theerasak Rojanarata, Ph.D.)

...../...../.....

..... Member

(Associate Professor Praneet Opanasopit, Ph.D.)

...../...../.....

54356801 : MAJOR : PHARMACEUTICAL CHEMISTRY AND NATURAL PRODUCTS
KEY WORDS : GENE DELIVERY SYSTEM / SIRNA DELIVERY / CATIONIC POLYMER / ADSORPTION DYE / DICHLOROFLUORESCEIN / CHITOSAN / POLY L ARGININE

SAMARWADEE PLIANWONG: DEVELOPMENT OF DETERMINATION METHOD AND FORMULATION OF POLYPLEX FOR NUCLEIC ACID DELIVERY. THESIS ADVISORS: ASSOC. PROF. THEERASAK ROJANARATA, Ph.D. AND ASSOC. PROF. PRANEET OPANASOPIT, Ph.D. 149 pp.

In this study, a new method for estimation of polyplex formation and carrier system for siRNA delivery was developed. The dye adsorption method was developed for the estimation of cationic polymer i.e. polyethylenimine (PEI) and chitosan (CS) to nucleic acid ratio at which the polyplex was completely formed. The assay relied on the attraction of dichlorofluoresceinate dye to adsorb on self-assembling particles as induced by the positive surface charge of the polyplex as cationic polymer associated equivalently with nucleic acid. This phenomenon resulted in the appearance of pink colored pellets of the polyplex after centrifugation. By the other means, sodium hydroxide solution was added to free the adsorbed dye into the solution, producing green fluorescence solution under UV light (366 nm). This method was well applied to the polyplex formulations of polymers and plasmid DNA or siRNA and gave the results in agreement with those from gel retardation method and zeta potential analysis. The proposed method was a fast, facile, cost-effective and safely, suited for the investigation of the optimal polymer to nucleic acid ratio for gene delivery. The new cationic polymer system was also developed for delivering siRNA. For the development of carrier system for siRNA delivery, CS combined with PLA was formulated and evaluated its performance regarding the delivery of siRNA to HeLa cells expressing enhanced green fluorescent protein (EGFP). The combination of CS and PLA could reduce the amounts of the polymers required for the complete complexation with siRNA, as compared with the single polymer using. Thereby forming positively charged, nanosized CS/PLA/siRNA polyplex was formed at the weight ratio of 5/0.5/1. The gene silencing efficiency of CS/PLA/siRNA at the optimal weight ratio of 5/0.5/1 satisfactorily silenced the endogenous EGFP gene at pH 7.4 as well as at pH 6.4 without deterrent effect from serum. In contrast, the transfection efficiency of CS/siRNA and PLA/siRNA was very low at physiological pH (7.4). The combined polymers could protect siRNA from RNase degradation over a period of at least 6 hr. Furthermore, MTT assay demonstrated that CS/PLA/siRNA complexes showed acceptably low cytotoxicity with 75 % cell viability. The uptake mechanism study showed CS/PLA/siRNA internalized into cell via clathrin-mediated endocytosis, caveolae-mediated endocytosis and enhanced transfection efficiency by facilitating acidification of endosome-lysosome system. Therefore, CS combined with PLA is easy-to-prepare, safe and promising for use as an efficient siRNA delivery vehicle.

Program of Pharmaceutical chemistry and Natural product Graduate School, Silpakorn University
Student's signature ..... Academic Year 2015
Thesis Advisors' signature 1.....2.....

54356801 : สาขาวิชาเภสัชเคมีและผลิตภัณฑ์ธรรมชาติ

คำสำคัญ : ระบบนำส่งยีน / การนำส่งเอสไออาร์เอนเอ / พอลิเมอร์ประจุบวก / สีชนิดดูดซับ / ไดคลอโรฟลูออเรสซีน / ไคโตซาน / พอลิแอลอาร์จินีน

สมาวดี เปลี่ยนวงษ์ : การพัฒนาวิธีตรวจสอบและการตั้งตำรับพอลิเพล็กซ์สำหรับนำส่งกรดนิวคลีอิก อาจารย์ที่ปรึกษาวิทยานิพนธ์ : ภก. รศ. ดร. ธีรศักดิ์ โรจนราธา, ภญ.รศ.ดร.ปราณีต โอปณะโสภิต. 149 หน้า

การศึกษานี้เป็นการพัฒนาวิธีวิเคราะห์ชนิดใหม่สำหรับการประมาณค่าการเกิดพอลิเพล็กซ์ที่สมบูรณ์ และการพัฒนาระบบนำส่งเอสไออาร์เอ็นเอ โดยวิธีการใช้สีชนิดดูดซับนั้นพัฒนาขึ้นเพื่อประมาณค่าอัตราส่วนการเกิดพอลิเพล็กซ์ที่สมบูรณ์ระหว่างพอลิเมอร์ประจุบวก เช่น พอลิเอทิลีนอิมีน และ ไคโตซาน กับกรดนิวคลีอิก วิธีการวิเคราะห์นี้อาศัยหลักการของการที่สีไดคลอโรฟลูออเรสซีนถูกดูดซับบนผิวอนุภาคที่มีประจุบวกของพอลิเพล็กซ์ที่เกิดขึ้นได้เองจากการรวมตัวกันของพอลิเมอร์ประจุบวกและกรดนิวคลีอิก ณ จุดที่ปริมาณของพอลิเมอร์ประจุบวกสมมูลกับกรดนิวคลีอิก ปรากฏการณ์นี้ทำให้สามารถเห็นพอลิเพล็กซ์เป็นสีชมพูหลังจากผ่านการปั่นเหวี่ยง ในอีกวิธีการหนึ่งนั้น การเติมสารละลายโซเดียมไฮดรอกไซด์จะทำให้สีที่ถูกดูดซับอยู่ถูกปลดปล่อยออกมาจากผิวของพอลิเพล็กซ์และทำให้เกิดเป็นสารละลายที่สามารถเรืองแสงสีเขียวได้เมื่อสังเกตภายใต้แสงยูวี (ความยาวคลื่น 366 นาโนเมตร) วิธีที่พัฒนาขึ้นนี้สามารถนำไปใช้ได้กับตำรับของดีเอ็นเอและเอสไออาร์เอ็นเอ โดยวิธีที่พัฒนาขึ้นนี้ให้ผลไปในทางเดียวกันกับผลที่ได้จากการวิเคราะห์ด้วยเจลและการวิเคราะห์ประจุบนพื้นผิว วิธีที่พัฒนาขึ้นนี้เป็นวิธีที่รวดเร็ว ง่าย มีความคุ้มทุน และปลอดภัยต่อผู้ปฏิบัติงาน โดยมีความเหมาะสมในการใช้สำหรับตรวจสอบอัตราส่วนที่เหมาะสมของพอลิเมอร์ประจุบวกและกรดนิวคลีอิกสำหรับการนำส่งยีน สำหรับการพัฒนาระบบตัวพาในการนำส่งเอสไออาร์เอ็นเอนั้น ศึกษาโดยการใช้ไคโตซานร่วมกับพอลิแอลอาร์จินีนในการนำส่งเอสไอาร์เอ็นเอเข้าสู่เซลล์ HeLa ที่มีการแสดงออกของโปรตีนเรืองแสง เมื่อเปรียบเทียบกับการใช้พอลิเมอร์แต่ละชนิดเพียงชนิดเดียว พบว่าการใช้ไคโตซานร่วมกับพอลิแอลอาร์จินีนสามารถลดปริมาณของพอลิเมอร์แต่ละชนิดในการรวมตัวกับเอสไอาร์เอ็นเอได้ โดยเกิดเป็นอนุภาคขนาดนาโนที่มีประจุบนพื้นผิวเป็นบวกที่อัตราส่วนไคโตซานต่อพอลิแอลอาร์จินีนต่อเอสไอาร์เอ็นเอเท่ากับ 5/0.5/1 โดยน้ำหนัก ที่อัตราส่วน 5/0.5/1 นี้ สามารถยับยั้งการแสดงออกของยีนโปรตีนเรืองแสงในเซลล์ได้ที่พีเอช 7.4 และ 6.4 โดยซีรัมไม่มีผลต่อประสิทธิภาพในการนำส่ง ในทางตรงกันข้าม ประสิทธิภาพในการนำส่งเอสไอาร์เอ็นเอของไคโตซาน หรือพอลิแอลอาร์จินีนนั้นมีค่าต่ำที่พีเอชของสภาวะในร่างกาย (7.4) การใช้พอลิเมอร์ร่วมกันนี้ยังสามารถปกป้องเอสไอาร์เอ็นเอจากการถูกทำลายด้วยเอนไซม์อาร์เอ็นเอสเป็นเวลาอย่างน้อย 6 ชั่วโมง นอกจากนี้ จากการศึกษาความเป็นพิษต่อเซลล์ พบว่าตำรับของไคโตซาน/พอลิแอลอาร์จินีน/เอสไอาร์เอ็นเอนั้นมีความเป็นพิษต่อเซลล์ต่ำ โดยมีค่าการรอดของเซลล์เท่ากับร้อยละ 75 การศึกษากลไกการผ่านเข้าเซลล์ของตำรับไคโตซาน/พอลิแอลอาร์จินีน/เอสไอาร์เอ็นเอ พบว่า ตำรับนี้เข้าสู่เซลล์โดยใช้แคลทริน, คาวีโอเล และสามารถเพิ่มประสิทธิภาพในการนำส่งเอสไอาร์เอ็นเอได้โดยการเพิ่มความเป็นกรดให้แก่ระบบเอนโดโซม-ไลโซโซมอีกด้วย ดังนั้น ตำรับที่พัฒนาขึ้นโดยใช้ไคโตซานร่วมกับพอลิแอลอาร์จินีนนับเป็นระบบที่ง่ายต่อการเตรียม มีความปลอดภัยสำหรับการนำส่งเอสไอาร์เอ็นเอได้อย่างมีประสิทธิภาพ

สาขาวิชาเภสัชเคมีและผลิตภัณฑ์ธรรมชาติ บัณฑิตวิทยาลัย มหาวิทยาลัยศิลปากร

ลายมือชื่อนักศึกษา..... ปีการศึกษา 2558

ลายมือชื่ออาจารย์ที่ปรึกษาวิทยานิพนธ์ 1..... 2.....

ACKNOWLEDGEMENTS

This Thesis would not be success without support and guidance from many people. First of all, I would like to express my sincere appreciation to my advisor, Assoc. Prof. Dr. Theerasak Rojanarata for his invaluable guidance, excellent experience and support throughout my study. I also would like to express my gratitude to my co-advisors, Assoc. Prof. Dr. Praneet Opanasopit for valuable advice and support, as well as my co-advisor at University of Alberta, Canada, Prof. Dr. Hasan Uludag who gave me the excellent opportunity to improve my research experience and always support and gave the valuable suggestion. I also would like to thank my thesis committees, Assoc. Prof. Dr. Tanasait Ngawhirunpat and Asst. Prof. Dr. Warisada Sila-on for giving me insightful comments and suggestions.

I am grateful to thank the Commission of Higher Education (Thailand), the Thailand Research Funds through the Royal Golden Jubilee PhD Program (Grant No.PHD/0069/2553) for financial support during my study as well as Faculty of Pharmacy, Silpakorn University for facility support and partial financial support.

My special thanks goes to my friends and members of the Pharmaceutical Development of Green Innovation Group (PDGIG), especially Miss Areerut Sripattanaporn, Miss Orapan Paecharoenchai and Miss Jintana Tragulpakseerojn for valuable laboratory technique. I would like to thank Mr. Phuwadat Pasarj and my friends in Edmonton who always support and beside me while I was staying in Canada. I also would like to thank my graduated friends, especially Miss Kotchamon Yodkhum, Miss Sunanta Srisopon and Miss Siripran Tidjarad who support and encourage me during my study.

Finally, my deepest gratitude goes to my lovely parents and my family who always take care, support, encourage and staying beside me all the time.

TABLE OF CONTENTS

LIST OF TABLES

LIST OF FIGURES

Figure Page

Figure Page

Figure Page

Figure Page

LIST OF ABBREVIATIONS

%	percentage
λ	wavelength
˚C	degree Celsius
<	less than
>	more than
®	registered trademark
µL	microliter (s)
µm	micrometer(s)
µM	micromolar
Abs	Absorbance
cm	centimeter (s)
cm^2	square centimeter
CO_2	carbon dioxide
CS	chitosan
DCF	2′,7′-Dichlorofluorescein
DNA	deoxyribonucleic acid
Eq.	equation
et al.	and others
etc.	et cetera (Latin); for example, such as
FI	Fluorescence intensity
g	gram (s)
hr	hour (s)
i.e.	id est (Latin); that is
k	kilo (s)
kDa	kilodalton (s)
L	liter (s)
M	molar (s)
MEM	modified Eagle’s medium
mg	milligram (s)
min	minute (s)
mL	milliliter (s)

mM	millimolar (s)
mRNA	messenger ribonucleic acid
MTT	3-(4,5-dimethylthiazol-2-yl)-2,5diphenyltetrazolium bromide
MW	molecular weight
nm	nanometer (s)
nM	nanomolar (s)
pDNA	DNA plasmid
pEGFP	Enhanced Green Fluorescent Protein plasmid
pH	potentia hydrogenii (latin); power of hydrogen
pKa	the negative logarithm of the ionization constant of an acid
PLA	poly L arginine
pM	picomolar (s)
pmol	picomole (s)
RNA	ribonucleic acid
RNAi	ribonucleic acid interference
rpm	revolutions per minute or rounds per min
SD	standard deviation
siRNA	short interfering ribonucleic acid
UV	ultraviolet (spectroscopy)
v/v	volume by volume
w/v	weight by volume
w/w	weight by weight
β	beta

CHAPTER 1

INTRODUCTION

1.1 Rational and problem statement

Gene therapy is currently a promising approach to the treatment of inherited and acquired diseases caused by genetic deficiencies and abnormalities, such as cancer, acquired immune deficiency syndrome (AIDS), cardiovascular diseases, certain autoimmune disorders and infectious diseases. It is carried out by transferring genetic materials to target cells in order to compensate for defective genes or produce therapeutic proteins [1, 2].

However, it is difficult for delivering the naked nucleic acids directly through plasma membrane due to their size and their physicochemical properties. Therefore the various gene delivery systems have been developed. Although viral system has high transfection efficiency, several limitations are associated with viral vectors, including carcinogenesis, immunogenicity, limited DNA packaging capacity and difficulty of vector production [3]. Non-viral gene therapy has been developed in order to improve these limitations. Over the years, a significant number of cationic polymers have been explored as carriers for in vitro and in vivo gene delivery. It has positively charged on the structure such as amine group, which able to mask the negative charge of nucleic acid (pDNA and siRNA) via electrostatic interaction and condense to small structure [4]. In addition, cationic polymer able to protect DNA or siRNA from nuclease degradation and facilitating the endocytosis and endolysosomal escape [5, 6].

In the study of gene delivery, the properties of complexes such as size and charge are characterized before in vitro study. It has been revealed that the optimal cationic polymer to nucleic acid ratio has a significant correlation to the complete formation and suitable properties of complexes which are resulting in transfection efficiency [5, 7] since too low amounts of polymers cannot efficiently compact nucleic acid and neutralize the negative charge whereas a significant excess of

polymer turns out to be cytotoxic [8]. Accordingly, the investigation of polymer to nucleic acid ratio in terms of weight ratio or molar ratio of polymer nitrogen atoms to nucleic acid phosphate (N/P ratio) that brings about the complete complex formation is usually a prerequisite step prior to *in vitro* and *in vivo* transfection experiments. For this purpose, a range of techniques have been used to monitor the self-assembly process e.g. light scattering, the inhibition of ethidium bromide fluorescence, zeta potential measurement [9] and the most commonly used gel retardation assay which is based on the loss of electrophoretic mobility of nucleic acid when it binds a critical amount of cationic polymers [10, 11]. Nevertheless, some methods need costly specialized instruments such as zeta sizer. Furthermore, a potent carcinogenic ethidium bromide [12, 13] is commonly employed in gel retardation. Despite the current availability of less mutagenic alternatives for nucleic acid stains, most of them are significantly expensive.

In the analytical chemistry, dichlorofluorescein (DCF) has been used as an adsorption indicator in Fajan's precipitate-forming titration of chloride using silver nitrate as a titrant [14, 15]. In water, weakly acidic DCF dissociates to green dichlorofluoresceinate anions. Once the titration reaches the equivalence point and the excess of silver ion titrant adsorbs on silver chloride surface imparting a positive charge, anionic DCF ions are attracted to the particles as the counter ions, and undergo the color change to pink upon adsorption, representing the endpoint. In analogue to this phenomenon, nucleic acid which is anionic like chloride ion is titrated with various amounts of cationic polymer. When a critical amount of polymer is added to completely form the complex particles with nucleic acids and totally masks the negative charge, the surface charge of the complexes becomes positive and DFC anions are attracted to adsorb on the particles as counterions. [16-18].

Based on the aforementioned rationale, the first part of thesis is the development of a new determination technique by using DCF for the estimation of polymer to nucleic acid ratio at which the complete polyplexes was formed. In this study, polyethyleneimine (PEI) which is one of the most effective and widely accepted cationic polymer for gene delivery is used as the represented synthetic polymer and chitosan (CS) is chosen as the natural polymer. The effect parameters

include the size and amount of plasmid DNA, the molecular weight of PEI and the minimum concentration of DCF required for the assay are studied. In addition, the applicability of the method to the formulation of PEI/siRNA polyplex is investigated and demonstrated.

The second proposed of thesis is to improve the siRNA transfection efficiency using chitosan combined with poly-L-arginine (PLA). Since RNA interference (RNAi) represents a promising new approach towards the inhibition of gene expression of specific genes in targeted cell as the potential means for the treatment of diseases. However, the delivery of naked siRNA to the desired targets is usually limited by rapid degradation by nucleases and poor cellular uptake, leading to the low transfection efficiency [19, 20]. Currently, cationic polymers such as PEI and poly(amidoamine) (PAMAM) have been reported for siRNA delivery [21-23]. Although these polymers bind efficiently to nucleic acid, their highly positive charge may interact with negatively charged serum proteins and tissue components *in vivo*, therefore hindering the effective transfection. Moreover, the excessive positive charge may be toxic to cells.

Chitosan (CS) is a biodegradable and biocompatible natural polymers consisting of repeating units of D-glucosamine and N-acetyl-D-glucosamine. It is a weak base and is soluble only in acidic solution where the pH is lower than pKa (≈ 6.5). Once the amino groups are protonated, CS binds and condenses negatively charged siRNA into smaller particles, enabling this polymer for use as gene delivery vehicle [24]. To date chitosan and its derivatives have been used to formulate with siRNA where it has been shown that the optimal complex formation greatly depended on the weight ratio of CS/siRNA. Nevertheless, low complex stability and transfection efficiency are usually obtained at physiological pH when native chitosan was employed [25-27]. Besides natural polymers, synthetic cationic polypeptides such as poly-L-lysine (PLL) [28-30] as well as PLA have also been used as gene carriers. Since PLA alone is known to be cytotoxic via its highly positive charge. In addition, PLA damage the mitochondria which lead to disturbance of cell metabolism and cell death [31]. Therefore, attempts were made to resolve this drawback e.g. by mixing

PLA with hyaluronic acid [32] or chemically conjugating it with CS [33] prior to use for siRNA delivery. The physical mixture of PLA and CS was previously reported to have the higher transfection efficiency and lower cytotoxicity than the polypeptide itself for use to deliver plasmid DNA (pDNA) [34]. Despite siRNA and pDNA share some common properties i.e. they are both double-stranded nucleic acids with anionic backbones to interact with cationic agents, but these two molecules possess distinct characteristics. By these reasons, the delivery strategies should be developed to suit each case individually. However, until now there have not been any reports about the use of easy-to-prepare CS combined with PLA formulations for siRNA delivery.

Therefore, in this experiment, the mixtures consisting of different ratios of these two polymers were therefore formulated and evaluated for their performance to form the complexes with siRNA. In addition to the characterization of the size and surface charge, the resulting complexes were tested for *in vitro* transfection efficiency with HeLa cells expressing stable and constitutive enhanced green fluorescent protein (EGFP) at the different pH and in the presence of serum. Furthermore, their RNase protection ability and cytotoxicity were investigated.

Since the investigation of cellular uptake pathway of complex is important to be taken into account when optimizing transfection efficiency of gene delivery systems. The majority of reports on cellular uptake mechanisms suggest that endocytosis is the preferred route of cell entry of non-viral gene carriers [35]. For determining the cellular uptake mechanism, selective inhibition of the different endocytic pathways has been shown to be a powerful approach for investigating the cellular uptake of gene carriers. For example, treatments that specifically inhibit clathrin mediated endocytosis (CME) is chlorpromazine. Inhibitors such as filipin, nystatin, and methyl-β-cyclodextrin perturb internalization through the caveolae. Genistein, a tyrosine kinase inhibitor, causes local disruption of the actin network at the endocytic site and inhibits the recruitment of dynamin II that are known to be essential for caveolae-mediated uptake. Nocodazole causes the depolymerization of microtubules. Wortmannin is a phosphatidyl inositol-3-phosphate inhibitor, which can inhibit micropinocytosis [36]. Based on selective inhibition of endocytosis pathway,

there are many researches which report the cellular uptake pathway of cationic polymer. However, the detailed uptake pathway of CS/PLA/siRNA complexes remains to be not investigated. Therefore, the cellular uptake mechanisms are also investigated by using selective inhibitors of endocytic pathway in HeLa cells stably expressing EGFP.

1.2 Objectives

1.2.1 To develop and optimize a method for determining the complete complex formation using adsorption dye.

1.2.2 To investigate the efficiency of chitosan (CS) combined with poly-L-arginine (PLA) for siRNA delivery in HeLa stably expressing green fluorescence protein.

1.2.3 To investigate the cellular uptake pathways of CS/PLA/siRNA polyplex.

1.3 Hypothesis

1.3.1 The optimal ratio of cationic polymer to nucleic acid for the complex formation can be determined by using adsorption dye.

1.3.2 A chitosan combined with poly-L-arginine is effective for delivery of siRNA into the cells with low cytotoxicity.

1.3.3 CS/PLA/siRNA complex is taken up into cells by certain pathways.

CHAPTER 2

LITERATURE REVIEWS

2.1 Gene therapy

2.2 Gene delivery systems

2.2.1 Viral vectors

2.2.2 Non-viral vectors

2.2.2.1 Physical methods

2.2.2.2 Chemical methods

2.3 Biological barrier to gene delivery

2.4 Cellular uptake pathway for non-viral gene delivery system

2.5 Tools to Study cellular uptake in Nonviral Gene Delivery

2.6 RNAi therapeutics

2.6.1 Mechanism of RNA interference

2.6.2 Challenge of siRNA therapeutic

2.6.3 Therapeutic application of RNAi

2.7 General methods for determining the carriers/nucleic acid complexes formation

2.7.1 Gel retardation

2.7.2 Zeta potential analysis

2.7.3 Dye exclusion assay

2.8 Dichlorofluorescein as an adsorption indicator and its application

2.1 Gene therapy

Gene therapy has been pronounced for over half century since we know that the mutation of genetic materials can cause the diseases. The European Medicines Agency (EMA) defines a gene therapy medicinal product as a biological medicinal product which accomplishes the following two characteristics: (1) an active substance which contains or consists of a recombinant nucleic acid used in or administered to human in order to regulating, repairing, replacing, adding or deleting a genetic sequence; (2) its therapeutic, prophylactic or diagnostic effect relates directly to the recombinant nucleic acid sequence it contains, or to the product of genetic expression of this sequence. In addition, the US Food and Drug Administration (FDA) also defines that a gene therapy is the products that mediate their effects by transcription and/or translation of transferred genetic material and/or by integrating into the host genome and that are administered as nucleic acids, viruses, or genetically engineered microorganisms. The products may be used to modify cells *in vivo* or transferred to cells *ex vivo* prior to administration to the recipient [37]. Gene therapy was generally categorized in four strategies: (1) gene replacement therapy for monogenic diseases, (2) gene addition for complex disorders and infectious diseases, (3) gene expression alteration targeting RNA, and (4) gene editing to introduce targeted changes in host genome [38].

Up to date, gene therapy was used for treatment of several diseases. For example, cystic fibrosis, peripheral vascular disease, arthritis, neurodegenerative disorders, acquired immunodeficiency syndrome (AIDS), combined immunodeficiency syndromes, muscular dystrophy, hemophilia, infectious diseases and cancers result from the presence of defective genes [39, 40]. The examples of diseases that treated by gene therapy are summarized in Table 2.1.

Table 2.1 Applications of gene therapy

Disorders/diseases
Cancer
Vaccines/immunotherapy, e.g. HLA-B7
Tumor suppressor genes
BRCA1 in ovarian cancer
Retrovial *p53* in pulmonary carcinoma
Ad-*p53* in head and neck cancer, non-small-cell lung cancer and hematologic malignanies
Liposome-*p53* in hepatocellular carcinoma
Suicide genes
Leptomeningeal carcinomatosis (*tk* gene)
Adenocarcinoma (prostate-*tk* gene)
Glioblastoma
GvDH control in allogenid bone marrow transplantation
Cytokines
IL-2 in solid tumors
IL-12, melanoma vaccination
IL-7, melanoma vaccination
Cytokine transfected xenogeneic cells
Monogenic diseases
X-linked severe combined immunodeficiency
Mucopolysaccharidosis
Familial hypercholesterolemia
Cystic fibrosis, e.g. CFTR cDNA
Hemophilia B
Chronic granulomatosis disease
Infectious diseases
AIDS-DNA-based vaccine
HIV-1 specific cytotoxic
Other diseases
Coronary heart disease
Angiogenesis trials using Ad-VEGF
Amyotrophic lateral sclerosis (ALS)
Neurotrophic factor in ALS
Rheumatoid arthritis

Source: Mhashilkar, A., et al. (2001). "Gene therapy: Therapeutic approaches and implications." **Biotechnology Advances** 19, 4: 279-297.

In addition, gene therapy is taking place in clinical trials worldwide. Among of these diseases, cancer is the most common indication which composes over 60% of all

clinical trials worldwide, following by monogenic diseases and cardiovascular diseases (Figure 2.1).

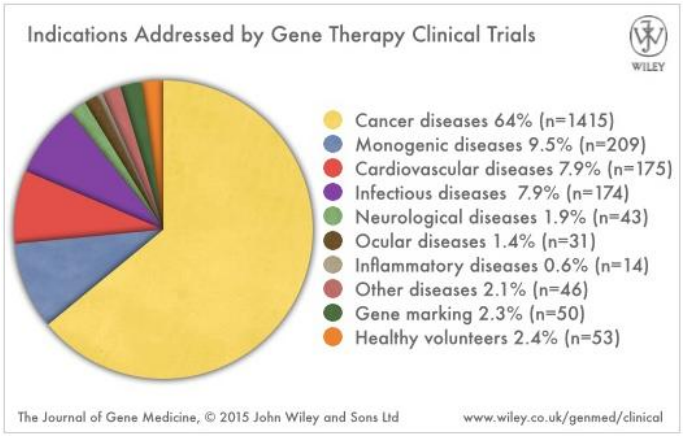

Figure 2.1 Graphical presentation of indications that have been addressed by gene therapy in clinical trials from 1989 to 2015. Source: The Journal of Gene Medicine, Wiley and Sons (http://www.abedia.com/wiley/index.html).

2.1.1 Classification of gene therapy

Gene therapy is classified into two major categories, germ line gene therapy and somatic gene therapy. Although germ line gene therapy may have a great potential, to date it cannot be used in human because it is currently ethically prohibited [41, 42].

2.1.1.1 Germ line gene therapy

This type of gene therapy is the insertion of functional gene into the reproductive cells as sperm and zygote. This gene will be integrated into the individual genomes, causing a heritable modification in the patient's genetic characteristics [43].

2.1.1.2 Somatic gene therapy

Somatic gene therapy involves the insertion of genes into non-reproductive cells which means that the effect appears in only one generation and is not passed on to next generations. However, somatic cell therapy show short-effected and transporting the gene to the target cells or tissue is also

challenging. Regardless of these problems, somatic cell gene therapy is appropriate and acceptable for many inherited and acquired disorders [43].

2.1.2 Strategies for gene therapy

There are 2 possible strategies for gene administration; *ex vivo* and *in vivo.*

2.1.2.1 *Ex vivo* gene therapy

In this approach cells are harvested and cultivated from patients after surgical biopsy or organ resection. The cells are then manipulated and transfected therapeutic genes *in vitro*. Finally, the transfected cells are reintroduced back into the target tissues. The *ex vivo* strategies is that many of the biological barriers can be avoided. The several diseases were investigated by *ex vivo* protocol e.g. Severe combined immunodeficiency diseases (SCID XI and SCID/ADA deficiency), X-linked disorder, hemoglobinopathies, cervical dysplasia and malignant tumors [44, 45]. The advantage of this method is the lack of immune response. However, *ex vivo* gene therapy has limitation when the target organ is internal such as the lung, heart or brain [46].

2.1.2.2 *In vivo* gene therapy

In vivo gene therapy involved the direct administration of the transgene into the target organ or patient as well as the transfer of genetic material through an appropriate vector which can be a viral or non-viral vector into the target tissue [44, 47]. The limitation of in vivo are usually the permanent integration of the recombinant gene may not occur and only transient expression of the gene product takes place until the sequences undergo degradation or elimination from the cell. In addition, another problem is insufficient targeting of vectors to the correct tissue sites thus the improvement in targeting and vector development is required [47].

2.2 Gene delivery system

The success of gene therapy essentially depends on ensuring that the therapeutic gene reaches the targeted cell without any biodegradation [48]. Naked therapeutic genetic molecules are generally difficult to deliver primarily due to rapid clearance, nucleases which limit serum half-life of unmodified small interfering RNA

to 5–60 minutes [49] and DNA to 10 minutes [50]. In addition, the hydrophilic anionic nature of the DNA macromolecule and its size inhibit it from penetrating passively through the cell [51]. Thus the development of gene vectors is importance in order to achieve high transfection efficiency. The biological barriers include cellular internalization, endosomal and lysosomal escape, resistant from enzymatic degradation, nuclear transport, and release of plasmid DNA for the smooth transcription [52].

The ideal gene carriers or vectors should have several criteria [48, 53] including:

It must not trigger a strong immune response.

It must be capable of transporting nucleic acids in wide range of size.

It must lead to the sustained and regular expression of gene.

The vector must deliver the gene to only certain types of cells.

It must be easy to prepare and be inexpensive.

It must either remain in episomal position or integrate into a specific region of the genome.

The gene delivery vectors are divided in two major categories, viral vectors and non-viral vectors.

2.2.1 Viral vectors

A virus can penetrate into the cell nucleus of the host and exploit the cellular machinery to express its own genetic material and replicate it, then spread to the other cells [54]. To use a virus as a vector to transfer a gene, it must be modified by genetic engineering. The pathogenic part of its genes is removed and the therapeutic gene is integrated [55]. The virus still retains its non-pathogenic structures such as envelope proteins, fusogenic proteins, etc. which allow it to infect the cell. To date, viral vectors are the vectors most often used to transfer genes. Although viral vectors show high transfection efficiency *in vitro* and *in vivo*, they have some drawbacks [51, 56] including:

The acute immune response that may be occurred.

The production of viral vectors in large quantities is very difficult and too expensive.

The limited size of gene that can be delivered by the virus.

The viral vectors available today are such as retrovirus, adenovirus, adeno-associated virus, herpes virus, pox virus, human foamy virus (HFV) and lentivirus.

2.2.1.1 Retroviral vectors

Retroviral vectors are one of the most frequently used for delivering genetic materials in somatic and germ line gene therapies. Retroviruses can transfect dividing cells because they can pass through the nuclear pores of mitotic cells [57]. In addition, all of the viral genes have been removed, creating approximately 7-10 kb of space for transgenic incorporation. Retroviruses have been used for human gene therapy of X-SCID successfully but incidence of leukemia in some patients occurred because of integration of retroviruses to the LMO2 gene and inappropriate activation of it [58]. Retroviral vectors also have been applied for familial hyperlipidemia gene therapy and tumor vaccination. However, the main limitations of retroviral vectors are their low efficiency *in vivo*, immunogenic problems, the inability to transduce the nondividing cells and the risk of insertion, which could possibly cause oncogene activation or tumor-suppressor gene inactivation [59].

2.2.1.2 Adenovirus vectors

Among the most commonly used viral vectors for the gene delivery into human cells are the adenoviruses. Adenoviral vectors have been isolated from a large number of different species, and more than 100 different serotypes have been reported. The adenovirus serotypes which most commonly used in gene therapy are types 2 and 5. They can be used for transferring both dividing and nondividing cells and have low host specificity so can be used for gene delivery into large range of tissues [60]. An additional attractive property of adenoviruses is the great efficiency with which they exploit the cellular machinery to drive synthesis of viral mRNAs and translation of viral proteins. Given these considerations, it is not surprising that, since the second half of the 1990s, adenoviral vectors have become the focus of a vast

series of both animal and clinical experimentations [61]. Adenoviruses are able to deliver large DNA particles up to 38 kb but they would not integrate into the host genome resulting in their short term gene expression.

2.2.1.3 Adeno‑associated vectors

Adeno-associated vectors (AAV) are like adenoviral vectors in their features but their replication and pathogenicity are deficient. Thus they are safer than adenoviral vectors and not caused any disease. Another special benefit of AAV is their ability to integrate into a human chromosome 19 which no undesirable effects. The major disadvantages of AAV are complicated process of vector production and the limited transgene capacity of the particles (up to 4.8 kb). AAVs have been used in the treatment of some diseases, such as CF, hemophilia B, meliorates muscular dystrophy and Leber congenital amaurosis [62-66].

2.2.1.4 Herpes simplex virus

HSV has broad host range, high natural infectivity of both replicating and non-replicating cells and capacity to establish a latent infection in neurons. Since the early days of gene therapy, all these properties have appeared very appealing in view of developing viral vectors [61]. When the defective HSV propagated in complementing cells' viral particles are generated, they can infect in subsequent cells permanently replicating their own genome but not producing more infectious particles. Herpes vectors can deliver up to 150 kb transgenic DNA and because of its neuronotropic features, it has the greatest potential for gene delivery to nervous system [67, 68], other tissues such as muscle, heart, liver [69, 70] and cancer [71].

2.2.1.5 Lentivirus

Lentiviruses are a subclass of retroviruses. They are able to naturally integrate with nondividing cells, contrast with other retroviruses which can infect only the dividing cells. Lentiviral vectors can deliver 8 kb of sequence. Because lentiviruses have strong tropism for neural stem cells, extensively used for *ex vivo* gene transfer in central nervous system with no significant immune responses and no unwanted side effects. Lentiviral vectors have the advantages of high-efficiency infection of dividing and nondividing cells, long-term stable expression of a

transgene, low immunogenicity, and the ability to accommodate larger transgenes [72, 73].

2.2.2 Non-viral vectors

As mentioned above, viral vectors have the drawbacks especially severe immune response. Consequently, non-viral vectors have been designed for transferring transgenes. Non-viral vectors are relatively safe, generally causes low immune response, they can be prepared easily, at low cost and in large quantities. In addition, they can transfer different and large transgenes, and they can be stored for long periods due to their stability. However, they show low transfection efficiency and a large scale usage is required [43]. Non-viral DNA delivery systems are classed into two groups [74]:

Physical methods: Therapeutic gene is delivered to target without using any carriers, by using physical forces to weaken the cell membrane and make it more permeable to the transgene.

Chemical methods: Therapeutic gene is carried into the cells by a carrier which can be prepared by several types of chemical reactions.

2.2.2.1 Physical methods

Physical approaches have been explored for gene transfer into cells *in vitro* and *in vivo*. These approaches induce transient injuries or defects on cell membranes, so that transgene can enter the cells. Gene delivery using mechanical (microinjection and gene gun), electric (electroporation), ultrasonic, hydrodynamic (hydrodynamic gene transfer), or laser-based energy has been explored.

2.2.2.1.1 Microinjection

This is a microsurgical procedure that is conducted on a single cell, using a glass needle (i.e., a fine, glass, microcapillary pipette), a precision positioning device (a micromanipulator) to control the movement of the micropipette, and a microinjector. This technique was successfully used for the first time in 1980 when DNA was microinjected into both the cytoplasm and nucleus of cultured mammalian cells [75]. Microinjection is the simplest gene delivery method. However,

it is difficult to apply. While pronuclear injection of DNA is very efficient, it is a laborious procedure; only one cell at a time can be injected [76].

2.2.2.1.2 Gene gun or particle bombardment

In this method transgene delivery into the target cell and tissue is carried out by using accelerated particle carriers biocompatible heavy metals such as gold, tungsten or silver. Ideally, particle carriers should be biocompatible, inert and have small diameters (usually 1–1.5 μm) [76]. The efficiency of this delivery technique depends on several parameters, such as the loading of DNA onto the particles, the particle size, and the timing of delivery. Such a simple and effective method of gene delivery is expected to have important applications as an effective tool for DNA based immunization [77].

2.2.2.1.3 Electroporation

Electroporation is impermanent destabilization of the cell membrane by insertion of a pair of electrodes so that transgene molecules in the surrounding media of the destabilized membrane would be able to penetrate into cytoplasm and nucleoplasm of the cells [78]. However, there are some problems in this method that are the difficulty in surgical procedure in the placement of electrodes into the internal tissues and that the high voltage applied to tissue might damage the organ and affect genomic DNA stability [79].

2.2.2.1.4 Hydrodynamic

Hydrodynamic is a simple and highly efficient method for direct intracellular delivery of any water-soluble compounds and particles into internal organs. Currently, this method is considered to be the most efficient nonviral gene transfer method for *in vivo* gene delivery in rodents such as the expression of hemophilia factors, cytokines, erythropoietin, and hepatic growth factors [80-83].

2.2.2.1.5 Sonoporation

Sonoporation enhances cell permeability via the application of ultrasound. It has been thought that cavitation is the most probable mechanism.

Cavitation causes mechanical perturbation and collapse of active bubbles, and the associated energy release can permeabilize adjacent cell membranes. The efficiency can be enhanced by the use of contrast agents or conditions that make membranes more fluidic [76, 84]. Unlike electroporation, which delivers transgenes along the electric field, ultrasound creates membrane pores and facilitates intracellular gene transfer through passive diffusion of transgene across the membrane pores. Therefore, the size and local concentration of plasmid DNA play an important role in determining the transfection efficiency [74].

2.2.2.1.6 Megnetofection

Magnetofection is a new efficient transfection method that has the advantages of the nonviral biochemical and physical transfection systems in one system. The idea of this method is to associate magnetic nanoparticles with genetic materials and either its transfection reagent. The magnetic particles are then concentrated preferentially into the target cells by the influence of an external magnetic field [85, 86].

2.2.2.2 Chemical methods

Chemical methods are more common than physical methods and generally are nanomeric complexes, which include compaction of negatively charged nucleic acid by polycationic nanomeric particles, belonging to cationic liposome/micelle or cationic polymers

2.2.2.2.1 Cationic lipids

Cationic lipid vectors are the most widely used non-viral gene carriers. It was first shown in 1980 that liposomes composed of the phospholipid phosphatidylserine could entrap and deliver SV40 DNA to monkey kidney cells [87]. Currently, hundreds of lipids have been developed and used for gene transfer. They share the common structure of positively charged hydrophilic head and hydrophobic tail that are connected via a linker structure. The positively charged head group is necessary for binding with negatively charged phosphate groups in nucleic acids. The examples of cationic lipids is illustrated in Figure 2.2. The positive-charged liposomes

spontaneously form uniquely compacted structures with the negatively charged DNA, called lipoplexes. In lipoplex structure, DNA molecules are surrounded with positively charged lipids which grant them protection against extracellular or intracellular nucleases. Furthermore, lipoplexes tend to electrostatically interact with the negatively charged molecules of the cell membrane (glycoproteins and proteoglycans) that may facilitate their cellular uptake [88].

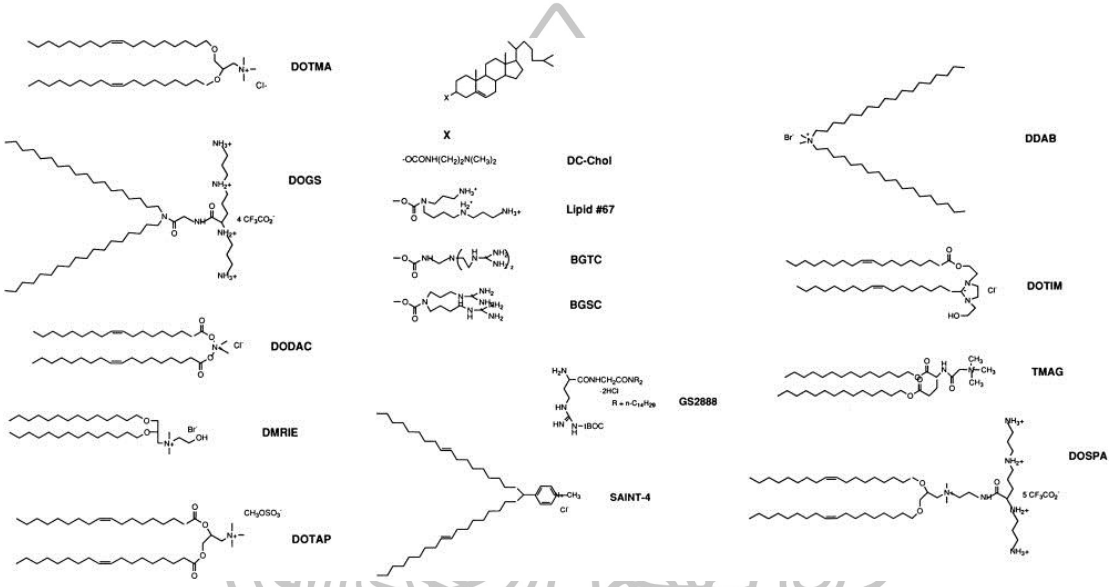

Figure 2.2 Examples of cationic lipids used for gene delivery.

Source: Tros de Ilarduya, C., Y. Sun, and N. Düzgüneş. (2010). "Gene delivery by lipoplexes and polyplexes." **European Journal of Pharmaceutical Sciences** 40, 3 (6/14/): 159-170.

The common neutral lipids such as dioleoyl phosphatidylethanolamine (DOPE) or cholesterol are generally added in cationic lipid–DNA complex as helper lipids. It shows facilitating the release of plasmid DNA from the endosome after endocytic uptake of the complexes [89]. Limitations of cationic lipids include low efficacy owing to poor stability and rapid clearance, as well as the generation of inflammatory or anti-inflammatory responses.

2.2.2.2.2 Cationic polymers

Cationic polymers have also been used extensively for gene transfer. These polymers form nanosized complexes with nucleic acid, often called

polyplexes. Cationic polymers can condense DNA molecules to a small size compared to cationic liposomes. This can be essential for gene delivery, as small particle size may be favorable for improving transfection efficacy [90].

2.2.2.2.2.1 Poly(L-lysine) (PLL)

PLL is one of the first cationic polymers employed for gene transfer. The biodegradable nature of PLL is an advantage for *in vivo* applications. However, PLL polyplexes are rapidly bound to plasma proteins and cleared from the circulation [90]. At physiological pH, all primary amino groups of PLL are protonated, yielding a structure with no buffering capacity to aid in endosomal escape. In general, only polylysine structures with molecular weights >3000 Da can effectively condense DNA to form stable complexes, indicating the significance of primary amine number for complex formation [91]. However, PLLs with high molecular weight showed a relatively high cytotoxicity.

Since the polyelectrolyte property of complexes is generally mediated by non-specific adsorption of the complex with the negatively charged plasma membrane via ionic interaction, the cationic property of the complex surface may be the cause for cytotoxicity. In addition, the charged surface can induce the nonspecific adsorption of serum proteins, resulting in rapid clearance of the complexes from the blood circulation [92]. Poly(ethylene glycol) (PEG) was conjugated to prevent the inter-particular aggregation of the complexes and to increase complex stability in the presence of serum proteins. In addition, specific targeting moieties such as;

Sugar conjugate PLL

Lactose and galactose have been used as conjugation partners with polymeric gene carriers for targeting asialoglycoprotein of hepatocytes [93].

Arterial-wall binding peptide (AWBP) conjugated PLL

The AWBP was conjugated to PLL via a PEG linkage (AWBP-PEG-g-PLL). AWBP-PEG-g-PLL showed dramatic increase of

transfection efficiency (150–180 fold), compared to PLL and PEG-g-PLL, in bovine aorta endothelial cells and smooth muscle cells [94].

Antibody–PLL conjugates

A monoclonal antibody against leukemia-specific JL-1 antigen (anti-JL-1-Ab) was conjugated with PLL. The anti-JL-1-Ab-PLL conjugate could specifically interact with the target antigen (JL-1) of leukemia cells (Molt 4) and was successfully internalized into the cells. The anti-JL-1-Ab-PLL conjugate demonstrated significantly higher transfection efficiency than PLL or lipofectin in Molt 4 cells [95].

2.2.2.2.2.2 Polyethylenimine (PEI)

PEI has been one of the most popularly employed cationic gene carriers due to its superior transfection efficiency in many different types of cells. PEI has primary (25%), secondary (50%) and tertiary amines (25%), of which two-thirds of the amines are protonated in a physiological pH. The unprotonated amines with different pKa values confer a buffering effect over a wide range of pH. The buffering property gives PEI an opportunity to escape from the endosome (proton sponge effect) [96].

Transfection efficiency of PEI has been studied over a wide range of molecular weights. The published study showed that transfection efficiency of PEI polyplexes increases with increased molecular weight ranging from 600 to 70000 Da [97]. The optimal molecular weight for PEI polyplex formation is typically between 5 and 25 kDa [98]. In addition to the molecular weight, the degree of branching of polyethylenimine has been shown to affect DNA complex formation and stability. Dunlap et al. showed that linear PEI is less effective at condensing DNA compared to the branched form for similar molecular weights [99].

PEI-PEG

When PEI graft with PEG, cell cytotoxicity of PEI-g-PEG was greatly reduced, while the transfection efficiency of PEI-g-PEG was

still comparable to that of PEI. Cytotoxicity was independent of molecular weight of PEG but affected by the degree of PEG substitution [100].

PEI conjugates with targeting moieties

PEI-g-PEG-RGD

An angiogenic endothelial cell targeted gene delivery system (PEI-g-PEG-RGD) was developed by incorporating the arh3/arh5 integrin binding RGD peptide. The PEI-g-PEG-RGD showed comparable binding affinity compared to unconjugated RGD peptide and could form a tight and stable complex with DNA [101]. The PEI-g-PEG-RGD/DNA complexes showed much lower cytotoxicity and about five times higher transfection efficiency in VEGF-stimulated angiogenic human dermal microvascular endothelial cells (HDMEC) than PEI/DNA complexes. However, much lower transfection efficiency of PEI-g-PEG-RGD was observed in angiostatic HDMEC compared to that of PEI, suggesting that the PEI-g-PEG-RGD is highly selective toward angiogenic endothelial cells.

Antibody-conjugated PEIs

The HER-2 antibody-PEI conjugate showed enhanced transfection efficiency in HER-2 overexpressing human breast adenocarcinoma cells (Sk-Br-3) compared to unmodified PEI. The conjugate also exhibited as high transfection efficiency as unmodified PEI in HER-2 low-expressing breast cancer cells (MDA-MB-231), suggesting that the conjugation of the antibody to PEI can provide target-specific transfection without loss of original properties of PEI [102].

Folate-conjugated PEIs

Folate-polyethylene-glycol-folate-grafted-polyethylenimine (FPF-g-PEI) was synthesized by grafting folate-PEG-folate to PEI. In CT-26 colon cancer cells, the FPF-g-PEI showed lower cytotoxicity as well as higher transfection efficiency than unmodified PEI. The enhanced transfection of

FPF-g-PEI could not be observed in normal smooth muscle cells, suggesting the specificity toward the folate-receptor overexpressing cancer cells [103].

Poly(α-(4-aminobutyl)-l-glycolic acid) (PAGA)

PAGA is a biodegradable analog of PLL. PAGA showed a significantly higher transfection efficiency than PLL, while no significantly cytotoxicity was detected in the experimental range, suggesting that the PAGA would be biocompatible [104].

Poly(b-amino ester)s

Poly(α-amino ester)s were synthesized by the addition of primary or secondary aliphatic amines to diacrylate esters. The polymers presented much lower cytotoxicity than PEI. The poly(α-amino ester)s could combine with plasmid DNA to form complexes in physiological condition, of which the size was 50–200 nm [105].

β-cyclodextrin

Cyclodextrin, CD is one of polysaccharide based polymers. CDs have an amphiphilic structure, which consists of a hydrophobic cavity and hydrophilic exterior. CDs are water-soluble, relatively non-toxic, and non-immunogenic [106]. Transfection results obtained with cyclodextrin-based polymers showed comparable efficiency with PEI and Lipofectamine at N/P ratios above 10 as well as limited toxicity in both fibroblast (BHK-21) and epithelial (CHOK1) cell lines at N/P ratios as high as 70 in the presence of serum [107]. However, the intracellular trafficking studies showed β-cyclodextrin-based polyplexes do not exhibit buffering capacity in the endosomal environment unless derivatized to form imidazole-terminated structures.286 Like most other cationic vector systems, in vivo use of β-cyclodextrin was shown to be hindered by the formation of aggregates at high ionic strengths. While PEGylation can generally reduce the formation of aggregates, it also reduces the cationic charge density of the polymer. Treating _-cyclodextrin polymers

with either adamantane-PEG-galactose288 or adamantane-PEG-transferrin289 copolymer has shown successful cell-targeted gene transfer potential.

Chitosan

Chitosan, obtained by deacetylation of chitin, is a biodegradable polysaccharide composed of two subunits, D-glucosamine and N-acetyl-D-glucosamine, which are linked by a (1,4) glycosidic linkage. Chitosan shows good properties i.e. biodegradability, biocompatibility, and cationic potential which has helped it become one of the most prominent, naturally derived nonviral vectors for gene transfer [108]. Investigations indicated that molecular weight of chitosan polymers can strongly influence gene transfer efficiency. In addition, several other factors have been shown to affect the transfection efficiency of chitosan polyplexes, including the N/P ratio, pH, the degree of deacetylation, and cell type [109]. Several approaches were developed to improve the properties of chitosan. The strategies included to increase charge density of chitosan by N-quaternization at terminal amines, which resulted in improved transfection efficiency regardless of higher cytotoxicity [110]. This higher cytotoxicity of the trimethyl chitosan derivatives was reduced by grafting of the polymer with PEG [111]. The charge density also increased by grafting chitosan with polylysine. The chitosan-*g*-PLL polymer showed better DNA-binding ability, reduced cytotoxicity, and increased transfection efficiency [112].

The chitosan has been conjugated with cell targeting ligands for delivering chitosan complex to specific cell types. For example, hepatic cell-targeting using galactose and lactose improved gene transfer to HepG2 cells. Complex stability was further enhanced for galactosylated complexes by conjugating chitosan- galactose polymers with either PEG or dextran. In addition, tumor cell-targeting was stimulated by conjugating chitosan with folate [113].

From the development of non-viral vectors, up to date, the non-viral vectors can be designed from a variety of different chemical compositions and constructed into various shapes (Figure 2.3). This flexibility in compositional design is beneficial for specific clinical applications. Therefore, vector composition must be

considered to enable optimal gene-delivery potential since the chemical, physical, and biological structure will primarily dictate the final gene-delivery outcomes [114]. In addition, there are non-viral vectors which address in clinical studies (Table 2.2)

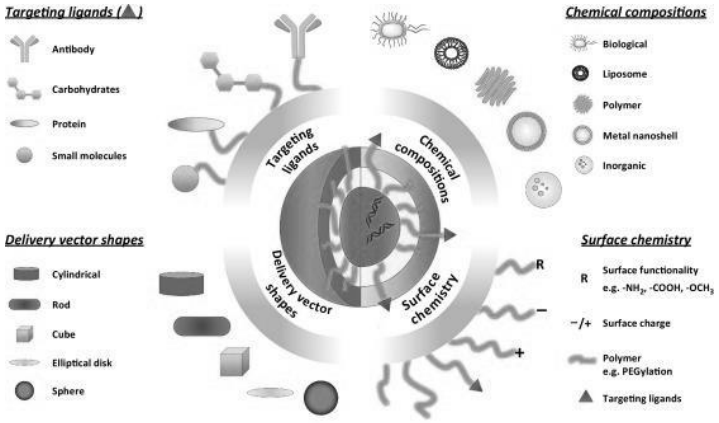

Figure 2.3 Compositional Design Considerations for Nonviral Gene-Delivery Vectors.

Source: Hill, A.B., et al. (2016). "Overcoming Gene-Delivery Hurdles: Physiological Considerations for Nonviral Vectors." **Trends in Biotechnology** 34, 2: 91-105.

Table 2.2 Non-viral DNA vectors under clinical evaluation

Delivery system	**Gene therapy drug**	**Sponsor**	**Indications**	**Phase**	**Status**
DOTAP–cholesterol	DOTAP– Chol-fus1	MD Anderson Cancer Center	Non-small-cell lung cancer	I	Completed
				I/II	Active
GAP-DMORIE–DPyPE	Tetravalent dengue vaccine	US Army Medical Research and Materiel Command	Dengue disease vaccine	I	Active
GL67A–DOPE–DMPE–PEG	pGM169/GL67A	Imperial College London	Cystic fibrosis	II	Active
PEI	BC-819/PEI	BioCancell Ltd.	Bladder cancer	II	Active
	BC-819	BioCancell Ltd.	Ovarian cancer	I/II	Completed
	DTA-H19	BioCancell Ltd.	Pancreatic cancer	I/II	Completed
	SNS01-T	Senesco Technologies, Inc.	Multiple myeloma and B cell lymphoma	I/II	Recruiting
	CYL-02	University Hospital, Toulouse	Pancreatic ductal adenocarcinoma	I	Completed
PEG–PEI–cholesterol	EGEN-001	Gynecologic Oncology Group	Ovarian, tubal and peritoneal cancers	I	Recruiting
				II	Active
	EGEN-001-301	EGEN, Inc.	Colorectal peritoneal cancer	I/II	Recruiting
PEI–mannose–dextrose	DermaVir/LC002	Genetic Immunity	HIV vaccine	II	Active
Poloxamer CRL1005–benzalkonium chloride	ASP0113	Astellas Pharma Inc.	CMV vaccine	III	Recruiting
				II	Recruiting
	VCL-CB01	Astellas Pharma Inc.	CMV vaccine	II	Completed

CMV, cytomegalovirus; PEG, polyethylene glycol; PEI, polyethylenimine

Source: Yin, H., et al. (2014). "Non-viral vectors for gene-based therapy." **Nature Reviews Genetics** 15, 8: 541-555.

From the overall of gene delivery system, although viral and nonviral gene delivery systems have been developed, all of them have some disadvantages that have made some limitations in their clinical application and yet no delivery system has been designed that can be applied in gene therapy of all kinds of cell types *in vitro* and *in vivo* with no limitation and side effects; however, some delivery systems has been explored, which can be efficient for gene delivery to specific cells or tissues. The comparison of advantages and disadvantages of both gene delivery systems are showed in Table 2.3.

Table 2.3 Comparison between viral and non-viral vectors

Vectors	**Comparison**	
	Advantages	**Disadvantages**
Viral	1. High transduction efficiency 2. Natural tropism confers the capability for infection of many cell types. 3. Intrinsic mechanism for endosomal escape 4. Virus evolved natural mechanism for nuclear import of genes.	1. Immune response is strong and multiple-injections are limited. 2. Can cause chromosomal insertion and proto-oncogene activation. 3. Difficult for construction and production. 4. Size of genes is limited. 5. Toxicity and contamination of live virus can be occurred.
Non-viral	1. Low immunogenicity 2. No risk of chromosomal insertion 3. Easy to synthesize and control the quality in mass production 4. Can carry large-sized DNA. 5. Can be functionalized for targeting, endosomal escape and nuclear import.	1. Transfection efficiency is low. 2. At high dose, current vectors show toxicity. 3. Lack of intrinsic tropism. 4. Lack of intrinsic mechanism for endosomal escape. 5. Lack of intrinsic mechanism for nuclear import of genes.

Source: Wang, T., J.R. Upponi, and V.P. Torchilin. (2012). "Design of multifunctional non-viral gene vectors to overcome physiological barriers: dilemmas and strategies." **International journal of pharmaceutics** 427, 1 (May): 3-20.

2.3 Biological barrier to gene delivery

Gene delivery presents an irresistible challenge to gene therapy research. It is clearly that transportation to target sites is usually inefficient. So gene delivery system represents a very important challenge to deliver the therapeutic gene to the target sites. The improvement of the efficiency in any individual step would be expected to improve the overall efficiency [115]. The biological barriers of gene delivery can be

divided in two major categories, extracellular delivery and intracellular delivery as presented in Figure 2.4.

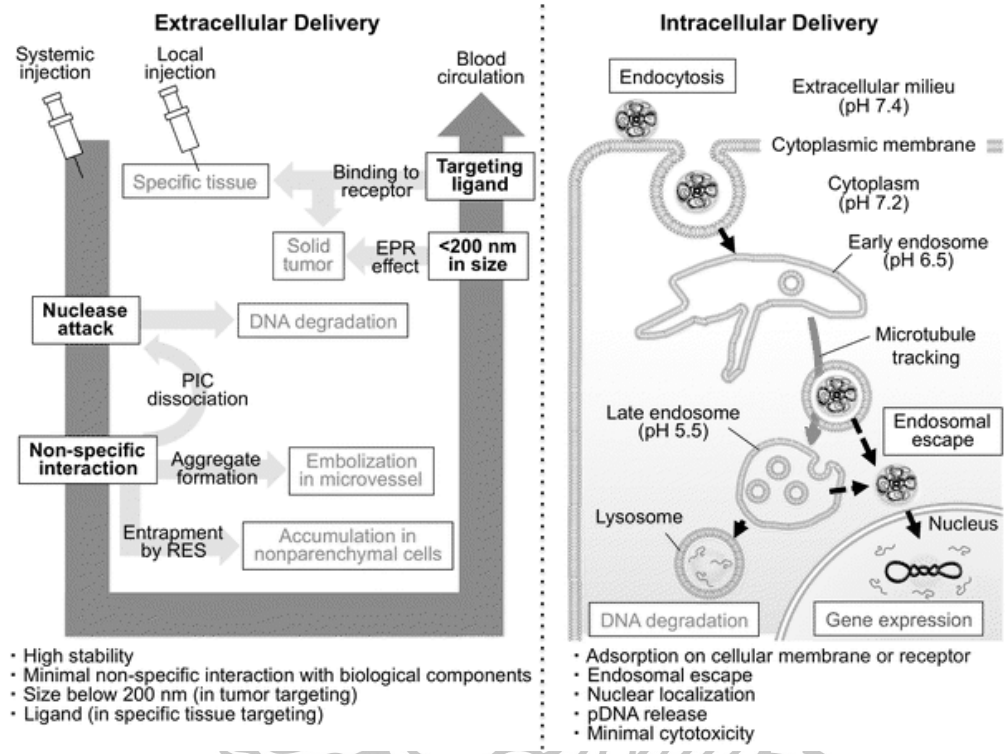

Figure 2.4 Schematic illustration of extracellular and intracellular delivery of therapeutic gene by injection.

Source: Miyata, K., N. Nishiyama, and K. Kataoka. (2012). "Rational design of smart supramolecular assemblies for gene delivery: chemical challenges in the creation of artificial viruses." **Chemical Society Reviews** 41, 7: 2562-2574.

2.3.1 Extracellular barriers

The exact barriers are dependent on the gene therapy strategy and particularly the route of administration of the genetic material in the body. In the case of *in vivo*-based strategies, the route of administration has been considered for gene delivery, including systemic, intramuscular, oral, topical, ocular and alveolar. At present, the most significant obstacle hindering *in vivo* gene therapy is delivery of the gene to the target site, and at levels that are biologically relevant.

2.3.1.1 Physicochemical properties

The complexes of cationic lipid and polymer with DNA have their unique particulate characteristics depending on the properties of the vector used, the mixing ratio, and the diluents used in the mixing protocol. Of the various properties, particle size is an important factor determining the tissue distribution process [116]. The particle that can pass through the capillaries is about 5 μm and through the fenestrae between discontinuous endothelial cells (30–500 nm). The entrance of a particle into cells via endocytosis is also a size-limiting process [117]. The electrical charge of the complex also greatly affects its biodistribution. Cell surface membrane containing glycoproteins and glycolipids show negatively charged membrane. Thus this is a good target for cationic complex to induce cellular uptake, followed by gene expression. However, this nonspecific interaction is also a hurdle for cell-specific delivery of DNA after local or systemic administration [118].

2.3.1.2 Route of administration

The administration of therapeutic gene is required to be intravenous or by other parenteral routes. Direct injection of gene medicines into a target tissue represents a far simpler task than targeting delivery to a specific tissue from the systemic circulation.

2.3.1.3 Interaction with blood components

The therapeutic gene or complex administered into the blood distributes to downstream tissues via blood circulation. When it interacts with serum proteins and/or blood cells, its biodistribution will depend on newly acquired physicochemical properties that are generally difficult to control. Negatively charged proteins such as albumin could bind with cationic non-viral vectors. Adsorption of negatively charged proteins neutralizes the cationic charge of the complex and increases its size, which leads to reduced gene expression [119]. To overcome this aggregation problem, the surface of the complex can be modified with hydrophilic compounds such as polyethylene glycol [120].

2.3.1.4 Recognition by immune system

Therapeutic gene-containing complexes are generally become targets for elimination by cells of the reticuloendothelial system (RES), and is recognized as a foreign material and is phagocytosed by immune cells, especially by the mononuclear phagocyte system (MPS) mainly Kupffer cells in the liver and splenic macrophages [121]. MPS plays a key role in systemic removal of hydrophobic particles. Modification of non-viral vectors with hydrophilic molecules such as poly(ethylene glycol) (PEG), creates a hydrophilic cloud around the particle surface, causing steric hindrance between the opsonins and the delivery vectors [122].

2.3.2 Intracellular barriers

2.3.2.1 Intracellular delivery

Intracellular delivery of therapeutic gene to the cytoplasm or nucleus is essential for its therapeutic action. The cytoplasmic membrane is typically impermeable to nucleic acids due to their large size and hydrophilic nature. The strategies of delivery gene involve physical means assist nucleic acid molecules to penetrate into cells by transiently penetrating through the cellular membrane. However, their clinical application is limited because of their invasive nature and potential damage to the structure of cells, as well as less successful to deeper tissues. An alternative strategy, chemical vectors capable of actively targeting internalization pathways that lead to an efficient transfection. There is convincing evidence showing that endocytosis is the predominant route for the internalization of a lipoplex/polyplex [123]. Lipoplexes and polyplexes are generally formulated into nanoparticles with net positive charges. From these reasons, endocytosis can be triggered by non-specific electrostatic interaction between the positively charged complexes and the negatively charged heparin sulfate proteoglycan on the cell surface followed by an internalization process termed adsorptive pinocytosis [124]. Receptor-mediated endocytosis is the most common route of nanoparticle uptake, and includes a variety of entry pathways such as clathrin- and caveolae-mediated endocytosis, macropinocytosis, and pathways that are both clathrin- and caveolae-independent [125]. It is not clear whether or not one pathway is more favorable than another in terms of the effectiveness of internalization, cytosol release and eventual gene

expression, but caveolae-dependant trafficking seems to be an attractive pathway for lipoplex/polyplex-targeting since the pathway is a non-acidic and non-digestive route . Particle size is also an important factor for the internalization pathway. Lipoplexes/polyplexes with a size less than 200 nm followed clathrin-mediated endocytosis, and particles with a size greater than 300 nm entered cells via a caveolae-mediated pathway. Macropinocytosis is on the order of 500 nm, and phagocytosis is capable of accommodating sizes up to 10 μm [126]. In addition, there was the illustration suggested that the translational diffusion of large DNAs (>250 bp) in cytoplasm was greatly slowed compared with that of smaller DNAs [127]. This was due to the major barrier of actin cytoskeleton which could restrict cytoplasmic transport of non-complexed DNA in non-viral gene transfer.

2.3.2.2 Endosome escape

After lipoplexes or polyplexes internalize via the endocytic pathway, endosomal entrapment and subsequent lysosomal degradation are a major bottleneck that limits the efficiency of gene delivery. Design of gene vectors with endosome-escape properties is considered critical for high transfection efficiency. The early endosome slowly matures by fusing with other sorting vesicles (from which material can be recycled back to the cell surface by exocytosis) and change to late endosome by the rapid acidification (pH 5−6) due to the action of the ATPase proton-pump enzyme. Sequential trafficking to the lysosome leads to further acidification (pH ~4.5) and the activation of various degradative enzymes. At this point, those nucleic acids that are unable to escape into the cytoplasm are rapidly degraded [128].

Several strategies are employed to facilitate nucleic acid release. Lipoplexes release their cargo into the cytosol by a lipid mixing mechanism, which presumably involves fusion of carrier lipids with the endosomal membrane, where local perturbations are formed that allow nucleic acid release. The proposed underlying mechanism is that cationic lipid form nonbilayer structures that participate in the lipoplex-induced flip-flop of negatively charged phospholipids from the cytoplasmic to the inner face of the endosome. This phenomenon is followed by the formation of charge-neutral ion pairs with the lipoplex, thereby destabilizing the

endosomal lamellar membrane organization and causing dissociation of the nucleic acids into the cytosol.

For cationic polymers, they are believed to release their therapeutic agents by “proton sponge effect” (Figure 2.5). Cationic polyplexes that contain a large number of titratable secondary and tertiary amines confer pKa values between physiological and lysosomal pH (typically 5.5−6). Thus, upon endolysosomal acidification, the amines become protonated and promote the influx of additional H+ ions and the concomitant influx of Cl− counterions. In order to compensate for increased ion uptake, vesicles introduce additional water molecules, causing osmotic swelling and eventual rupture.

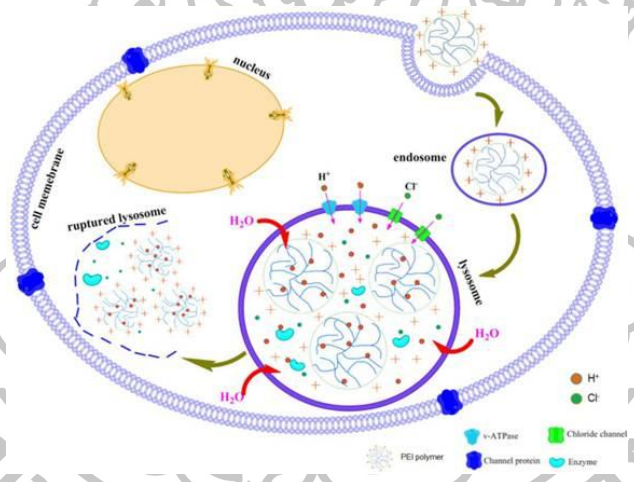

Figure 2.5 Proton sponge effect of cationic polymers [129]

2.3.2.3 Stability in cytoplasm, nuclear import

After endosomal escape and cytoplasmic release, nucleic acids should be delivered to their target side to obtain desired biological activity. For cytoplasmic activity-based nucleic acids, such as siRNA, the nuclear translocation barrier is nonexistent. However, the mobility of larger molecules, such as pDNA, is extremely low in the cytoplasm, making the payload susceptible to cytoplasmic nucleases. It has been reported that the half-life of naked pDNA in the cytoplasm is 50−90 min [130]. Previously, researchers believed that, after escape from the endosome, remaining of carriers may protect larger nucleic acid constructs from degradation. However, recent

studies contradicted these assumptions by observations of empty lipoplexes that were in the endosomal membrane, and free polymer being expelled into the cytosol with no accompanied translocation away from the endosomal vesicles at the time of nucleic acid release [131].

Nuclear expression requires overcoming an additional intracellular barrier, transnuclear passage. For dividing cells, nucleic acids can enter the nucleus during nuclear membrane breakdown; however, in nondividing cells, gene cargo must cross the membrane via the nuclear pore complex (NPC) which only permits entry of molecules up to 9 nm in size and <40 kDa by free diffusion [132]. Introduction of specific sequences, termed nuclear localization sequences (NLS), to nucleic acids can promote the attachment of proteins that are expected to enter the nucleus and mediate transnuclear transport through the NPC. Despite noted success, attachment of NLS-recognition proteins can affect biological expression/activity of pDNA and attempts at *ex vivo* attachment require a complex synthesis mechanism [133]. Overcoming nuclear translocation is requires more extensive research to investigate potential solutions.

2.4 Cellular uptake pathway for non-viral gene delivery system

The uptake pathways are divided into two major groups: endocytic pathways and non-endocytic pathways. The endocytic pathways include two types: phagocytosis and non-phagocytosis. The non-phagocytosis pathways are also divided into clathrin-mediated endocytosis (CME), caveolae-mediated endocytosis (CvME), and macropinocytosis. Non-viral gene complexes tend to be trapped in intracellular vesicles and eventually fuse with lysosomes when they are internalized through endocytic pathways. For nonendocytotic pathways, there are two categories of non-viral gene delivery systems: invasive and non-invasive systems. For the invasive systems such as microinjection, permeabilization, and electroporation, they are the techniques that are designed to break through the barrier of cytosolic lysosomes. For the non-invasive systems such as fusion and penetration, they are the naturally existing pathways that are useful to enhance the intracellular availability of non-viral gene complexes [134].

2.4.1 Phagocytosis

Phagocytosis is a special type of endocytic pathway which primarily exists in professional phagocytes such as macrophages, monocytes, neutrophils, and dendritic cells (DCs) . In contrast with other nonphagocytic pathways such as CME, CvME, and macropinocytosis which occur in almost all kinds of cells including phagocytes [135]. Phagocytic pathway is mediated by cup-like membrane extensions that are usually larger than 1 μm to internalize large particles such as bacteria or dead cells. In addition, a phagocytosis-like mechanism was proposed for the uptake of large lipoplexes and polyplexes that are larger than can be taken up by the classic CME or CvME pathway. There are three steps usually involved in phagocytosis. First, the complexes are recognized by opsonins in the bloodstream. Then, the opsonized complexes adhere to phagocytes and are ultimately ingested by them. Opsonization is the key step of the phagocytosis pathway. It involves complexes tagged by some major opsonins including immunoglobulins G and M (IgG and IgM), as well as complement components C3, C4, and C5 in the bloodstream [136]. These opsonized complexes become visible to macrophages and bind to their surface through the interaction between receptors (such as fragment crystallizable receptors (FcR) and complement receptors (CR)) and the constant fragment of particle-adsorbed immunoglobulins. Therefore, antibodies that lack constant fragments are sometimes used to help non-viral vectors avoid recognition and clearance by macrophages *in vivo.*

2.4.2 Clathrin-mediated endocytosis

CME is the best-characterized type of endocytosis, which is receptor-dependent, clathrin-mediated, and GTPase dynamin-required [137]. The most common examples of molecules that are internalized by CME are the cholesterol-laden low-density lipoprotein (LDL) that binds to LDL receptors, and the iron-laden transferrin (Tf) that binds to Tf receptors [138]. In this pathway, a series of downstream events are activated after the recognition of ligands by receptors on the cell surface. Clathrins assemble in the polyhedral lattice right on the cytosolic surface of the cell membrane, which helps to deform the membrane into a coated pit with a

size about 100–150 nm. As the clathrin lattice formation continues, the pit becomes deeply invaginated until the vesicle fission occurs. Dynamin, a kind of GTPase, is necessary in the vesicle fission. Dynamins usually self-assemble at the neck of the budding vesicle immediately before vesicle fission . The previous study indicated that cholesterol is also important for vesicle formation because cholesterol depletion causes the failure of the coated pits to detach from the plasma membrane [139]. In the next step of the CME pathway, the endocytosed vesicles internalized from the plasma membrane are integrated into late endosomes. Late endosomes then deliver their cargos to lysosomes [140].

In terms of gene delivery, CME can be targeted by using specific ligands, such as transferrin, which can recognize certain receptors on the cell surface. This results in an increase in the internalization of the particles and offers the possibility of targeting specific cells that substantially overexpress the receptors. However, genes that are internalized through CME are usually trapped in endosomes followed by enzymatic degradation in lysosomes, and the final result is that genes have little or almost no access to their target sites. Actually, entrapment and degradation can be regarded as two separate barriers, because preventing lysosomal degradation results in an accumulation of genes in intracellular vesicles without enhancing cytosolic release. Therefore, to reach the nucleus, genes must avoid degradation in lysosomes and must also released from intracellular vesicles into the cytosol. Several strategies have been developed to enhance the cytosolic release of endocytosed genes. This involves the incorporation of vesicular destructive elements to the DNA-carrier complexes, which perturb the integrity of the vesicular membrane and allow the cytosolic release of their contents, while not damaging the DNA. Some cationic polymers, e.g., polyethyleneimine (PEI), and some lipids also have the ability to enhance the cytosolic release of genes through different mechanisms as will be subsequently discussed.

2.4.3 Caveolae-mediated endocytosis

CvME begins in a special flask-shaped structure on the cell membrane called caveola, which is a kind of cholesterol- and sphingolipidrich smooth invagination

[141]. Caveolae have a diameter range of 50–100 nm and are typically between 50 and 80 nm with a neck of 10–50 nm [142]. CvME is also a type of cholesterol, dynamin-dependent, and receptor-mediated pathway. The fission of the caveolae from the membrane is mediated by the GTPase dynamin, which locates in the neck of caveolae and then generates the cytosolic caveolar vesicle. Caveolae are also involved in transcytosis and endocytosis of certain viruses such as simian virus 40 (SV40), as well as some bacteria and bacterial toxins, e.g., cholera toxin. Compared with CME, CvME is generally considered a non-acidic and non-digestive route of uptake, which means it does not suffer a drop in pH, and most pathogens can be directly transported to the Golgi and/or endoplasmic reticulum, thus avoiding the normal lysosomal degradation [143]. Therefore, this pathway seems to be advantageous in terms of gene delivery. However, this issue remains under discussion. There was the report that sometimes caveosomes join the classical endocytic pathway, in which fusion with lysosomes cannot be avoided. Another report also revealed that the size of particles affected on the pathway of their entry into the cell and their subsequent intracellular routing. The particles which microspheres with a diameter of < 200 nm were internalized via clathrin-mediated endocytosis and were ultimately delivered to the lysosomes, while 500-nm particles entered the cells via caveolae and never reached the lysosomal compartment [126].

Another term associated with caveolae is *lipid rafts.* Markers for lipid rafts are frequently found within caveolae. In general, caveolin-containing rafts are referred to as caveolae, whereas caveolin-devoid rafts are denoted by a variety of names such as glycolipid-enriched membranes and caveolae-like domains [144].

2.4.4 Macropinocytosis

Macropinocytosis is a type of distinct pathway that nonspecifically takes up a large amount of fluid-phase contents through the mode called fluid-phase endocytosis (FPE). Macropinocytosis usually accompanies cell surface ruffling that is induced in many cell types upon stimulation by growth factors or other signals [145]. Macropinocytosis occurs via the formation of actin-driven membrane protrusions, which is similar to phagocytosis. However, in this case, the protrusions do not zipper

up the ligand-coated particle; instead, they collapse onto and fuse with the plasma membrane [135]. Distinct from clathrin-coated vesicles (CCVs) and caveosomes, the macropinosomes have no apparent coat structures and are heterogenous in size, but are generally considered larger than 0.2 μm in diameter [146].

Macropinocytosis has recently received attention as an entry route for gene and drug delivery. Recent reports have demonstrated that the uptake of the TAT peptide and its cargos occurs by macropinocytosis [147]. This pathway provides some advantageous aspects such as the increased uptake of macromolecules, the avoidance of lysosomal degradation and the ease of escape from macropinosomes because of their relatively leaky nature. However, the basis for the different fates of macropinosomes and the relationship with lysosome is still unclear because sometimes they are cell type dependent.

2.4.5 Non-endocytic pathways

Although the endocytic pathways are efficient cellular uptake pathways, most of them have to meet the harsh environment inside the lysosomes, which cause the poor intracellular availability of DNA or siRNA. Therefore, it will be more advantageous to look for non-endocytic pathways to achieve a better intracellular availability of DNA or siRNA.

There are three technologies that are designed to bypass the endocytic pathways. One is microinjection, by which each cell is injected with the gene materials using glass capillary pipettes. The second one is permeabilization by using pore-forming reagents such as streptolysin O or anionic peptides such as HA2 subunit of the influenza virus hemagglutinin. The third one is electroporation, which uses an electric field to open pores in the cell. All of them are highly invasive and not ideal for in vivo gene delivery.

Another non-endocytic pathway is called “fusion”, which is special for lipoplexes, as it can cause a direct release of DNA to the cytoplasm before entering the endocytic pathways. However, more and more evidences suggest that fusion with

the cell membrane contributes minimally to the overall uptake of lipoplexes, while the CME plays an important role in the uptake of lipoplexes [148].

2.5 Tools to Study cellular uptake in Nonviral Gene Delivery

2.5.1 Specific inhibiors

Certain cell treatments can inhibit internalization via endocytosis, which is generally useful in determining the uptake pathways is illustrated in Table 2.4.

Table 2.4 Perturbation of endocytosis and intracellular trafficking

Treatment	Effect	Mechanism
Low temperature	General inhibitor of endocytosis	Energy depletion
Metabolic inhibitors	General inhibitor of endocytosis	Energy depletion
Potassium depletion	Specific inhibitor of CME	Dissociation of clathrin lattice
Cytosol acidification	Specific inhibitor of CME	Dissociation of clathrin lattice
Hypertonic medium	Specific inhibitor of CME	Dissociation of clathrin lattice
Chlorpromazine	Specific inhibitor of CME	Dissociation of clathrin lattice
Filipin	Specific inhibitor of caveolae	Cholesterol binding
Nystatin	Inhibitor of caveolae	Sequester cholesterol
Methyl- β -cyclodextrin	Inhibitor of caveolae	Deplete cholesterol
Genestein	Inhibitor of caveolae	Tyrosine kinase inhibitor
Cytochalasins	Inhibitors of caveolae and macropinocytosis	Actin depolymerization
Amiloride	Specific inhibitor of macropinocytosis	Inhibits the Na+/H+ exchange protein
Phorbol esters	Specific stimulators of macropinocytosis	Protein kinase C activators
Wortmannin	Inhibitor of macropinocytosis	Phosphatidyl inositol-3-phosphate inhibitor
Monensin	Inhibitor of endosome maturation	Prevents endosome acidification
Chloroquine	Disrupting endosomes and lysosomes	Prevents endosome acidification and causes swelling to endosomes and lysosomes
Ammonium chloride	Disrupting endosomes and lysosomes acidification	Increases pH of late endosomes and lysosomes
Nocodazole	Inhibit vesicular transport	Depolymerises microtubules

Source: Khalil, I.A., et al. (2006). "Uptake pathways and subsequent intracellular trafficking in nonviral gene delivery." **Pharmacological reviews** 58, 1: 32-45.

However, none of the commonly used inhibitors of different uptake pathways is absolutely specific. All of them either affect the actin cytoskeleton with their side effects, or interfere with alternative uptake pathways simultaneously. In addition, they usually show cell type variations.

The most direct way to distinguish endocytic pathways and nonendocytic pathways is to use the inhibitor or method of energy depletion, because most endocytic pathways are energy dependent. The commonly used inhibitors and methods are: low temperature (4 °C) and sodium azide (an ATPase inhibitor).

To distinguish the phagocytic and macropinocytic pathways with CME and CvME pathways, the commonly used inhibitors and methods for phagocytic and macropinocytic pathways are: inhibitors of sodium-proton exchange “amiloride and its derivatives”, F-actin depolymerizing drugs “cytochalasin D and latrunculins”, inhibitors of phosphoinositide metabolism “wortmannin and LY290042”, and protein kinase C activator “phorbol esters”. Except phorbol esters, the specificity of all the inhibitors is still in doubt as depolymerizing F-actin and inhibition of phosphoinositide metabolism may also disrupt the other two endocytic pathways. For example, cytochalasin D is also used as the inhibitor for CvME [149]. Within these inhibitors, amiloride and its derivatives may be considered as the first choice for their fewest side effects.

The commonly used inhibitors and methods for clathrin-mediated endocytosis are: Hypertonic sucrose (0.4–0.5 M), potassium depletion, cytosolic acidification, chlorpromazine, monodansylcadaverine (MDC), phenylarsine oxide. However, all of them have been shown to be able to inhibit macropinocytosis, thus cannot be used to distinguish the clathrin-mediated endocytic pathway and the macropinocytic pathway. Besides this, all these inhibitors can influence the cortical actin cytoskeleton more or less, which can cause non-specific cytotoxicity. However, potassium depletion, chlorpromazine, and MDC are the relatively better choices than the other ones for the initial discrimination of clathrin-mediated endocytic pathway [150].

As to caveolae-mediated endocytic pathway, the commonly used inhibitors and methods are: statins, methyl-β-cyclodextrin (MβCD), filipin, nystatin, genestein,

and cholesterol oxidase. Among them, the incubation with filipin, nystatin, and cholesterol oxidase produce the fewest side effects. The chronic inhibition of cholesterol synthesis by statins or acute cholesterol depletion by MβCD nonspecifically disrupts intracellular vesicle trafficking and the actin cytoskeleton. Also, the specificity of genestein is still in doubt for its nonspecific disruption of the actin network. That being so, appropriate controls should be included when filipin, nystatin, and cholesterol oxidase are used [150].

The inhibitors for the study of intracellular fates of complexes are also very important. Monensin, bafilomycin A can inhibit the acidification of endosomes, thus preventing their maturation and fusion into lysosomes [151]. Chloroquine is another inhibitor that accumulates in endosomes/lysosomes and causes the swelling and disruption of endocytic vesicles by osmotic effects [152].

However, a range of concentration with lowest cytotoxicity and sufficient inhibitory efficiency should be determined first when the inhibitor is used on the cell for the first time. Then, the lack of absolute specificity can be compensated by the combined application of biological methods such as siRNA silencing, transient or stable expression of dominant-negative proteins, and reconstruction of proteins by knockout mutants, all of which are more specific than classical chemical inhibitors.

2.5.2 Molecular probes, markers, and dyes

Apart from specific inhibitors, there are several classical molecular probes that are known to be specifically internalized through each uptake pathway. Transferrin is often used as a probe of CME pathway in many studies [153]. Cholera toxin beta subunit (CTBs) is commonly used as a probe for CvME [153]. In addition, caveolin-1 is also an important marker for CvME, as it is specifically involved in the formation of caveosome. Dextran is the popular probe for macropinocytosis in some studies because it can accumulate in the endolysosome compartment [153]. To solve the issue about the intracellular fate of complexes, a group of the specific markers or biological dyes are necessary to colocalize the non-viral gene complexes and intracellular organelles. TFR is used as a classical early endosome marker because it is transported into an early endosome when transferrin is internalized. EEA-1 is a hydrophilic

peripheral membrane protein present in cytosol and membrane fractions. It colocalizes with TFR, and immunoelectron microscopy shows that it is associated with tubulovesicular early endosomes. The lysosome-associated type 1 membrane glycoproteins LAMP-1 and LAMP-2 are localized primarily on the periphery of the lysosome, and can be used as markers for lysosome. The different roles of EEA-1 and LAMP in the endolysosome pathway allow us to know the stage in which the uptake carries on. Other endosome or lysosome markers are the Rab family proteins. They are small GTPases that control multiple membrane trafficking events in the cell, and there are at least 60 Rab genes in the human genome [154, 155]. The organelle specific dyes are other ideal tools for the detection of colocalization, and they are relatively convenient. LysoTracker (red) and Lyso Sensor (green) are the widely used dyes for lysosomes. Cell light (red or green) are the widely used dyes for early endosomes. Combined with the confocal imaging technology, the colocalization of labeled non-viral gene complexes and intracellular compartments can be viewed intuitively. However, the classical confocal imaging technology can only provide the monolayer images, the information from which is not convincing enough.

2.6 RNAi therapeutic

RNAi therapeutics is a fundamentally new strategy to treat human disease at post transcriptional step. RNAi was first described in the nematode *Caenorhabditis elegans* by Fire and colleagues [156]. The injection of double-stranded RNA (dsRNA) could suppress the expression of a target gene by triggering specific degradation of the complementary mRNA sequence. After that, RNAi has rapidly become one of the most powerful and widely used tools for gene therapy. In addition, it has been developed as a novel therapeutic tool to target disease genes for treatment.

2.6.1 Mechanism of RNA interferance

RNA interference is a conserved biological process among multicellular organisms as diverse as plants, worms, yeast and humans. At the first time, by infection of dsRNA is able to suppress the expression of a target gene by triggering specific degradation of the complementary mRNA sequence. It is now clear that higher eukaryotes contain a large number of genes that encode small RNA namely

micro RNAs (miRNA) [157]. These miRNA generally have only incomplete sequence homology to their targets, often recognizing sequences in the untranslated 3′ end of a gene, and usually work by blocking the translation of mRNA into protein rather than by destroying the mRNA transcript. The naturally occurring miRNA are synthesized in the nucleus in large precursor forms, which are processed in the nucleus by Drosha, an RNase III enzyme, into pre-miRNA (60–80 nucleotides). Subsequent to transport to the cytoplasm and processing by Dicer, mature miRNA (22 nucleotides) are taken up into a multisubunit ribonucleoprotein complex called RNA-induced silencing complex (RISC). The heart of RISC is the Argonaute (AGO) proteins which are 8 AGO protein in human. Not all AGO proteins are cleavage competent. Only AGO2 is the executer that accomplishes siRNA-induced silencing . RISC incorporates the antisense strand of the unwound siRNA and defines the target region of the mRNA via sequence complementarity to promote its specific cleavage [158]. The pathway of RNAi shows in Figure 2.6.

For siRNA, it has a well-defined synthesized structure, a short (usually 21-bp) double-stranded RNA with phosphorylated 5′ ends and hydroxylated 3′ ends with two overhanging nucleotides. This type of small RNA directly incorporates into RISC, where its guide strand binds to and cleaves the complementary mRNA with a perfect match. When the cleaved mRNA is released, the guide-strand bound RISC binds to another mRNA and starts a new round of cleavage [159].

Since the half-life of siRNA is short, shRNA has been developed as an alternative RNA molecule. shRNA is transcribed in the nucleus from an external expression vector bearing a short double stranded DNA sequence with a hairpin loop by RNA polymerase II or III. The shRNA transcript is then processed by Drosha, an RNase III endonuclease. The resulting pre-shRNA is exported to cytoplasm, where it is processed by Dicer (another RNase III enzyme) and incorporated into RISC, followed by the same cytoplasmic RNAi process as in siRNA . Comparing with siRNA, shRNA is constantly synthesized in host cells, leading to more durable gene silencing.

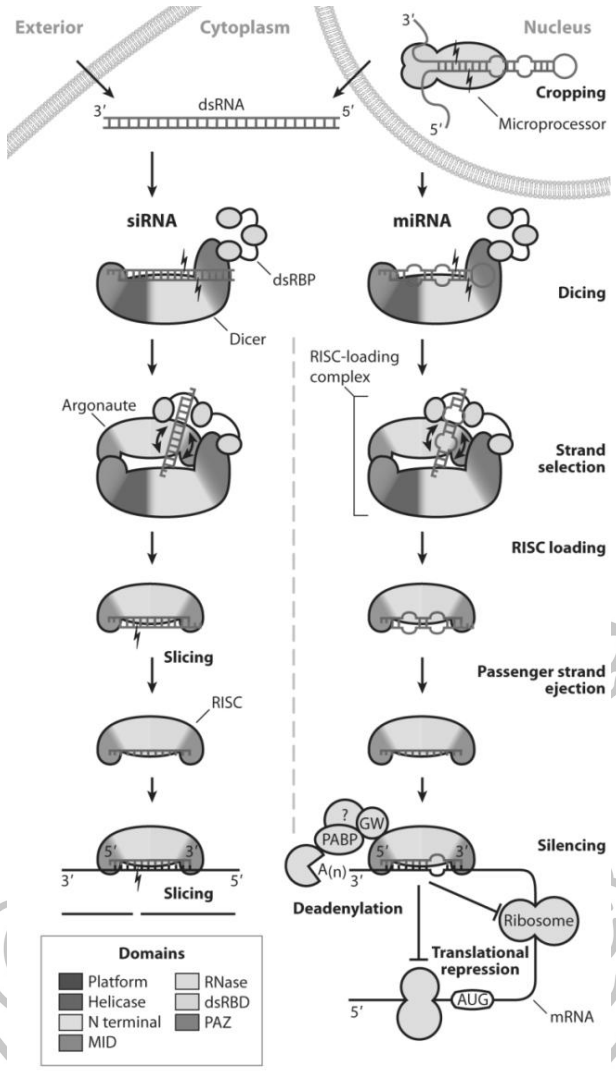

Figure 2.6. The siRNA (*left*) and miRNA (*right*) pathways of RNA interference.

Source: Wilson, R.C. and J.A. Doudna. (2013). "Molecular mechanisms of RNA interference." **Annual review of biophysics** 42: 217-239.

2.6.2 Challenge of siRNA therapeutic

2.6.2.1 siRNA stability and targeting

Generally, unmodified siRNAs are quite stable in a variety of conditions by avoiding nucleases. Neither brief exposure to high temperature (up to 95 °C) nor long incubation time at lower temperatures (1 year at 4 °C) had any effect on activity [160]. To be effective in a disease-relevant setting, siRNAs must not only

survive in the serum, but also reach their target cells in the specific tissues. The large size and negative charge of naked siRNAs frustrates their diffusion across the plasma membrane. In addition, siRNA delivery strategies that take advantage of endocytosis also must provide for endosomal escape. Once it is in the cell cytoplasm, siRNAs need to be recognized by and incorporated into RISC with high efficiency with no degradation by intracellular nuclease [161].

2.6.2.2 Off-target silencing

It is believed that RNAi is gene specific and only the gene with complementary sequence should be affected. However, the truth is that RNAi can sometimes induce nonspecific off-target effects. Among of off-target mechanism, miRNA-like binding in the 3′ UTRs is a major cause. Indeed, siRNAs or shRNAs can function as miRNAs due to the similarities between these silencing pathways. It has shown that siRNA can regulate unintended transcripts via “seed region” complementarity in their 3′ UTRs. This can be mitigated by siRNA redundancy or chemical modification [162]. However, Off-target silencing cannot be ignored in developing siRNA-based therapeutics, and all potential therapeutic siRNA candidate sequences must be heavily tested for perturbation of normal protein expression profiles. Also, predictive bioinformatics approaches implemented at the stage of siRNA design promise to significantly reduce and eventually eradicate off-target silencing [161].

2.6.2.3 Activation of immune response

Double-stranded RNA induces innate immune response via interaction with RNA-binding proteins such as Toll-like receptors (TLRs) and protein kinase receptor (PKR). The innate immune response is mediated mainly by type I interferon (IFN) and pro-inflammatory cytokines, like IL-6 and TNFα. siRNA can stimulate the immune system in a sequence-dependent manner, certain shRNAs or siRNAs can bind and activate TLR7 if they contain 5′-GUCCUUCAA-3′motif or similar GU-rich sequences [163]. Furthermore, longer double-stranded RNA increased cytokine production markedly.

2.6.3 Therapeutic application of RNAi

RNAi-induced gene silencing hijacks the inhibitory effects of conventional pharmaceuticals, mainly achieved by blocking their targets' function. However, some disease-related molecules, primarily proteins, do not have an enzymatic function or have a conformation that is hardly accessible to conventional drugs, therefore are considered as “non-druggable” targets. Recently, these “non-druggable” targets have been targeted by RNAi approach.

2.6.3.1 Cancer

Cancer is a genetic disease which involves mutational and epigenetic changes which lead to uncontrollable cell proliferation and differentiation [164]. siRNA and shRNA have been extensively used to silence cancer-related gene targets. A lot of preclinical studies have shown that gene silencing can inhibit tumor cell growth, angiogenesis, metastasis and chemo-resistance [165, 166].

For example, an oncogene Bcl-2 is over expressed in many human tumors [167]. The report demonstrated that siRNA targeting Bcl-2 induced apoptosis of the cells *in vitro* and shRNAs against Bcl-2 suppressed tumor growth in mice with xenograft tumor [168]. Angiogenesis is also a key factor for neoplasia and tumor metastasis. The vascular endothelial growth factor (VEGF) pathway is the well-known target of tumor angiogenesis [169]. RNAi technology has been used to inhibit angiogenesis by selectively silencing VEGF pathway. For example, shRNAs against VEGF was intravenously and intratumorally delivered to a pancreatic tumor xenograft model. Both treatment significantly inhibited cancer cell proliferation and tumor growth, down-regulated the expression of VEGF-C mRNA, and reduced tumor microvessel density (MVD) and microlymphatic vessel density (MLVD). Interestingly, shRNA showed a weaker inhibitory effect on tumor growth, compared to Gemcitabine but a stronger inhibitory effect of MLVD and MVD [170]. Basic fibroblast growth factor (bFGF) is also an important pro-angiogenic growth factor. siRNA against bFGF significantly reduced the bFGF mRNA amount and showed inhibitory effects on endostatin secretion in different pancreatic cancer cell lines.

These will provide therapeutic targets for antiangiogenic treatment of pancreatic cancer and other tumors [171].

Drug resistance is another major barrier that limits the effectiveness of chemotherapy. A common phenomenon is multidrug resistance (MDR), that is simultaneous resistance to a number of structurally and functionally unrelated chemotherapeutic agents. The mechanism involves the overexpression of trans-membrane transporter proteins P-glycoprotein (P-gp) and multidrug resistance-associated protein-1 (MRP1), encoded by MDR1 and MRP1 genes, respectively [172]. RNAi approach may be an efficient tool to reverse MDR and increase the success of chemotherapy. Selective MDR1 siRNA duplex treatment induced 85–90% reduction in MDR1 expression in doxorubicin-resistant MCF-7 breast cancer cells, relocalization of doxorubicin to the nucleus and 70% resensitization of doxorubicin resistant cells [173].

2.6.3.2 Cardiovascular disease

In cardiovascular system, renin–angiotensin system (RAS) plays important roles in the development and progression of atherosclerosis and hypertension. In RAS, angiotensinogen (AGT) is the precursor of angiotensin II (AngII). The increased AGT in liver may significantly elevate the production of Ang II, which increases the blood pressure and accelerates the progression of atherosclerosis. Meanwhile, a larger amount of superoxides and reactive oxygen species (ROS) are produced, but the production of nitric oxide (NO) is reduced and the endothelium-dependent dilation is impaired. Thus, inhibition of RAS may reduce the generation of ROS, promote the synthesis of NO, control the blood pressure, and delay the development of atherosclerosis. AGT was selected as the target gene to design corresponding GPE nanoparticles carrying shRNA, since it is the initial substrate of RAS. After AGT shRNA treatment, the mRNA and protein expressions of AGT in the liver were remarkably reduced and the blood levels of AGT and Ang II also significantly decreased. The blood pressure was reduced during the first few days. Moreover, microscopy showed that the atherosclerotic lesions were markedly

attenuated in AGT shRNA treated rats, resulting in the delayed development of early atherosclerotic lesions [174].

On the other hand, aldosterone (Aldo) is a principal signaling factor in the functional cascade of the RAS. Like Ang II, Aldo also plays an important role in the progression of hypertension. Aldo excess increases ROS generation by activating NADPH oxidase (NOX) and the increased ROS in the brain may be a key mechanism in the development of hypertension. A number of studies demonstrated that intracerebroventricular (i.c.v.) infusions of NADPH oxidase inhibitors attenuate Aldo-induced hypertension. There was the study which investigated the brain regional specificity of NOX2 and NOX4 NADPH oxidase subunits in the hypothalamic paraventricular nucleus (PVN) in Aldo-induced hypertension. PVN injections of adenoviral vectors expressing siRNA targeting NOX2 or NOX4 significantly attenuated the increase in mean arterial pressure (MAP) induced by Aldo in mice. As for in vitro study, silencing either NOX2 or NOX4 protein by culturing PVN cells with NOX2 siRNA or NOX4 siRNA remarkably attenuated Aldo-induced ROS generation [175]. These indicate that silencing NOX2 or NOX4 in the PVN via siRNAs could normalize the hypertensivogenic actions induced by Aldo excess.

2.6.3.3 Neurodegenerative diseases

Neurodegenerative diseases are considered by the progressive loss of neurons, which leads to the gradual appearance of disable neurological symptoms and premature death. Current available therapies aim to improve the symptoms but not to prevent the progress. The increasing prevalence and economic burden of the diseases such as Huntington's disease (HD), Alzheimer's disease (AD), or Parkinson's disease (PD) have facilitated the development of new inventions, including RNAi. Several lines of evidence have shown that therapeutic manipulation of RNAi to selectively suppress disease linked genes has a potential for the treatment of neurodegenerative diseases [176]. In HD studies, RNAi directed against mutant human hunting in successfully suppressed expression of the transgene in the stritum and cerebellum in HD mice, resulting in a significant pathological and behavioral improvement [177]. In AD studies, RNAi targeted for amyloid precursor protein (APP), β-site APP cleavage

enzyme 1 (BACE1) or tau has been proposed as therapies for AD. Singer using lentiviral delivery of shRNA targeting endogenous BACE1 to the hippocampi significantly reduced Aβ production, amyloid plaques and neuronal death, which leads to improved learning and memory in a transgenic mouse model of AD after disease onset [178]. In addition, studies using herpes simplex virus RNAi directed against the APP transcript significantly reduced the accumulation of AD related Aβ in the lentiviral mouse model [179]. In PD studies, RNAi manipulation has been proposed to silence the expression of α-synuclein, which may interfere with the pathogenic cascade and thus be therapeutically helpful in PD [180].

2.6.3.4 Human immunodeficiency virus (HIV)

HIV belongs to the retroviral family which led to acquired immunodeficiency syndrome (AIDS). Due to the lack of effective anti-retroviral drugs, CD4+ T lymphocytes may continue to decrease and weaken the immune system, resulting in opportunistic infections and tumors. The alternative strategies were developed to overcome these problems and RNAi studies presented favorable outcomes. Synthetic siRNAs and expressed shRNAs have been used to target several early and late HIV-encoded RNAs in cell lines [181]. Although the success of RNAi-mediated inhibition of HIV encoded RNAs in vitro, targeting the virus directly is still difficult because the virus can escape from being targeted by viral mutation. Therefore, down-regulation of the cellular cofactors, such as CD4, can be an alternative strategy [182]. In addition, down-regulation of CXCR4 and CCR5 resulted in the inhibition of HIV replication in numerous human cell lines and primary cells [183]. The first clinical trial using a lentiviral gene therapy was initiated in early 2007 (NCT00569985; 04047). The lentivirus vector induces 3 forms of anti- HIV RNA: RNAi in the form of a shRNA targeted to an exon in HIV-1 tat/rev (shI) to destroy viral mRNA, a decoy for HIV TAT-activated RNA (TAR) to antagonize viral transactivation, and a ribozyme that targets the host T cell CCR5 cytokine receptor (CCR5RZ) to block viral entry. The vector is called rHIV7-shI-TAR-CCR5RZ and was used in the transduction and expansion of autologous CD4-enriched T cells.

2.6.3.5 Viral hepatitis

Current therapy for chronic hepatitis C virus (HCV) infection employed combined use of pegylated interferon (IFN-α) and ribavirin. Although these agents have improved the clinical outcome, few patients responded to them and IFN-α was associated with significant side effects, ranging from fatigue to mood disorders. Thus, there is a clear need for the development of additional agents that act specifically. Several studies have shown that HCV replication is very sensitive to siRNAs or shRNA targeting HCV RNA [184]. Moreover, increasing evidence has suggested that miR-122 can facilitate HCV replication and stimulate HCV translation at an early initiation stage by binding directly to two adjacent sites close to the 5′ end of HCV RNA. This can be a therapeutic target for HCV [184].

2.6.3.6 Other applications

RNAi can be used to silence endogenous genes involved in the cause of metabolic diseases. Current focus is laid on silencing target genes that control lipid packaging into lipoprotein particles. For instance, silencing apolipoprotein B (ApoB), a crucial component of LDL particles, has been proved to lower serum LDL cholesterol levels in both rodents and nonhuman primates [185]. Silencing proprotein convertase subtilisin/kexin type 9 (PCSK9), an enzyme responsible for the processing of secretory proteins could reduce serum LDL cholesterol content in mice.

On the other hand, the eye provides advantages for clinical application of siRNA, as it is a relatively isolated tissue compartment. Topical administration of siRNAs directed against VEGF or its receptors has proven effective on suppressing corneal neovascularization [186]. In addition, signaling through transforming growth factor-beta receptor 2 (TGFbetaR2) has been implicated in excessive ocular scarring and siRNA targeting TGFbetaR2 has shown a beneficial effect on excessive scarring after glaucoma filtration surgery [187]. The first clinical trial was initiated in 2004 by Acuity Pharmaceuticals in patients with age-relatedmacular degeneration (AMD). A siRNA targeting the angiogenic growth factor VEGF was administered by intravitreal injection. So far, there are at least 10 siRNA clinical trials for treating eye diseases,

such as AMD, ocular hypertension, ocular pain and glaucoma. The summary of RNAi application illustrated in Table 2.5.

Table 2.5 Small RNA-based therapeutics in clinical trials

Diseases	Disease category	Drug name	Drug type	Target	Phase
AMD	Ophthamology	Bevasiranib	siRNA	VEGF	III
		PF-4523655 (RTP801ni-14)	siRNA	RTP801	II
		AGN211745	siRNA	VEGF-R1	I/II
Macular edema	Ophthamology	Bevasiranib, Cand 5	siRNA	VEGF	II
		PF-4523655 (RTP801ni-14)	siRNA	RTP801	II
Chronic optic nerve atrophy	Ophthamology	QPI-1007	siRNA	proNGF	I
Pachyonychia congenita	Genetic disorder	TD1010	siRNA	Keratin K6a	I
Chronic lymphocytic leukemia	Oncology	SPC2996	LNA oligo	Bcl-2	I/II
Metastatic lymphoma	Oncology	Proteasome siRNA	siRNA	Immuno-proteasome β-subunits LMP2, LMP7 and MECL1	I
		gPLK SNALP	siRNA	PLK1	Pre-clinical
Solid tumors	Oncology	CALAA-01	siRNA	M2 subunit of ribonucleotide reductase	I
		Atu027	siRNA	PKN3	I
		EZN3042	LNA oligo	Survivin	I/II
		EZN2968	LNA oligo	HIF-1α	I/II
		FANG vaccine	shRNA	Furin	I
		ALN-VSP	siRNA	KSP and VEGF	I
		eIF-4E ASO	LNA oligo	eiF-4E	I
		Survivin ASO	LNA oligo	Survivin	II
Delayed graft function	Inflammation	I5NP	siRNA	p53	I/II
Acute kidney injury	Inflammation	I5NP	siRNA	p53	I
Familial adenomatous polyposis	Inflammation	CEQ508	shRNA	β-Catenin	I
Hypercholesterolemia	Metabolic disease	PRO-040201	siRNA	ApoB	I
		ApoB SNALP	siRNA	ApoB	I
		SPC4955	siRNA	ApoB	Pre-clinical
		ALN-PCS	siRNA	PCSK9	Pre-clinical
HCV	Viral infection	SPC3649	LNA oligo	miR-122	I
HIV	Viral infection	Lentivirus expressing shRNASI/SII-TAR decoy and anti CCR5 ribozyme	shRNA+TAR decoy +CCR5 ribozyme	HIV Tat and Rev proteins, HIV TAR RNA, and human CCR5	I
		pHIV7-shI-TAR-CCR5RZ	shRNA+TAR decoy +CCR5 ribozyme	HIV Tat protein, HIV TAR RNA and human CCR5	Pre-clinical
RSV	Viral infection	ALN-RSV01	siRNA	RSV nucleocapsids	II

Source: Lares, M.R., J.J. Rossi, and D.L. Ouellet. (2010). "RNAi and small interfering RNAs in human disease therapeutic applications." **Trends in Biotechnology** 28, 11: 570-579.

2.7 General methods for determining the carriers/nucleic acid complexes formation

Since the formation of carriers/nucleic acid is important for therapeutic gene transfer and involved in transfection efficiency. A range of techniques have been employed to monitor the self-assembly formation and to characterize properties of the polyelectrolyte complexes produced. Amount of these techniques, gel retardation is a common method that monitors the loss of electrophoretic mobility of DNA when it binds a critical amount of cationic polymer. Also, inhibition of ethidium bromide (EtBr)/DNA fluorescence resulting from DNA condensation by cationic polymers is a convenient method to monitor the polyelectrolyte interaction [188]. In addition, zeta potential analysis which could detect the surface charge of complexes was also common method for determining of complete complex formation.

2.7.1 Gel retardation

2.7.1.1 Principle of gel electrophoresis

Gel electrophoresis is a most commonly used method for separating nucleic acid. DNA and RNA have regularly repeating phosphodiester linkages that carry negative charges near neutral pH. These macromolecules migrate to the anode of the electrophoresis chamber under an applied constant voltage. Nucleic acid molecules are size separated by the aid of an electric field where negatively charged molecules migrate toward anode (positive) pole [189]. The migration flow is determined solely by the molecular weight where small weight molecules migrate faster than larger ones. In addition to size separation, nucleic acid fractionation using agarose gel electrophoresis can be an initial step for further purification of a band of interest. A voltage range of 1 to 10 V per cm gel length (V/cm) is used, depending on the size of the nucleic acid macromolecule. A voltage that is too high results in poor resolution and overheating, while a voltage that is too low results in diffusion of smaller-sized nucleic acids [190]. Extension of the technique includes excising the desired “band” from a stained gel viewed with a UV transilluminator.

2.7.1.2 Agarose

For agarose gel electrophoresis, Agarose is composed of long polymers of mainly uncharged repeating disaccharides. An agarose gel is formed when a solution of agarose polymers is first heated and then allowed to cool. As the agarose cools below around 40◦C, hydrogen bonds form to create the gel matrix. Agarose is the gelling component of agar (agar-agar), an extract from red algae (mainly *Gelidium* and *Gracilaria species*) [190]. The percentage of agarose used depends on the size of fragments to be resolved. Prepare a higher-percentage gel to create smaller pores (~100 nm) to resolve small DNA fragments, and a lower-percentage gel to create larger pores (~300 nm) to resolve larger DNA fragments. In general a 0.8-1% gel may be used for effective separation of DNA fragments of 100-1500 base pairs. The percentage of agarose for separating DNA was illustrated in Table 2.6.

Table 2.6 Percentage of agarose for Separating DNA Fragments

Effective range of resolution of linear DNA fragments (kb)	Percentage of agarose
30 to 1	0.5
12 to 0.8	0.7
10 to 0.5	1
7 to 0.4	1.2
3 to 0.2	1.5

Source: Voytas, D., Agarose Gel Electrophoresis, in **Current Protocols in Molecular Biology**. 2001, John Wiley & Sons, Inc.

2.7.1.3 Running buffer

The running buffer is also an importance component in gel electrophoresis. For DNA gels, one may use Tris-acetate-EDTA (TAE) or Tris-borate-EDTA (TBE) running buffer. TAE is commonly used since it is easy to make and store since TBE may form precipitates upon storage. However, TBE has a superior buffering capacity, as the p*K*a of Tris (8.08) is closer to that of boric acid (9.24) than it is to the p*K*a of acetic acid (4.76). TBE is not necessarily always best for

large DNA fragments. Smaller DNA fragments (<1 kb) may be better resolved in TBE gels, since TBE interacts with agarose more tightly, effectively forming smaller pores [191]. TAE should be used if the DNA is to be purified from the gel, since the interaction between TBE and agarose can reduce the amount of DNA recovered [192].

2.7.1.4 Staining and visualization

Ethidium bromide is the common dye for nucleic acid visualization. EtBr binds DNA with no apparent sequence preference once every 4–5 base pairs [193]. Although the with a lower efficiency compare to the double- stranded DNA, EtBr is also used to stain single- stranded DNA or RNA. Under UV illumination, the maximum excitation and fluorescence emission of EtBr can be obtained from 500-590 nm. Exposing DNA to UV fluorescence should be performed rapidly because nucleic acids degrade by long exposures and thus, the sharpness of the bands would be negatively affected.

An alternative dsDNA stain is SYBR Green I. Despite the fact that SYBR Green is more expensive, it is 25 times more sensitive than ethidium bromide [194]. SYBR Safe, a variant of SYBR Green, has been shown to have low levels of mutagenicity and toxicity compared with ethidium bromide while providing similar sensitivity levels EtBr. Nevertheless, similar to the SYBR Green, SYBR Safe is also more expensive when compared to EtBr.

2.7.1.5 Application

The agarose gel electrophoresis is widely employed to estimate the size of DNA fragments after digesting with restriction enzymes, e.g. in restriction mapping of cloned DNA. It has also been a routine tool in molecular genetics diagnosis or genetic fingerprinting via analyses of PCR products. Separation of restricted genomic DNA prior to Southern blot and separation of RNA prior to Northern blot are also dependent on agarose gel electrophoresis [189].

Agarose gel electrophoresis is commonly used to resolve circular DNA with different supercoiling topology, and to resolve fragments that differ due to DNA

synthesis. DNA damage due to increased cross-linking proportionally reduces electrophoretic DNA migration. In addition to providing an excellent medium for fragment size analyses, agarose gels allow purification of DNA fragments. Since purification of DNA fragments size separated in an agarose gel is necessary for a number molecular techniques such as cloning, it is vital to be able to purify fragments of interest from the gel [195].

Gel electrophoresis was also applied for determination of complex formation in gene delivery. Since condensation of DNA into nano-sized particles is a prerequisite for efficient delivery of DNA into cells and determination of complete complex formation generally done before *in vitro* study. The binding strength of the cationic polymers to nucleic acid was determined by gel retardation assay at various weight ratios. Form this aspect, the binding ability of cationic polymer to nucleic acid and complete formation was indicated by the ratio at which full retardation was achieved [196].

2.7.2 Dye exclusion assay

In general, the measurement of nucleic acid concentration is a critical step in molecular biology studies. Spectrophotometry is the principal method for evaluating quantity and quality of nucleic acids. In aqueous solution, DNA has maximal absorbance near 260 nm with an extinction coefficient of 50; protein absorbs light strongly near 280 nm. The *A*260/*A*280 ratio provides an estimate of DNA purity; values of 1.7–2.0 predict ‘clean DNA’. In addition, quantitative analysis of low concentrations of double stranded DNA (dsDNA) is now feasible using fluorometry with newer fluorophores (fluorescent stains). Fluorometric measurement of DNA concentration has gained popularity because it is simple and potentially much more sensitive than absorbance measurements [197]. Ethidium bromide preferentially binds to dsDNA by intercalation. However, because of high mutagenicity of EtBr, the newer fluorescent dyes have been develop for this purpose such as SYBR green and Picogreen. Both PicoGreen and SYBR Green I appear to exhibit high affinity for DNA and a large fluorescence enhancement upon DNA binding with similar excitation/emission maxima [198].

Upon the principle of intercalating dye which fluorescence will increase by intercalation into double-stranded regions of nucleic acids, it can be apply for detection of binding ability between nucleic acid and cationic polymer. For this aspect, inhibition of fluorescent dye/nucleic acid fluorescence resulting from DNA condensation by cationic polymers is a convenient method to monitor the polyelectrolyte interaction [199]. By forming complex between nucleic acid and cationic polymer, the studies show that loss of fluorescence coincides with expulsion of EtBr from the DNA, rather than quenching [188]. The common intercalating dyes used for determination of complex formation were following;

2.7.2.1 Ethidium bromide

Ethidium bromide is a phenanthridinium intercalator, structurally similar to propidium iodide. It binds strongly to both DNA and RNA at sites which appear to be saturated when EtBr molecule is bound for every 4 or 5 nucleotides [193]. However, ethidium bromide has significant intrinsic fluorescence, the dye displays a 20–25-fold increase in fluorescence upon intercalation into double-stranded regions of nucleic acids [200].The concentration of dsDNA which was able be linear over a range extending from 250 ng/ml to 20 μg/ml. However, EtBr has been no longer used and the new safer intercalating dyes have been developed. EtBr showed to inhibit replication in several organisms by interfering with both DNA and RNA synthesis and causes frameshift mutations in bacteria. These effects are presumably due to the presence on the genomic DNA of covalently bound metabolic or photoactivated products of the parent dye molecule that may intercalate, causing errors during replication [201].

2.7.2.2 PicoGreen

PicoGreen is a fluorochrome that selectively binds dsDNA and has characteristics similar to that of SYBR-Green I. It has an excitation maximum at 480 nm (lesser peaks in the short-wave UV range) and an emission peak at 520 nm. When bound to dsDNA, fluorescence enhancement of PicoGreen is exceptionally high; little background occurs since the unbound dye has virtually no fluorescence. PicoGreen is very stable to photobleaching, allowing longer exposure times and assay flexibility.

PicoGreen assays have a threshold of <1.0 ng dsDNA per sample, regardless of the detection equipment, or molecular complexity of the sample; ~250 ng per sample of genomic DNA and ~1.0 ng small PCR product are the practical limits of the assay [198].

2.7.2.3 SYBR green I

SYBR Green I, unsymmetrical cyanine dye is a sensitive dsDNA stain, making it useful for many applications where there is a low concentration of DNA. The capability of SYBR Green I to selectively assay dsDNA in the presence of contaminants (RNA, ssDNA, nucleotides, and protein) is advantageous. Also, the presence of SYBR Green I bound to DNA does not inhibit the activity of some restriction endonucleases, including *Hind*III and *Eco*RI [202]. Unlike EtBr, SYBR Green has minimal intrinsic fluorescence and exhibits a 800- to 1000-fold fluorescence enhancement and high quantum yield (~0.8) upon binding to dsDNA. The affinity of SYBR Green I stain for dsDNA is approximately 100-fold higher affinity than that of ethidium bromide. The later study showed that the 96-well microplate fluorescence assay accurately quantified different types of DNA over a broad linear dynamic range of concentrations (0.25–2,500 pg/μL), and was not affected by a variety of contaminants in the assay mixture [203]. Comparing four different fluorophores for DNA quantification, it was concluded that SYBR Green I and PicoGreen were substantially more sensitive than Hoechst 33258 or ethidium bromide, and that SYBR Green I and PicoGreen exhibited almost identical detectabilities, with SYBR Green I being approximately 30-times less expensive than PicoGreen at the effective working concentration [197].

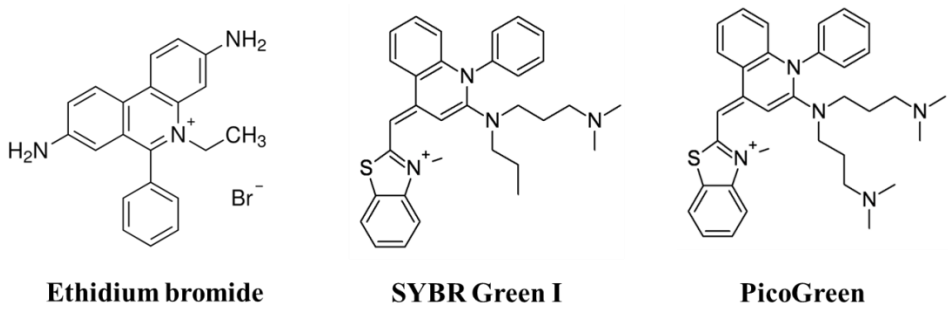

Figure 2.7 Structure of EtBr, SYBR Green I and PicoGreen

2.7.3 Zeta potential analysis

According to the positive charge characteristic of cationic polymers, they are able to mark the negative charge of nucleic acid and condense into nanoparticle. The surface charge of cationic polymers/nucleic acid complex was usually measured. The common practice is to determine the electric potential of a particle at a location away from the particle surface, somewhere in the diffuse layer. This location, related to particle movement in liquid, is called the slipping or shear plane. The potential measured at this plane is called zeta potential which is a very important parameter for colloids or nanoparticles in suspension (Figure 2.8). Its value is closely related to suspension stability and particle surface morphology [204].

There are three existing methods for zeta potential determination of suspended particles, electrophoretic light scattering (ELS), acoustic and electroacoustic. Due to its sensitivity, accuracy, and versatility, ELS is by far the best choice for many applications [205].

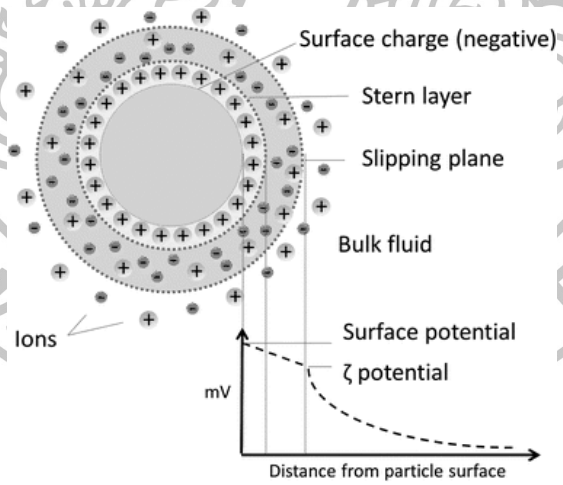

Figure 2.8 Zeta potential of particle

Source: Liese, A. and L. Hilterhaus. (2013). "Evaluation of immobilized enzymes for industrial applications." **Chemical Society Reviews** 42, 15: 6236-6249.

2.8 Dichlorofluorescein as an adsorption indicator and its applications

The property of fluorescein dye was employed for the first time in 1923 by Fajan [14] in marking the end-point in argentometric titrations of halide ion. The fluorescein is not sensitive to dissolved silver or halide ions, but changes its color at the equivalence point where colored compounds are formed on the precipitate due to adsorption phenomena.

In Fajan's precipitation titration, chloride ions are titrated with silver nitrate and the silver chloride precipitant form. At slightly over equivalent point, the silver chloride adsorbs silver ions on it. The "silver body" then adsorbs fluorescein ions from the solution and dark red silver fluoresceinate is formed on the surface of the precipitate. The majority of dyes used as adsorption indicators are acidic dyes and they are applicable generally in the titration of anions against cations. Fluorescein possesses a weak acidic character; in weak acid solution the concentration of fluorescein ions is so small that the color change no longer takes place [206]. So the fluorescein derivatives were then developed. The introduction of halogen atoms into the fluorescein molecule has two effects: the dissociation constant is increased and the adsorbability of the dye anions by the silver halide increases. It would therefore be expected that substances with a stronger acid character than fluorescein could be used as indicators in weak acid solutions. On the other hand, the stronger adsorbability might either interfere or be favorable. During the titration of chloride ions with silver nitrate the silver chloride formed at the beginning of the titration adsorbs chloride ions. In the presence of the anions of the indicator, the latter also have a tendency to be adsorbed and if their adsorption is larger than that of the chloride ions, the color change will take place during the early stages of the titration. Such is the case when eosin is used. Therefore this indicator cannot be used in the argentometric determination of chlorides, even though it gives highly accurate results when bromides, iodides and thiocyanates are titrated even in weak acid solutions. On the other hand, stronger adsorbability may exert a favorable influence in that it might make possible the titration of very dilute chloride solutions. In this case, the absorption of fluorescein ions is too small and no color change is observed [207].

Fluorescein dyes are widely used owing to their unique spectral properties. However, 2,7-dichlorofluorescein was numerously utilized in photophysical studies such as an adsorption indicator, a reactant in free radical chemistry [208], and a probe for examination of micellar media [209].

Particularly, 2,7-dichlorofluorescein possesses properties which are very promising from some viewpoints. For instance, the pKa values are lower than those of fluorescein, and this ensures the existence of the dye in form of the intensively fluorescing dianion in media of such kinds in which fluorescein is not yet completely dissociated. This is of special significance for the application of these dyes as tracers in water systems and in other unbuffered systems, as well as in biological systems within the 'physiological' pH region, etc. In addition, 2,7-dichlorofluorescein is more photostable as compared with the unsubstituted luminophore.

The most typical species of 2,7-dichlorofluorescein are presented in Figure 2.9. The negative 'phenolate' charge of the dianion R^{2-} is delocalized within the xanthene moiety. The neutral form H_2R exists in solutions as an equilibrium mixture of two tautomers, quinonoid and lactonic, the latter being colorless due to sp3-hybridization of the central carbon atom C-9. Contrary to fluorescein, the zwitterionic structure is less typical for 2,7-dichlorofluorescein due to an increase in the acidic strength of the hydroxy groups resulting from ortho-chloro substitution. This highly polar zwitterionic tautomer of dichloro-substituted fluorescein exists only in extremely small amounts even in water, evidently due to the marked strengthening of acidity of the OH groups by the orthochlorine substituents. Therefore, this structure is not included in Figure 2.9. Less clear and much poorer studied is the structure of monoanion HR^-, which can exist as 'carboxylate' and 'phenolate' tautomer. In the case of fluorescein, the 'carboxylate' tautomer predominates in all solvent systems studied, while in the case of eosin, erythrosin, Rose Bengal B, and other 2,4,5,7-tetrahalogen derivatives the monoanion HR^- exists as 'phenolate' tautomer. The relative population of the aforesaid HR^- tautomers of 2,7-dichlorofluorescein gradually changes along with alterations in the nature of the solvent, that is, pure and mixed solvents. On transferring from water to organic solvents, the tautomeric equilibrium shifts toward the right [210].

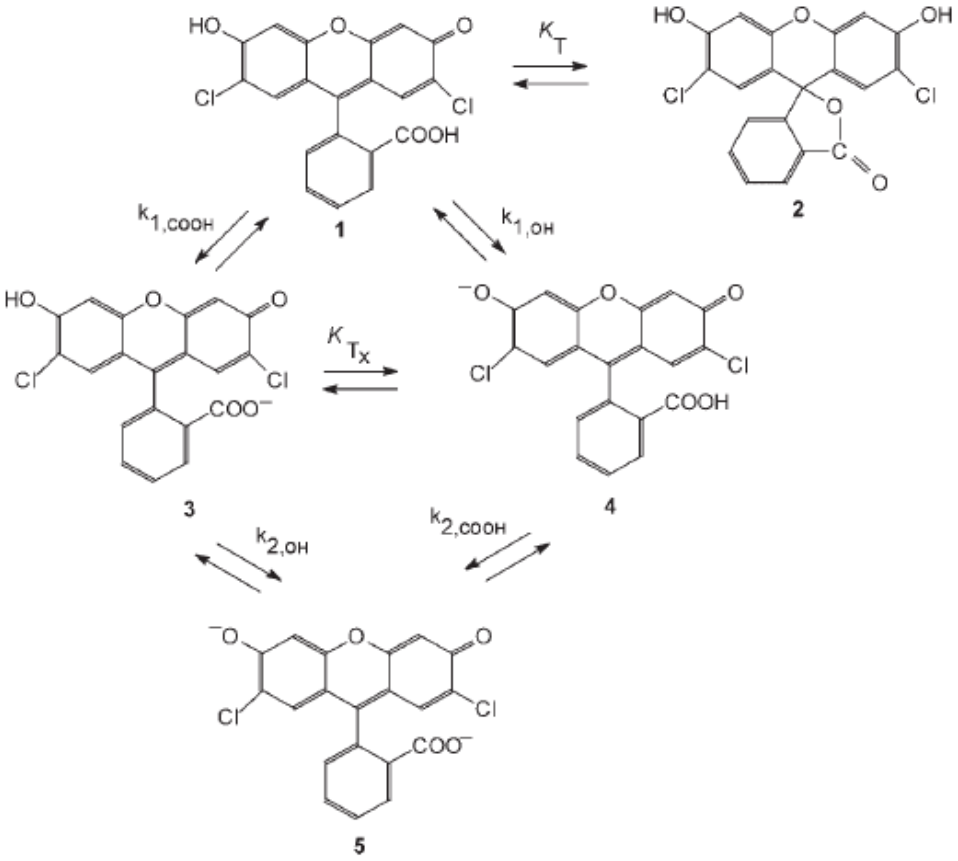

Figure 2.9 Protolytic conversions of 2,7-dichlorofluorescein in solution.

Source: Mchedlov-Petrossyan, N.O., et al. (2006). "A dibasic acid with reversed order of the stepwise ionization constants: 2, 7-dichlorofluorescein in the ternary solvent mixture benzene–ethanol–water." **Journal of physical organic chemistry** 19, 6: 365-375.

CHAPTER 3

MATERIALS AND METHODS

1. Materials
2. Equipment
3. Methods
    - 3.1 pDNA isolation and purification
    - 3.2 Preparation of siRNA-EGFP
    - 3.3 Cell culture and maintenance
        - 3.3.1 Generation of HeLa cell stably expressing green fluorescent protein
        - 3.3.2 Culture media preparation
        - 3.3.3 Subcultivation and maintenance
    - 3.4 Method development for complex formation using adsorption dye
        - 3.4.1 Preparation of polymers/pDNA complexes
        - 3.4.2 Development of dye adsorption protocol
        - 3.4.3 Optimization of dye adsorption method
            - 3.4.3.1 Size of pDNA
            - 3.4.3.2 Limit of pDNA amount
            - 3.4.3.3 Optimal DCF concentration
            - 3.4.3.4 Type of polymers
            - 3.4.3.5 Molecular weight of polymers
        - 3.4.4 Application of dye adsorption method for siRNA complex
        - 3.4.5 Zeta potential analysis
        - 3.4.6 Agarose gel retardation
        - 3.4.7 Transfection efficiency of PEI(25 kDa)/pEGFP in HeLa cell
        - 3.4.8 Gene silencing efficiency of PEI(25 kDa)/siRNA-EGFP

3.5 Chitosan combined with PLA for siRNA delivery

3.5.1 Polymers/siRNA-EGFP complex formation

3.5.2 Agarose gel retardation

3.5.3 Size and zeta potential analysis

3.5.4 *In vitro* gene silencing efficiency

3.5.5 Effect of serum on transfection efficiency

3.5.6 Cytotoxicity of polymers/siRNA complexes

3.5.7 RNase protection ability of CS/PLA

3.5.8 Uptake pathway of CS/PLA/siRNA complex

3.5.8.1 Optimization of inhibitor concentration

3.5.8.2Cellular uptake pathway

3.6 Statistical analysis

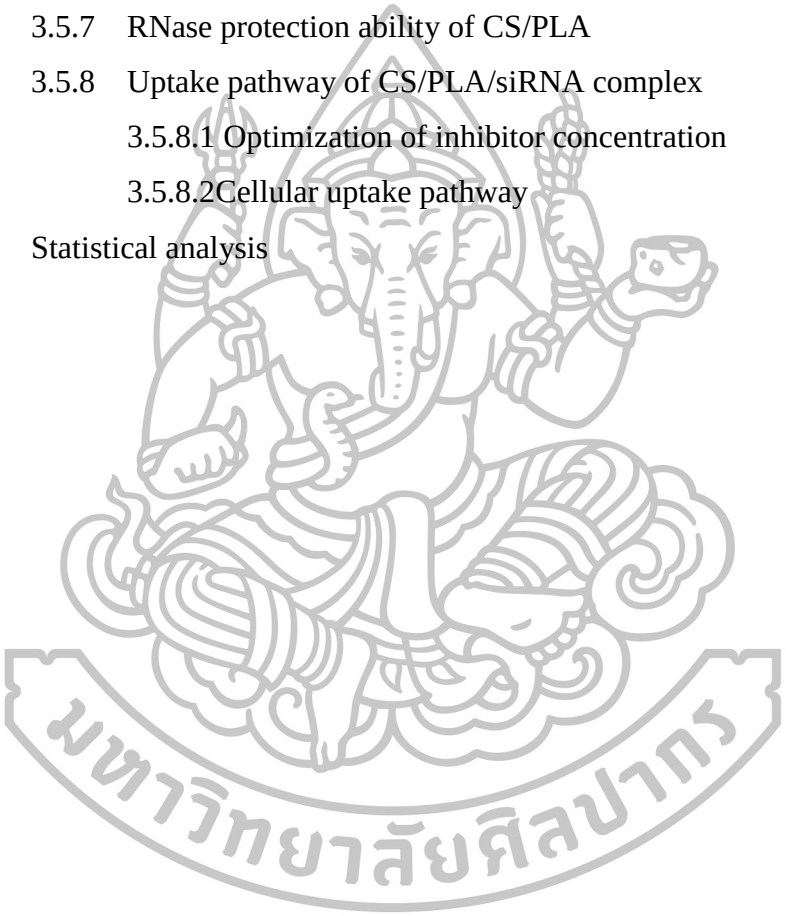

1. Materials

2′,7′-Dichlorofluorescein (Sigma-Aldrich ®, St Louis, MO, USA)

Ambion's Silencer™ siRNA Construction Kit (Ambion, USA)

Chitosan (45 kDa, 85% degree of deacetylation) (Seafresh Chitosan Lab., Thailand)

Chitosan (low molecular weight) (Sigma-Aldrich ®, St Louis, MO, USA)

Chlopromazine (Sigma-Aldrich ®, St Louis, MO, USA)

Dimethylsulfoxide (DMSO) (Fisher Scientific; analytical reagent grade)

DNA purification kit, QIAGEN® Plasmid Midi Kit (Qiagen, Santa Clarita, CA USA)

Ethidium bromide (Sigma-Aldrich ®, St Louis, MO, USA)

Fetal bovine serum (GIBCO™ , Grand Island, NY, USA)

Filipin complex, from Streptomyces filipinensis (Sigma-Aldrich ®, St Louis, MO, USA)

Gene Pure LE Agarose 500g (ISC BioExpress®, USA)

Geneticin® (GIBCO™ , Grand Island, NY, USA)

Genistein (Sigma-Aldrich ®, St Louis, MO, USA)

GlutaMAX™ supplement (GIBCO™ , Grand Island, NY, USA)

Kanamycin (GIBCO™ , Grand Island, NY, USA)

Lambda DNA / Hind III Markers (Promega, Madison, MI, USA)

MEM non-essential amino acids (GIBCO™ , Grand Island, NY, USA)

Methyl-β-cyclodextrin (Sigma-Aldrich ®, St Louis, MO, USA)

Minimum Essential Media (MEM) (GIBCO™ , Grand Island, NY, USA)

Nocodazole (Sigma-Aldrich ®, St Louis, MO, USA)

pEGFP-C2 (4.7 kbp) is amplified in *Escherichia coli*

Penicillin-Streptomycin (GIBCO™ , Grand Island, NY, USA)

Polyethylenimine (PEI) 0.8 kDa (Wako Pure Chemical Industries, Ltd., Osaka, Japan)

Polyethylenimine (PEI) 1.6 kDa (Wako Pure Chemical Industries, Ltd., Osaka, Japan)

Polyethylenimine (PEI) 10 kDa (Wako Pure Chemical Industries, Ltd., Osaka, Japan)

Polyethylenimine (PEI) 25 kDa (Sigma-Aldrich Chemie. GmbH, Germany)

Poly-L-arginine (Sigma-Aldrich ®, St Louis, MO, USA)

pSV-β-galactosidase (6.8 kbp) is amplified in *Escherichia coli*

RNase A (Sigma-Aldrich ®, St Louis, MO, USA)

Sodium bicarbonate (Analar® BDH ;VWR International Ltd.)

Sodium chloride (UNIVAR®Ajax Finechem; analytical reagent grade)

Sodium dodecyl sulfate (Sigma-Aldrich ®, St Louis, MO, USA)

Thiazolyl Blue Tetrazolium Bromide (MTT) (Sigma-Aldrich ®, St Louis, MO, USA)

Trypsin-EDTA (0.25%), no phenol red (GIBCO™, Grand Island, NY, USA)

Wortmannin (Sigma-Aldrich ®, St Louis, MO, USA)

2. Equipment

Analytical balances (Satorious CP224S, Scientific promotion Co., Ltd.)

Autoclave (Model: LS-2D; Scientific promotion CO., Ltd.)

Beakers (50, 100, 250, 500, 1000 ml)

Black clear-bottom, 96 well plate (Corning ®; Corning Incorporated)

Cell culture flask, 25 cm^3, 75 cm^3 (Corning ®; Corning Incorporated)

Centrifuge (Sorvall® Biofuge Stratos)

Conical centrifuge tube (15, 50 ml) (Corning ®; Corning Incorporated)

Electronic pipette controller (Powerpette Plus; Bio-Active Co., Ltd.)

Filter membrane, 0.22 micron (Sartorius AG. 37070 Goettingen, Germany)

Flat clear-bottom, 24 well plate (Corning ®; Corning Incorporated)

Flat clear-bottom, 48 well plate (Corning ®; Corning Incorporated)

Flat clear-bottom, 96 well plate (Corning ®; Corning Incorporated)

Fluorescence microscope (Model: GFP-B, wavelengths: excitation filter 480/40 and emission filter 535/50)

Gel electrophoresis apparatus (MyRUN intelligent electrophoresis unit, Cosmobio CO., Ltd., Japan)

GelDoc system (Multi Genus Bio- imaging system, Syngene™)

GeneRay UV-Photometer (Biometra® λ260/280 nm)

Hot air oven

Humid CO2 Incubator (37°C, 95% RH, 5% CO2) (HERA Cell 240 Hereaus)

Laminar air flow (BIO-II-A)

Magnetic stirrer and magnetic bar

Microcentrifuge tube 1.5 ml

Micropipette (0.1-2 µl, 2-20 µl, 20-200 µl, 100-1000 µl)

Micropipette tips (Corning ®; Corning Incorporated)

Microplate reader (Universal Microplate Analyzer, Model AOPUS01 and AI53601, Packard Bio-Science, CT, USA)

Multipoint pipette with 8 channel aspiration manifold 20- 200 µL

pH meter (Horiba compact-B212)

Syringe Filter, 0.22 micron, 17 mm

Thermo-regulated water bath

UV cabinet

UV spectrophotometer (NanoVue™, GE Healthcare, UK)

Vacuum filtration pump and filter set (Sartorius BORO 3.3 Goettingen, Germany)

Vortex mixer

Zetasizer Nano ZS (Malvern Instruments Ltd., Malvern, UK)

3. Methods

3.1 pDNA isolation and purification

In this study, the plasmid encoding green fluorescence protein, pEGFP-C2 (Figure 3.1) and the plasmid encoding β-galactosidase enzyme, pSV-β-gal (Figure 3.2) were amplified in *Escherichia coli*. pDNA was extracted and purified by using the plasmid midi kits (Qiagen® Plasmid Midi kit) according to manufacturer protocol. Briefly, bacterial culture was harvested and centrifuged at 6000 g for 15 min at 4 ˚C. The bacterial pellet was resuspended in 4 ml of P1 buffer (50 mM Tris Cl, pH 8.0; 10 mM EDTA; 100 µg/mL RNase A) and cells were lysed with P2 buffer (200 mM NaOH, 1% w/v SDS, Lyseblue reagent). The solution was then neutralized by P3 buffer (3.0 M potassium acetate, pH 5.5) and centrifuged at 20,000 g for 30 min at 4 ˚C. The supernatant was filtered using QIAGEN-tip and washed with QC buffer (1.0 M NaCl; 50 mM MOPS, pH 7.0; 15% v/v isopropanol). Plasmid was then eluted by QF buffer (1.25 M NaCl; 50 mM Tris.Cl, pH 8.5; 15% v/v isopropanol) and then precipitated by adding isopropanol and centrifuged at 15000 g for 30 minutes at 4 ˚C. The supernatant was removed and the pellets were washed with 70% ethanol followed by the centrifugation at 15000 g for 10 minutes at 4 ˚C. The pellets were dried at room temperature and dissolved in TE buffer, pH 8.0. The concentration of purified pDNA was evaluated by measuring optical density at 260 nm (GeneRay) and calculated by the following equation.

$$\text{Plasmid concentration } (\mu g/mL) = \varepsilon_{260} \times OD_{260} \times DF \qquad \text{(Eq. 1)}$$

Where; ε_{260} is an extinction coefficient of double stand DNA at 260 nm which is equal to 50 µg/mL

OD_{260} is an optical density from the measurement

DF is a dilution factor

The OD_{260}/OD_{280} value of plasmid solution was used to evaluate the purity of plasmid. This value is usually in the range of 1.8 to 2.0.

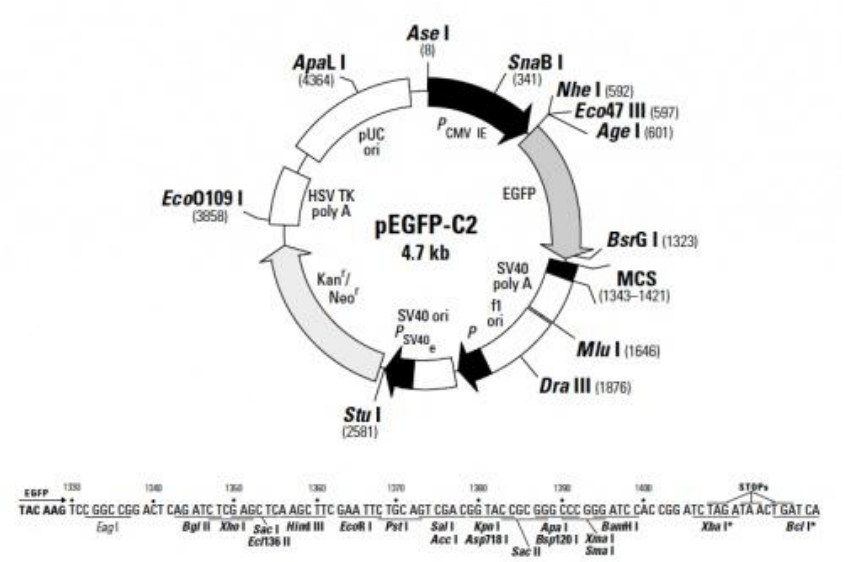

Figure 3.1 Plasmid map of pEGFP-C2

Available from: https://www.addgene.org/vector-database/2488/

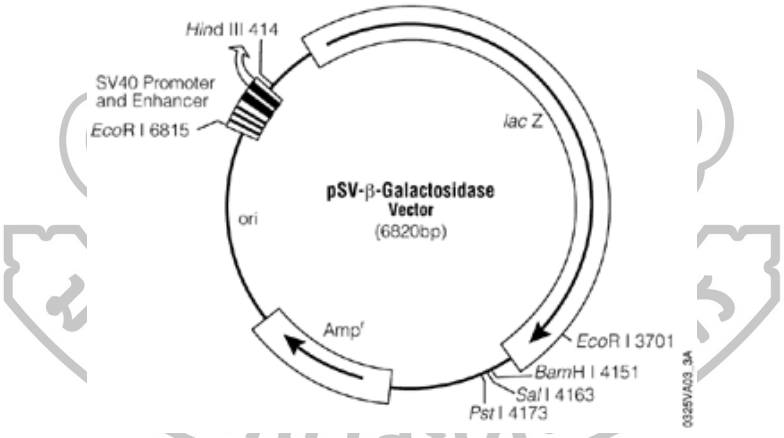

Figure 3.2 Plasmid map of pSV-β-gal

Available from: https://worldwide.promega.com/products/reporter-assays-and-transfection/reporter-vectors-and-cell-lines/psv_beta_galactosidase-control-vector/?activeTab

3.2 Preparation of siRNA-EGFP

The EGFP targeted siRNA, siRNA-EGFP, and the mismatch siRNA were synthesized from Ambion's Silencer™ siRNA Construction Kit. The sequence of

DNA oligonucleotide templates for duplex EGFP targeted siRNA and mismatch siRNA were following:

For EGFP targeted siRNA,

Antisense template oligonucleotide;

5’-AAG CTG ACC CTG AAG TTC ATC CCT GTC TC-3’

Sense template oligonucleotide;

5’-AAG ATG AAC TTC AGG GTC AGC CCT GTC TC-3’

For mismatch siRNA,

Antisense template oligonucleotide;

5’-AAG CAC CGC TTA CGT GAT ACT CCT GTC TC-3’

Sense template oligonucleotide;

5’-AAA GTA TCA CGT AAG CGG TGC CCT GTC TC-3’

After the duplex siRNA was synthesized according to construction protocol, the siRNA-EGFP(+) contained sense 5’-GCU GAC CCU GAA GUU CAU CUU-3’ and antisense 5’-GAU GAA CUU CAG GGU CAG CUU-3’. The mismatch siRNA contained sense 5’-GCA CCG CUU ACG UGA UAC UUU-3’ and antisense 5’-AGU AUC ACG UAA GCG GUG CUU-3’. The siRNA-EGFP targeted to position 124–144 of EGFP open-reading frame. The mismatch siRNA were designed by scrambling the nucleotide sequence of EGFP targeted siRNA and confirmed the sequences that lack of significant homology to human genes by blast analysis. The concentration of siRNA was determined by measuring the optical density at 260 (GeneRay) and kept at -20 ˚C.

3.3 Cell culture and maintenance

Human cervical carcinoma cell line (HeLa cell) and HeLa cell stably expressing green fluorescent protein (HeLa-EGFP cell) were used as the models for pDNA transfection and siRNA transfection, respectively.

3.3.1 Generating of HeLa cell stably expressing green fluorescent protein

HeLa-EGFP cell generating protocol was reported elsewhere [211]. Briefly, HeLa cells were seeded in 24 well plate and incubated at 37 ˚C, 5% CO_2 for 24 hr. The cells were then transfected with pEGFP-C2/Lipofectamine 2000 complexes in serum free media. After 12 hr, the transfection media was removed and cells were washed with Hanks' balanced salt solution (HBSS). The fresh complete media were added and cells were further incubated to 100% cell confluent. Cells were trypsinized and then cultured in cell culture dish with MEM supplemented with 10% FBS containing and 0.5 mg/mL G418, the select and maintain EGFP expression agent. The HeLa-EGFP colony was isolated and cultured in MEM supplemented with 10% FBS under normal maintenance condition. The EGFP gene expression was maintained by treating cells with 0.1 mg/mL G418 every 3-4 weeks.

3.3.2 Culture media preparation

Minimum Essential Media (MEM) was used for culturing both HeLa cell and HeLa-EGFP cell. For preparing 1 L of media, MEM powder was dissolved in 700 mL of sterile water and pH was then adjusted to 7.4 by adding 2.2 g of $NaHCO_3$. The solution was adjusted to 1 L and filtered through 0.22 μm cellulose acetate membrane filter using vacuum pump under sterile condition. The media was then supplemented with 10% v/v FBS (inactivated at 56 ˚C before used), 1% v/v non-essential amino acid and 1% v/v Glutamax™ (Gibco).

HeLa cell and HeLa-EGFP cell were cultured in complete MEM at 37 ˚C under a humidified atmosphere (5% CO_2, 95% RH). Cells were subcultured for 1-2 times per week at 80-90% confluence by following procedure;

a The media were discarded and cells were washed with PBS.

b Trypsin/EDTA (0.25%) solution was added and incubated at 37 ˚C for 5 min or until cells detached from flask.

c The complete media were added to dilute and inactivate trypsin.

d The cell suspension was centrifuged at 1,000 rpm for 2 min and supernatant was then removed.

e The cell pellet was resuspended in fresh complete media. The subcultivation ratio was 1:5.

3.4 Method development for polyplex formation using adsorption dye

3.4.1 Preparation of polymers/pDNA complexes

Polyethylenimine (PEI) and chitosan (CS) hydrochloride were used as the model of synthetic and natural cationic polymer, respectively. The polymers/pDNA complexes were prepared by adding the polymer solution (stock solution 1 mg/mL) to the plasmid solution (stock solution 1 mg/mL) in 1.5 mL microcentrifuge tubes at different weight ratios. The final volume of mixture was kept at 30 µL. The mixtures were gently mixed by pipetting and further incubated at room temperature for 30 min, sufficiently for the complex self-assembly.

3.4.2 Development of dye adsorption protocol

The protocol was first developed using pEGFP-C2 and PEI (25 kDa). The PEI (25 kDa)/pEGFP complex was prepared from pEGFP at 5 µg with PEI (25 kDa) at different weight ratios of 0, 0.01, 0.1, 0.25, 0.5, 0.75, 1 and 2. After the complexes were formed, 5 µL of DCF solution (0.15 mg/mL in 1X TAE buffer, pH 8.3) was added and gentle mixed. The mixture was centrifuged at 20,000 rpm for 10 min at 4 ˚C to precipitate the complexes. The supernatant was removed and measured the absorbance value of free DCF anion in supernatant at 504 nm by a cuvetteless drop-based NanoVue Plas. The PEI (25 kDa)/pEGFP pellet was washed with 30 µL of sterile water and centrifuged at 20,000 rpm for 5 min. The adsorbed DCF on complexes was then released by adding 30 µL of 0.01 N NaOH. The fluorescence of the solution was observed under UV light at 366 nm.

3.4.3 Optimization of dye adsorption method

3.4.3.1 Size of pDNA

Two different plasmid DNAs were used as models in this study, pEGFP-C2 (4.7 kbps) and pSV-β-gal (6.8 kbps). The protocol for determining the complete complex formation was the same as mentioned above.

3.4.3.2 Limit of pDNA amount

pEGFP was used for determining the lowest amount of pDNA which the dye adsorption method was able to detect. The amount of pDNA was varied at the amount of 5, 2.5, 1, 0.5 and 0.25 µg. The PEI (25 kDa)/pEGFP complex was prepared at the same weight ratios as mentioned above.

3.4.3.3 Optimum of DCF concentration

To determine the optimal DCF concentration, PEI(25 kDa)/pEGFP complexes were prepared using the lowest pDNA amount which this method could detect. DCF solutions were prepared at different concentrations i.e. 0.15, 0.1, 0.075 and 0.05 mg/ml in 1X TAE buffer (pH 8.3). The same volume of DCF solutions (5 µL) was added to the PEI (25 kDa)/pEGFP complex solutions and examined the lowest concentration of DCF solution by observing pink pellet and the fluorescence of solution after adding NaOH solution.

3.4.3.4 Type of polymers

Beside PEI (synthetic polymer), CS (low molecular weight) was used as representative of natural polymer. CS solution (1 mg/mL) was prepared by dissolving CS powder in 0.01 mM HCl and stirred until CS completely dissolved. The CS/pEGFP complexes were prepared by same protocol as mention above at various weight ratios of 0, 0.1, 0.5, 1, 5, 10, 15 and 20.

3.4.3.5 Molecular weight of polymers

The various molecular weights of PEI, 0.8, 1.6, 10 and 25 kDa were investigated for the effect of size of polymers. The PEI/pEGFP complexes were prepared using the lowest pDNA amount which was able to detect.

3.4.4 Application of dye adsorption method for siRNA complex

The PEI (25 kDa)/siRNA-EGFP complex was prepared at the same weight ratios as those for PEI/pDNA complex and determined the complete complex formation by the same protocol. The amounts of siRNA were 1 µg.

3.4.5 Zeta potential analysis

The surface charge of complexes was determined using Zetasizer Nano ZS (Malvern Instrument Ltd, Malvern, UK). The polymers/pDNA or PEI (25 kDa)/siRNA-EGFP complexes were prepared at the same weight ratios as previous method. The complex solutions were diluted with distilled water to 1 mL before measuring zeta potential. The measurement was performed in triplicate in each sample at 25 ˚C.

3.4.6 Agarose gel retardation

The polymers/pDNA and PEI (25 kDa)/siRNA-EGFP complexes were prepared using 0.25 µg pDNA and 0.112 µg siRNA-EGFP at the same weight ratios as previous experiment. For polymers/pDNA complexes, agarose gel electrophoresis was performed using 0.8% agarose in 1X TAE buffer. The complex solutions were mixed with 50% glycerol before loaded into gel. The electrophoresis was carried out in 1X TAE buffer for 45 min at 100 V. For PEI (25 kDa)/siRNA-EGFP complexes, agarose gel was prepared in 1X TBE buffer (1% agarose gel) and the electrophoresis system was 120 V, 20 min in 1X TBE buffer. The pDNA or siRNA on agarose gel was then stained with ethidium bromide and de-stained in sterile water. The pDNA and siRNA bands were then observed and photographed by a UV transilluminator using a GelDoc system.

3.4.7 Transfection efficiency of PEI (25 kDa)/pEGFP in HeLa cell

PEI (25 kDa)/pEGFP complex group was selected as the representative to compare the complete complex formation ratio from the previous studies with the ratio that exhibited the highest transfection efficiency. HeLa cells were seeded in 48 well plates in the density of 10,000 cells/well and incubated at normal maintenance condition for 24 hr before transfection. The PEI (25 kDa)/pEGFP complexes were prepared in serum-free media at the same weight ratio as the previous studies by using pEGFP amount of 0.5 µg in each well. Cells were transfected with complexes and then incubated in normal condition for 24 hr. The transfection efficiency was determined by the expression of green fluorescence protein under fluorescence microscope and calculated the transfected cells/cm^2 by following equation;

$$\text{Transfected cells } (\text{cells}/\text{cm}^2) = \frac{\text{Transfected cells (cells/well)}}{\text{Approximate growth area of well plate } (\text{cm}^2)} \quad \text{(Eq. 2)}$$

Where; Approximate growth area of 48 well plate = 0.95 cm^2

3.4.8 Gene silencing efficiency of PEI (25 kDa)/siRNA-EGFP

The efficiency of gene silencing was performed in HeLa-EGFP cells. Cells were seeded in 96 black flat-bottom well plate at the density of 9,000 cells/well and incubated at normal condition before transfection for 24 hr. The PEI(25 kDa)/siRNA-EGFP complexes were prepared at the same weight ratios as previous studies in serum-free media. The complexes were added to each well at the final siRNA-EGFP amount of 15 pmol/well. The plates were incubated in normal condition for 6 hr. The transfection media was removed and cells were washed with PBS. The fresh complete media was added and plates were further incubated for 4 days. The media was changed every day and the fluorescence intensity was measured daily. The percent of seeding variation, adjusted fluorescence intensity and percent of gene silencing were calculated according to Eq. 3, Eq.4 and Eq. 5, respectively.

$$\%\ \text{seeding variation} = \frac{(I_{\text{avg, day 0}} - I_{\text{n, day 0}}) \times 100}{I_{\text{avg, day 0}}} \quad \text{(Eq. 3)}$$

Adjusted fluorescence intensity

$$= I_{n,\ day\ 1\text{-}4} + \{\frac{(I_{n,\ day\ 1\text{-}4}) \times (\%\ seeding\ variation)}{100}\} \quad \text{(Eq. 4)}$$

$$\%\ EGFP\ gene\ silencing = \frac{(I_{ad,\ mismatch} - I_{ad,\ EGFP})}{I_{ad,\ mismatch}} \times 100 \quad \text{(Eq. 5)}$$

Where;

$I_{avg,\ day0}$ = the average fluorescence intensity of all wells prior to transfection (day 0)

$I_{n,\ day0}$ = the fluorescence intensity of individual well at day 0

$I_{n,\ d1-4}$ = the fluorescence intensity at days one to four of each well

I_{ad} = adjusted fluorescence intensity

$I_{ad,\ EGFP}$ = adjusted fluorescence intensity of each well with polymers/siRNA-EGFP complexes

$I_{ad,\ mismatch}$ = the average value of adjusted fluorescence intensity of all wells with polymers/mismatch siRNA complexes

3.5 Chitosan combined with poly-L-arginine for siRNA delivery

3.5.1 Polymers/siRNA-EGFP complex formation

The cationic polymers used in this study were chitosan, CS (45 kDa) and poly-L-arginine, PLA (> 70 kDa). The CS solution was prepared by dissolving CS powder in distilled water pH 4 which were adjusted pH by adding hydrochloric acid and continually stirred until clear solution was obtained. To form the CS/siRNA complexes, the CS solution (stock solution of 1 mg/mL) was added to siRNA solution at different weight ratios. The PLA/siRNA complexes were formed in a similar procedure at different weight ratios. For CS/PLA/siRNA complexes, the PLA solution was added to siRNA solution at the PLA/siRNA weight ratios of 0.01, 0.05, 0.1, 0.5,

1 and 5. After standing for 5 min, CS was added to the previous solution at the fixed CS weight ratio which gave the highest gene silencing efficiency. The final mixtures were gently mixed by pipetting and the complexes were allowed to completely form at room temperature for 30 min.

3.5.2 Agarose gel retardation

The binding ability of polymers was confirmed by gel retardation assay. The polymers/mismatch siRNA complexes were prepared at different weight ratios which contained 10 pmol of siRNA. After incubating the complexes in room temperature for 30 min, 2 µl of 50% glycerol was added and the solutions were loaded in the wells on 1% agarose gel. The electrophoresis was carried out for 20 min at 100 V in 1XTBE buffer, pH 8.3. Agarose gel was stained with ethidium bromide for 5 min and then de-stained in sterile water for 15 min. The siRNA bands were visualized under a UV transilluminator using a GelDoc system.

3.5.3 Size and zeta potential analysis

The size and zeta potential of CS/siRNA, PLA/siRNA and CS/PLA/siRNA complexes were measured using the Zetasizer Nano ZS (Malvern Instruments Ltd., Malvern, UK) at 25 ˚C. The CS/siRNA, PLA/siRNA and CS/PLA complexes were prepared according to the same procedure as previously described and the solutions were diluted with sterile water to 1 mL before measuring the zeta potential and size. All samples were measured in triplicate.

3.5.4 *In vitro* gene silencing efficiency

The efficacy of CS, PLA and CS/PLA to deliver siRNA into cells and targeted to mRNA was determined by investigating EGFP expression in HeLa-EGFP cells. The HeLa-EGFP cells were trypsinized and seeded at the density of 9,000 cells/well in 96 wells black clear-bottom plates for 24 hr before transfection. The fluorescence intensity of each well was measured before transfection in order to calculate the seeding variation. CS, PLA and CS/PLA were complexed with 15 pmol of siRNA-EGFP or mismatch siRNA at different weight ratios in serum-free MEM containing 100 U/mL penicillin G and 100 µg/ml streptomysin. The transfection

studies were performed in both physiological pH (7.4) and pH 6.4. After the complexes was added, plates were incubated at normal maintenance condition for 6 hr. The transfection media were removed and cells were washed with PBS. The fresh complete media (containing 100 U/ml penicillin G and 100 µg/ml streptomysin) were added and plates were further incubated for 4 days. The culture media were changed every day and the fluorescence intensity was measured daily. The EGFP gene silencing efficiency was determined by measuring the fluorescence intensity of each well using a fluorescence microplate reader (Universal Microplate Analyzer, Model AOPUS01 and AI53601, Packard Bio-Science, CT, USA) with excitation/emission at 485/530 nm. PEI (25 kDa)/siRNA complex at weight ratio of 2 was used as a positive control in this study.

The percentage of seeding variation, adjusted fluorescence intensity and percent EGFP gene silencing were calculated by Eq. 3, 4 and 5, respectively as mentioned above.

3.5.5 Effect of serum on transfection efficiency

The interfering effect of serum on the transfection efficiency of CS/PLA/siRNA complexes was investigated using the same protocol as *in vitro* gene silencing study, except the transfection media were serum-containing MEM (10% FBS).

3.5.6 Cytotoxicity of polymers/siRNA complexes

Cytotoxicity of polymers/ siRNA complexes was investigated by MTT assay. EGFP-HeLa cells were seeded at a density of 9,000 cells per well in 96-well plates and incubated for 24 h prior to transfection. Polymers/mismatch siRNA complexes were prepared in serum-free medium at the same weight ratios as *in vitro* transfection experiment. After 6 h of transfection, the media were removed and cells were washed with PBS and continually incubated in the complete media for 24 h. MTT solution (5 mg/mL in PBS) was added to give the final concentration of 1 mg/mL in each well and incubated in normal condition for 4 hr. The media were then removed and formazan crystals in the living cells were dissolved in 100µl DMSO.

The optical density was measured at 550 nm using a microplate reader (Universal Microplate Analyzer, Model AOPUS01 and AI53601, Packard BioScience, CT, USA). Relative viability (%) was calculated by Eq. 6.

$$\text{Relative viability (\%)} = \frac{OD_{\text{treated cells}}}{OD_{\text{non-treated cells}}} \times 100 \quad \text{(Eq. 6)}$$

Where;

$OD_{\text{treated cells}}$ = Optical density of formazan solution from cells were treated with complexes

$OD_{\text{non-treated cells}}$ = Optical density of formazan solution from non-treated cells.

3.5.7 RNase protection ability of CS/PLA

The CS/PLA/siRNA-mismatch complex was prepared at weight ratio of 5/0.5/1containing siRNA 0.21 µg. The complex was then incubated with RNase A (5 mIU/µg of siRNA) at 37 ˚C for 0.5, 1, 2, 4 and 6 hr. At the designated time points, the mixture was heated at 70 ˚C to inactivate RNase A activity for 30 min. siRNA was displaced from complex by adding 3 µL of 16 mM sodium dodecyl sulfate (SDS) and incubated at room temperature for 10 min. The released siRNA was analyzed by agarose gel electrophoresis carried out at 120 V, 20 min in 1X TBE buffer. The naked siRNA-mismatch was used as a control under the same condition.

3.5.8 Investigation of uptake pathway of CS/PLA/siRNA polyplexes

In this study, the uptake pathways of CS/PLA/siRNA complexes were investigated by using the inhibitors that involved in endocytosis pathway i.e.

a Chlorpromazine as an inhibitor for clathrin-mediated endocytosis (CME)

b Genistein, filipin and methyl-β-cyclodextrin as the inhibitors for caveolae-mediated endocytosis

c Nocodazole as an inhibitor for Polymerization of microtubules

d Wortmannin as an inhibitor for macropinocytosis

e Ammonium chloride as an inhibitor for endosomes and lysosomes acidification

3.5.8.1 Optimization of inhibitor concentration

The optimum inhibitor concentrations were investigated in terms of cell viability by MTT assay. HeLa-EGFP cells were seeded at a density of 9,000 cells per well in 96-well plate and incubated for 24 hr. The inhibitor solutions were prepared at different concentrations from 1 nM to 10 mM (depended on each inhibitor) in with serum-free medium. Cells were incubated with inhibitors for 6 hr at 37 ˚C under normal maintenance condition. Then the cells were washed with PBS and continually incubated in the complete media for 24 hr. Twenty five microlites of MTT solution (5 mg/mL) were added to each well and plates were continuously incubated for 4 hr. The media were then removed and formazan crystals in the living cells were dissolved in 100 μL of DMSO. The optical density was measured at 550 nm using microplate reader and relative viability (%) was calculated by Eq. 6 taken the viability of non-treated cells as 100%. The highest concentration of inhibitors which did not affect on cell viability (100% cell viability) was selected for cellular uptake study.

3.5.8.2 Cellular uptake pathway

To study the uptake pathway of polymers/siRNA-EGFP complexes, HeLa-EGFP cells were seeded at a density of 9,000 cells per well in black clear-bottom 96-well plates and incubated for 24 hr. At the day of transfection, cells were pre-incubated with 100 μL of inhibitor solutions in serum-free media for 30 min. Cells were then transfected with CS/PLA/siRNA-EGFP complex at weight ratio of 5/0.5/1. For uptake pathway study of CS/siRNA-EGFP complex, the complex was prepared at weight ratio of 5 and the transfection experiment was performed at pH 6.4. After 6 hr of transfection, cells were washed with PBS and further incubated in complete media for 4 days at 37°C under normal condition. The culture media were changed every other days and the fluorescence intensity was measured daily. The percent seeding variation, adjust fluorescence intensity and percent EGFP gene

silencing were calculated by Eq. 3, 4 and 5, respectively as previously described. Uptake pathway of complex was evaluated by comparing percent EGFP gene silencing between the inhibitor treated group and no-inhibitor treated group.

3.6 Statistical analysis

Data were presented as the means ± standard deviations (SD) for three experiments. The statistical significance of transfection efficiency, gene silencing efficiency and cell viability were determined using one way analysis of variance (ANOVA) followed by an LSD post hoc test. The effect of serum on transfection efficiency and cellular uptake pathway of complexes was determined using Student's t test. P values of < 0.05 were considered significant.

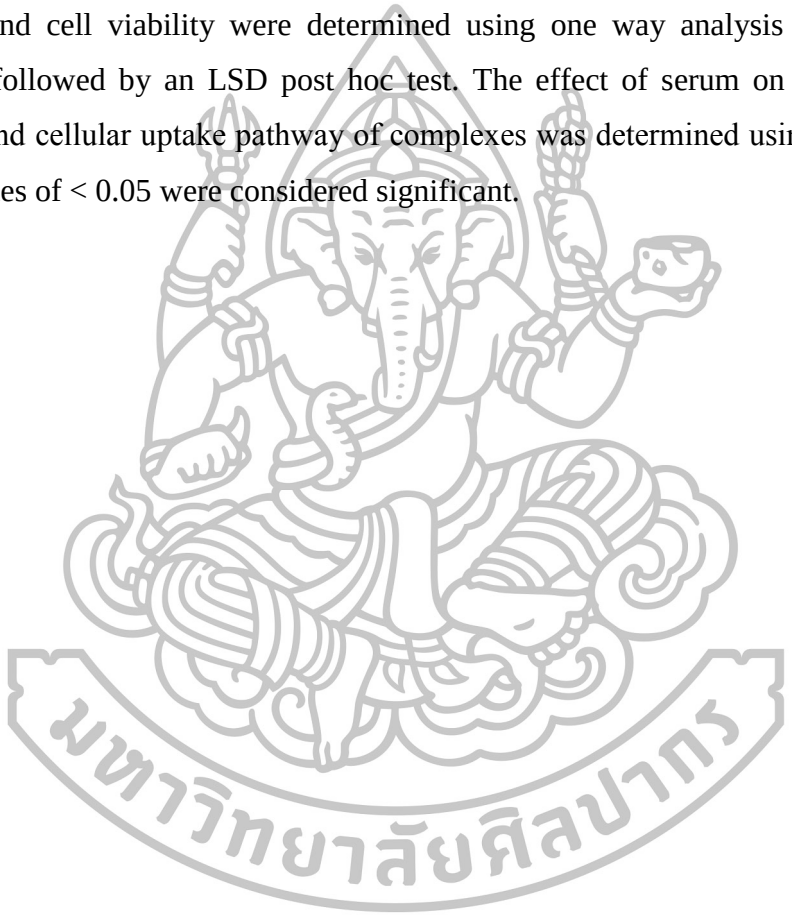

CHAPTER 4

RESULTS AND DISCUSSION

4.1 Dye adsorption method for determination of complete complex formation

4.1.1 Principle of dye adsorption method

4.1.2 Dye adsorption method for complete PEI/pDNA complex formation

4.1.3 Type of plasmid

4.1.4 Limit of plasmid amount

4.1.5 Optimum of dichlorofluorescein concentration

4.1.6 Type and molecular weight of polymers

4.1.7 Application of dye adsorption method for siRNA complex

4.1.8 General method for determination of complete complex formation

4.1.8.1 Agarose gel retardation

4.1.8.2 Zeta potential analysis

4.1.9 Transfection efficiency of PEI (25 kDa)/pEGFP complex

4.1.10 Gene silencing efficiency of PEI (25 kDa)/siRNA-EGFP complex

4.2 Chitosan combined with poly L arginine for siRNA delivery

4.2.1 Agarose gel retardation

4.2.2 Hydrodynamic size and zeta potential analysis

4.2.3 *In vitro* gene silencing efficiency

4.2.4 Effect of serum on transfection efficiency

4.2.5 Cytotoxicity of complexes

4.2.6 RNase protection ability of CS/PLA

4.2.7 Cellular uptake pathway of polymers/siRNA-EGFP complexes

4.1 Dye adsorption method for determination of complete complex formation

4.1.1 Principle of dye adsorption method

Since the estimation of complete complex formation was a preliminary test before *in vitro* transfection study, a new estimation method was developed in this study based on Fajan's titration using dichlorofluorescein as an adsorption indicator. The principle of the method for determining the optimal ratio of complex formation was illustrated in Figure 4.1. Firstly, DNA or siRNA was allowed to form complex with cationic polymer by self-assembly formation at different weight ratio for 30 min (A). The solution containing green anionic DCF was then added to the complexes (B). At this step, if the polymer amount was not adequate to form the complex with nucleic acid and resulted in negative charge on the surface of complex, DCF would not be adsorbed on the complexes because of electrostatic repulsion. Once the amount of polymer sufficiently associated with nucleic acid, the surface charge of complexes turned to positive and anionic DCF was attracted onto the particles as counterions. After spinning down to precipitate the complexes, the pink colored smear or pellets could be visualized under visible light (C). By the other mean, the adsorbed DCF could be released from complexes by adding sodium hydroxide solution and the green fluorescence could be seen under UV light at 366 nm (D).

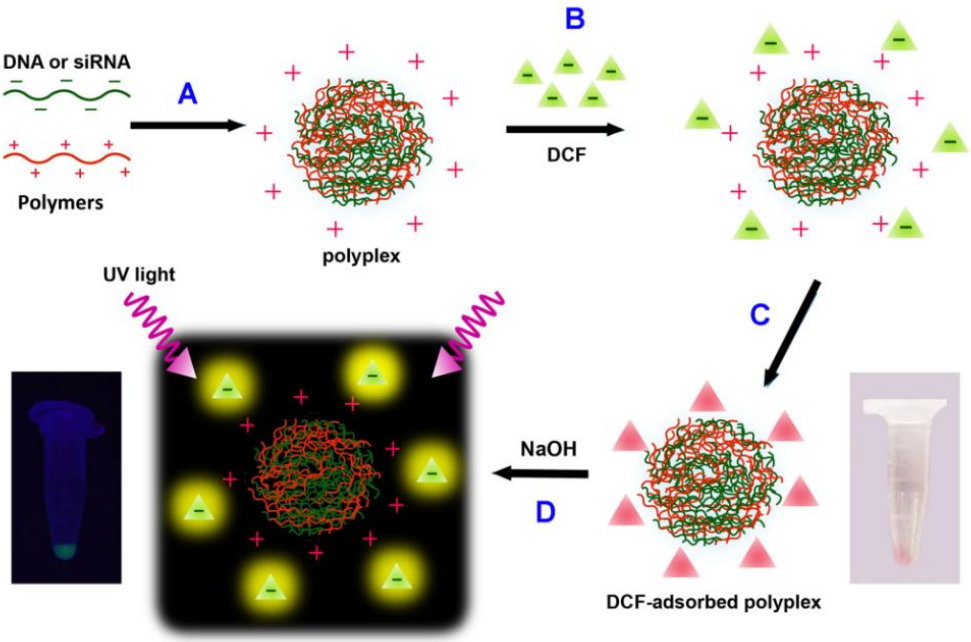

Figure 4.1 Scheme of dye adsorption method for estimation of complete complex formation.

4.1.2 Dye adsorption method for complete PEI/pDNA complex formation

According to the principle, the new method was first applied for estimating the complete polymer/pDNA complex formation using pEGFP and PEI (25 kDa) as representative plasmid DNA and polymer, respectively. The series of complex solution were prepared at PEI/pEGFP weight ratios of 0 to 2 containing 5 µg of pEGFP in each tube. DCF solution (0.15 mg/mL in TAE buffer, pH 8) was added and the solutions were then centrifuged. As shown in Figure 4.2, pink pellet appeared in the tubes which contained complexes at weight ratio of 0.5 and higher (Figure 4.2A). After adding sodium hydroxide solution, the green fluorescence was also observed in the same tubes under UV light (Figure 4.2B). This result indicated that PEI/pEGFP at weight ratio of 0.5 and higher was sufficient for complete self-assembling complexation, whereas the weight ratios of lower than 0.5 did not give the pink pellets or green fluorescence. Therefore, the estimated lowest weight ratio that PEI (25 kDa) completely complexed with pEGFP was 0.5.

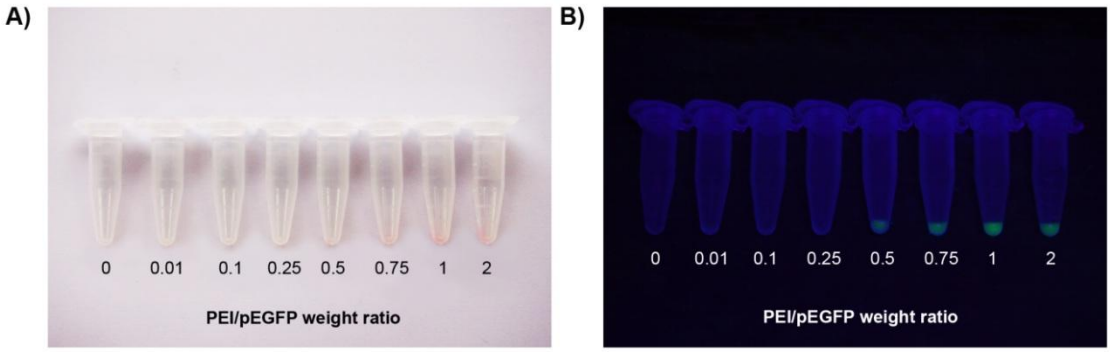

Figure 4.2 Estimation of complete PEI (25 kDa)/pEGFP complex formation by dye adsorption method as detected the pink pellets under visible light (A) or green fluorescence under UV light at 366 nm (B).

Apart from the observation of pink pellets and green fluorescence, the additional monitoring was done to confirm the adsorption phenomenon. For this purpose, the concentration of free DCF in supernatant (after spinning down the complexes) was determined by measuring the absorbance at 504 nm which was the maximum wavelength (λmax) of DCF solution. As seen in Figure 4.3, the absorbance value abruptly decreased at the weight ratio of 0.5 due to the adsorption of DCF on the positively charged surface of complexes. This result confirmed that the PEI/pEGFP complex completely formed at this point.

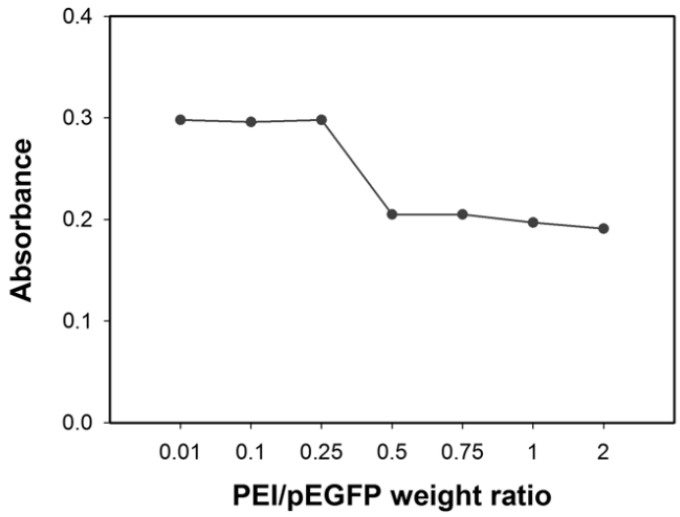

Figure 4.3 Absorbance value of free DCF in the supernatant at 504 nm.

4.1.3 Size of plasmid DNA

To prove whether this method was able to apply to other different plasmid with different size, pSV-β-gal (6.8 kbp) was tested. The PEI/pSV-β-gal complexes were prepared at the same protocol as PEI/pEGFP complex. The result showed that the dye adsorption method could also apply for different plasmid and the estimated complete complex formation ratio was at 0.5 (Figure 4.4).

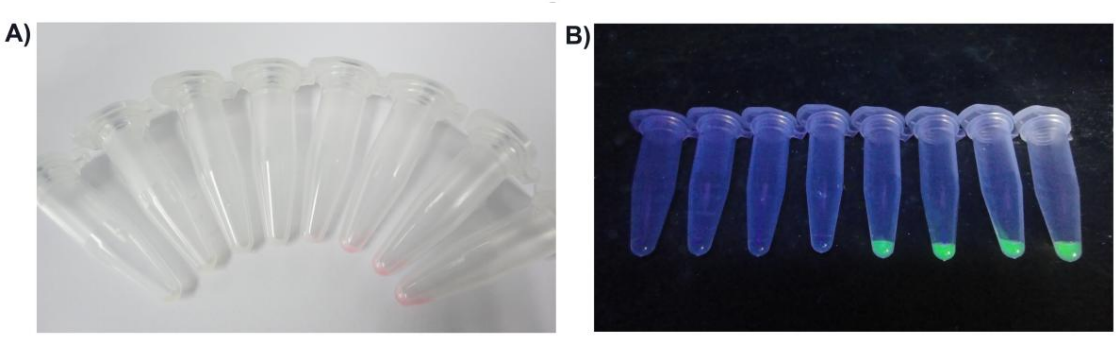

Figure 4.4 Estimation of complete PEI(25 kDa)/pSV-β-gal complex formation using dye adsorption method as detected the pink pellets under visible light (A) or green fluorescence under UV light at 366 nm (B). The complexes were prepared at weight ratio of 0, 0.01, 0.1, 0.25, 0.5, 0.75, 1 and 2 (from left to right).

4.1.4 Limit of pEGFP amount

The sensitivity of method was determined by varying pEGFP amount of 5, 2.5, 1, 0.5, 0.25 and 0.1 µg. The PEI/pEGFP complex was prepared at the same weight ratios of 0.5 and the concentration of DCF solution was 0.15 mg/mL. As seen in Figure 4.5, the lowest pEGFP amount that this method could clearly detect the complete complex formation under visible light was 0.5 µg pEGFP (Figure 4.5A). It was likely due to the too low amount of dye-adsorbed complexes formed at this weight ratio thus it was not able to detect by eyes. However, after DCF was released from the complexes by adding NaOH solution, the lowest pEGFP amount which was able to detect under UV light was 0.25 µg pEGFP (Figure 4.5B). This caused from the sensitivity of UV detection was higher than visible light detection. From this result, the recommended lowest pEGFP amount of this method was 0.5 µg pEGFP which was detectable under both visible and UV light.

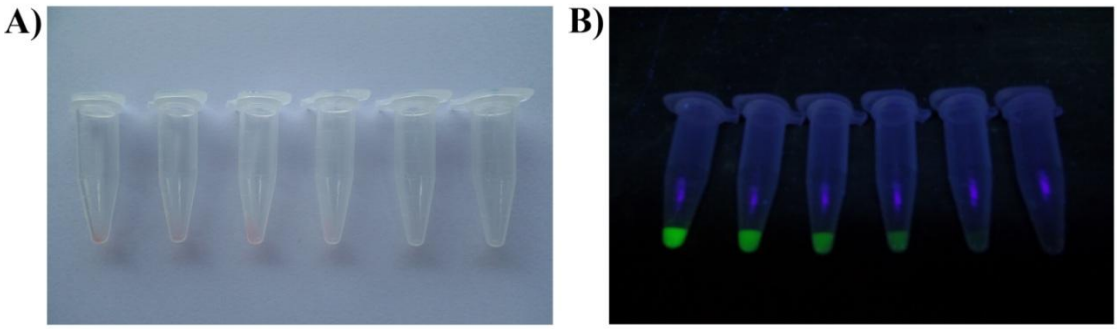

Figure 4.5 Effect of pEGFP amount on the detection of PEI (25 kDa)/pEGFP complex by observing the pink pellets under visible light (A) or green fluorescence under UV light at 366 nm (B). The complexes were prepared at same weight ratio of 0.5 using different pEGFP amount of 5, 2.5, 1, 0.5, 0.25 and 0.1 µg (from left to right).

4.1.5 Optimal of dichlorofluorescein concentration

The optimal concentration of DCF solution was determined by varying the concentration of DCF at 0.15, 0.1, 0.075 and 0.05 mg/mL in 1X TAE buffer (pH 8.3) while the other parameters were fixed. The results indicated that all tested DCF concentration were able to use for this method and could be detected under UV light. However, the pink pellets were difficult to observe under visible light by using the lowest concentration of DCF solution (0.05 mg/mL). Thus, the lowest concentration of DCF which was recommended to use for this method was 0.075 mg/mL (Figure 4.6).

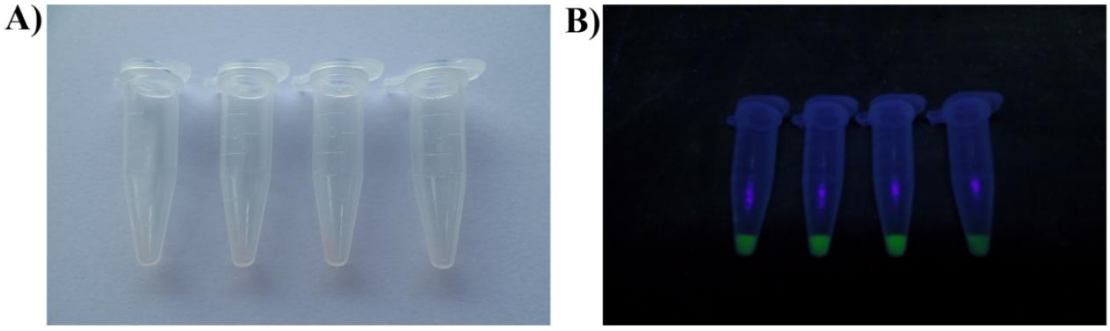

Figure 4.6 Effect of DCF concentration on the detection of PEI (25 kDa)/pEGFP complex by observing the pink pellets under visible light (A) or green fluorescence under UV light at 366 nm (B). The complexes were prepared at same weight ratio of 0.5 using 0.15, 0.1, 0.075 and 0.05 mg/mL of DCF solution (from left to right).

4.1.6 Molecular weight of polymers

Beside PEI 25 kDa, the different molecular weights of PEI at 10, 1.8 and 0.6 kDa were also tested. The PEIs/pEGFP complexes containing 0.5 µg pEGFP were formed at the same weight ratios for all MW of PEI. The result showed that PEI 25 kDa, 10 kDa (Figure 4.7), 1.8 kDa (Figure 4.8) and 0.6 kDa (Figure 4.9) could completely self-assembly form the complexes with pEGFP at weight ratio of 0.5 and gave green fluorescence under UV light. So the dye adsorption method could apply to wide range of molecular weight of polymers. However, the complexes of low molecular weight PEI (1.8 and 0.6 kDa) especially PEI 0.6 kDa did not clearly show the pink pellet by observing under visible light. It was possible that the complex association was loose and the surface charge was just slightly positive so anionic DCF could not strongly adsorb on it. Nevertheless, there were the reports indicated that low molecular weight PEI (< 2 kDa) had lack of DNA condensation and low transfection efficiency [212, 213]. Thereby, this difficulty of dye adsorption method to detect such a low MW of PEI under visible light was not the limitation.

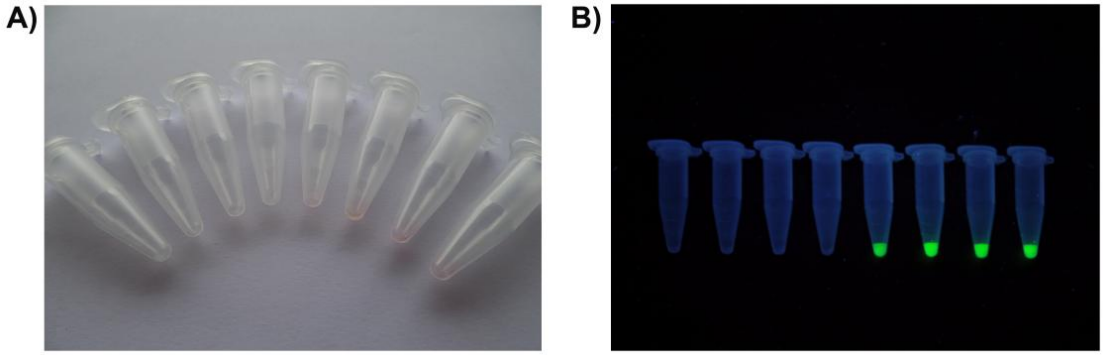

Figure 4.7 Estimation of complete PEI (10 kDa)/pEGFP complex formation using dye adsorption method detected by observing the pink pellets under visible light (A) or green fluorescence under UV light at 366 nm (B). The complexes were prepared at weight ratio of 0, 0.01, 0.1, 0.25, 0.5, 0.75, 1 and 2 (from left to right).

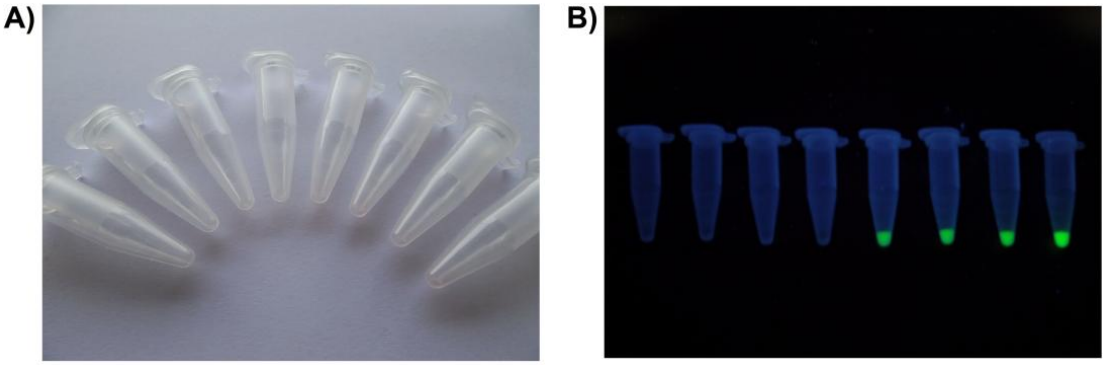

Figure 4.8 Estimation of complete PEI (1.8 kDa)/pEGFP complex formation using dye adsorption method detected by observing the pink pellets under visible light (A) or green fluorescence under UV light at 366 nm (B). The complexes were prepared at weight ratio of 0, 0.01, 0.1, 0.25, 0.5, 0.75, 1 and 2 (from left to right).

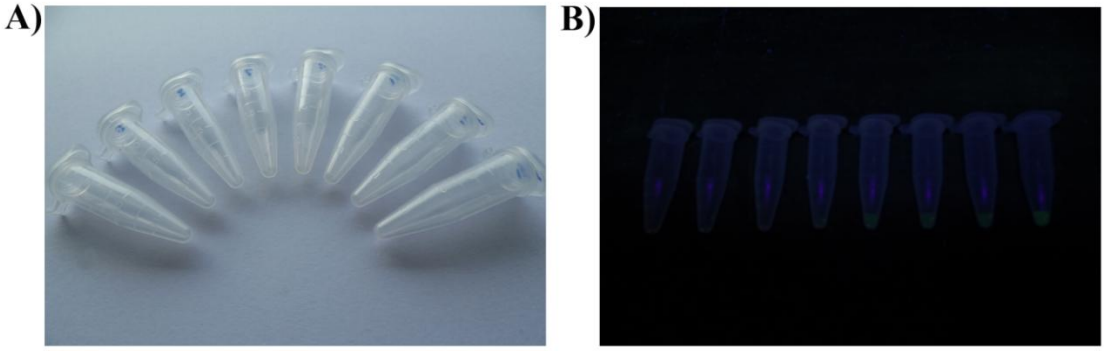

Figure 4.9 Estimation of complete PEI (0.6 kDa)/pEGFP complex formation using dye adsorption method detected by observing the pink pellets under visible light (A) or green fluorescence under UV light at 366 nm (B). The complexes were prepared at weight ratio of 0, 0.01, 0.1, 0.25, 0.5, 0.75, 1 and 2 (from left to right)

4.1.7 Type of polymer

Chitosan (low molecular weight), a natural polymer was also used as another representative polymer. The CS/pEGFP complexes containing 2.5 µg pEGFP were prepared at weight ratio of 0, 0.1, 0.5, 1, 5, 10, 15 and 20. The result showed pEGFP completely self-assembly complexed with CS at first weight ratio of 5 which was able to detect the pink pellets and green fluorescence (Figure 4.10).

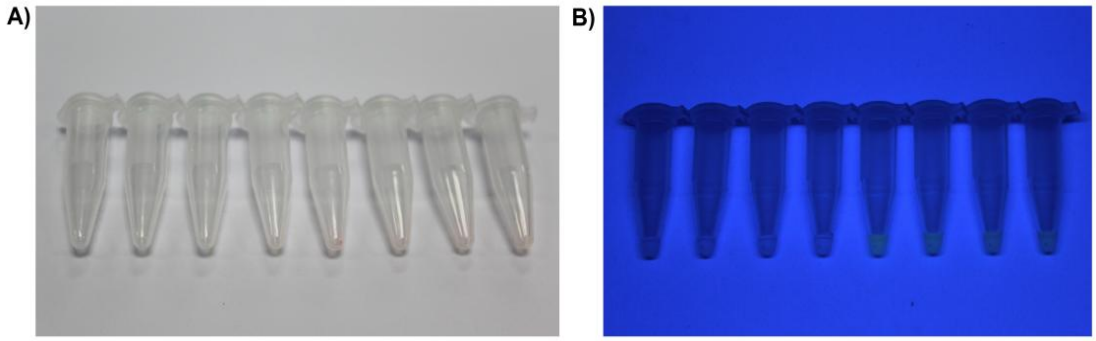

Figure 4.10 Estimation of complete CS/pEGFP complex formation using dye adsorption method detected by observing the pink pellets under visible light (A) or green fluorescence under UV light at 366 nm (B). The complexes were prepared at weight ratio of 0, 0.1, 0.5, 1, 5, 10, 15 and 20 (from left to right).

4.1.8 Application of dye adsorption method for siRNA complex

The dye adsorption method was also applied to determine PEI/siRNA-mismatch complex since siRNA and pDNA complexes showed the different properties eg. size and stability of complexes [214, 215]. The PEI (25 kDa)/siRNA-mismatch complexes were prepared at same weight ratio as PEI (25 kDa)/pEGFP complexes by containing 1 µg of siRNA. By using dye adsorption method, the complete complex formation was occurred at the weight ratio of 1 (Figure 4.11).

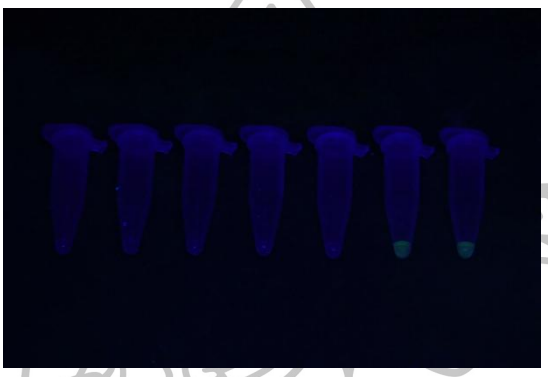

Figure 4.11 Estimation of PEI (25 kDa)/siRNA by dye adsorption method. The complexes were prepared at weight ratio of 0.01, 0.1, 0.25, 0.5, 0.75, 1 and 2 (from left to right).

4.1.9 General method for determination of complete complex formation

4.1.9.1 Zeta potential analysis

The complete complex formation was usually evaluated by the presence of positive charge on surface by zeta potential analysis. Thus, the zeta potential of PEIs/pEGFP, PEI (25 kDa)/pSV-β-gal, CS/pEGFP and PEI (25 kDa)/siRNA complexes were also determined in order to confirm the accuracy of dye adsorption method. For PEIs/pEGFP complex (Figure 4.12), the zeta potential increased with increasing weight ratios. For the complexes of PEI 25 kDa, 10 kDa and 1.8 kDa, the surface of complexes became positive at weight ratio of 0.5 whereas the complexes of PEI 0.6 kDa showed weakly positive charge. This result was in agreement with the result from dye adsorption method.

For PEI (25 kDa)/pSV-β-gal complexes, the surface charge became positive at weight ratio of 0.5 which was also at the same weight ratio of the first complete complex formation determined by dye adsorption method (Figure 4.13).

The surface charge of CS/pEGFP complexes was also determined and the result showed that the surface charge of complexes was positive at weight ratio of 1 and higher (Figure 4.14). However, the result was different from dye adsorption method which showed the complete formation at first weight ratio of 5. This was likely because CS must dissolve and form complexes with pDNA in acidic condition (pH < 6) in order to maintain the positive charge of CS. As the DCF in the basic solution was added to the CS/pEGFP complex, the pH of complex solution would be changed. This resulted in the decreasing of positive charge of CS and anionic DCF was not able to adsorb on complexes. On the other hand, zeta potential analysis was done in neutral or slightly acidic condition so CS quite contained positive charge and the surface of complexes remained positive. Therefore, it should be concerned that DFC-based method might not be appropriate for the polymers which have limited solubility under the basic condition.

For the zeta potential of PEI (25 kDa)/siRNA complexes, the surface of complexes was positive at weight ratio of 1 and higher (Figure 4.15). This was relatively in parallel with the result determined by dye adsorption method.

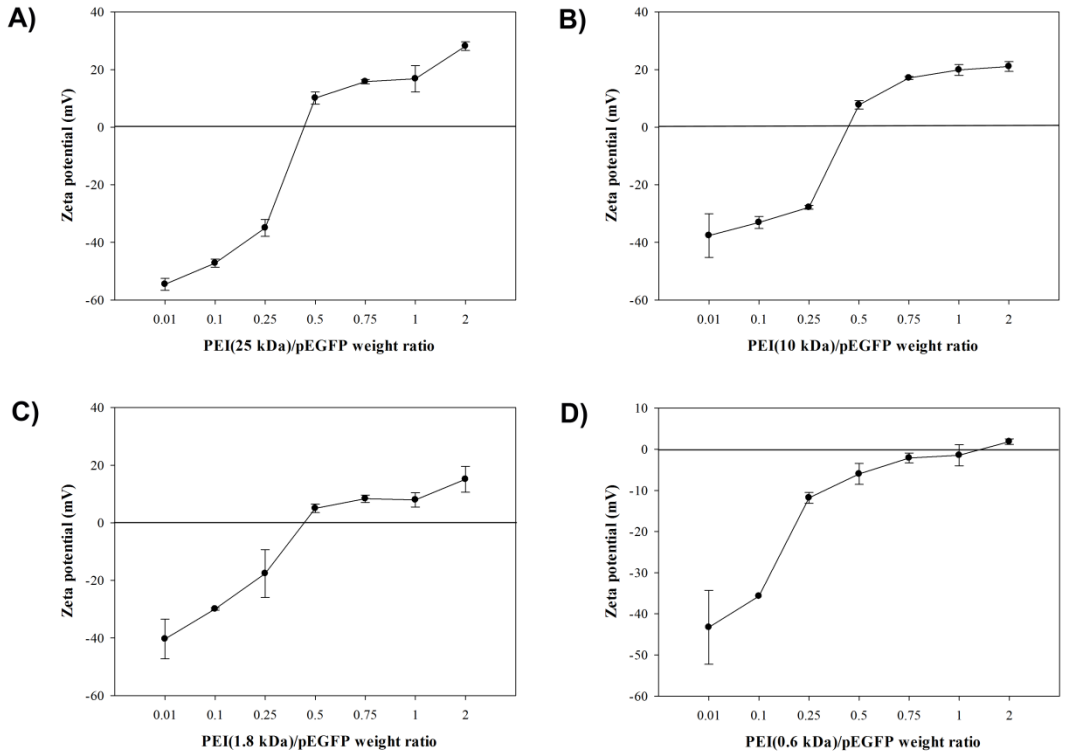

Figure 4.12 Zeta potential of PEI (25 kDa)/pEGFP complex (A), PEI(10 kDa)/pEGFP complex (B), PEI(1.8 kDa)/pEGFP complex (C) and PEI(0.6 kDa)/pEGFP complex (D). The results presented in mean ± SD of triplicate samples.

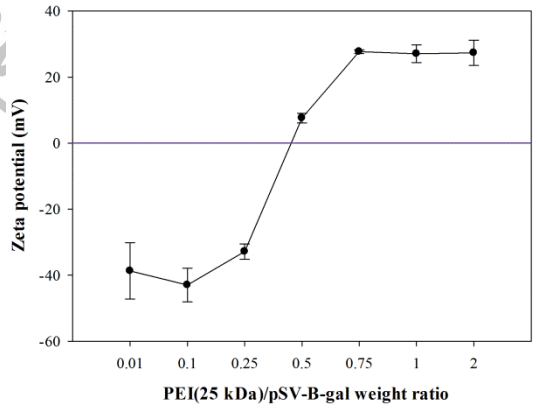

Figure 4.13 Zeta potential of PEI (25 kDa)/pSV-β-gal complexes at different weight ratio. The results presented in mean ± SD of triplicate samples.

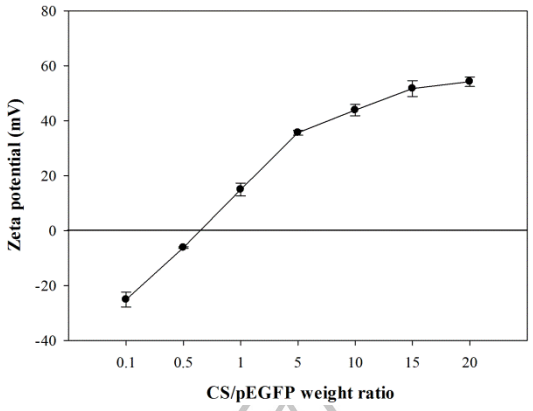

Figure 4.14 Zeta potential of CS/pEGFP complexes at different weight ratio. The results presented in mean ± SD of triplicate samples.

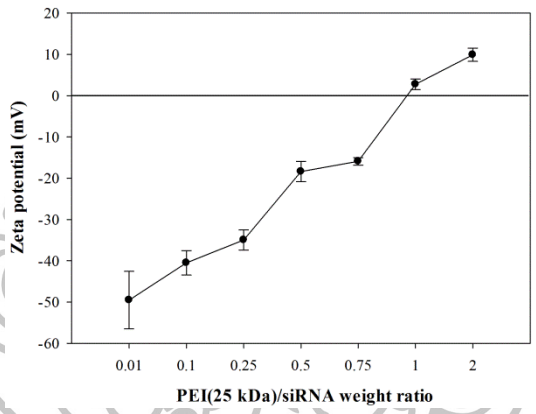

Figure 4.15 Zeta potential of PEI (25 kDa)/siRNA complexes at different weight ratio. The results presented in mean ± SD of triplicate samples.

4.1.8.2 Agarose gel retardation

To confirm the correctness of the results from dye adsorption method, the complete complex formation was determined by agarose gel retardation. The PEI (25 kDa)/pEGFP and PEI (25 kDa)/pSV-β-gal complexes were prepared at weight ratio of 0.01, 0.1, 0.25, 0.5, 0.75, 1 and 2. The result showed the complete complex formation at weight ratio of 0.5 and higher which pEGFP and pSV-β-gal were totally retained in the wells (Figure 4.16). The results were exactly the same as those from dye adsorption method.

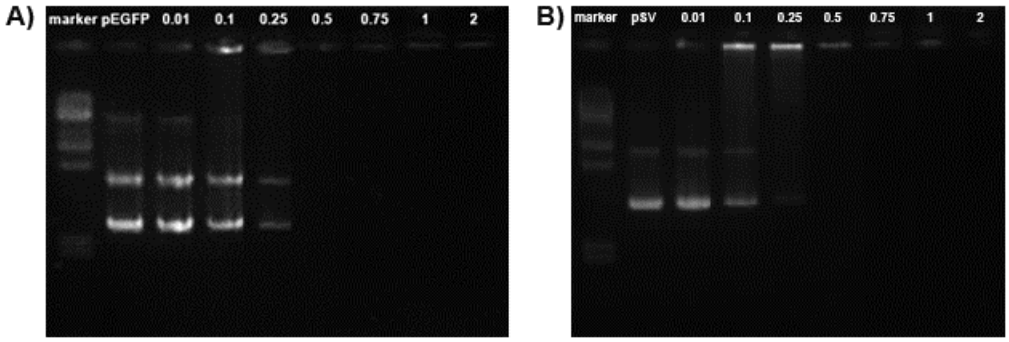

Figure 4.16 Agarose gel retardation of PEI (25 kDa)/pEGFP complexes (A) and PEI (25 kDa)/pSV-β-gal complexes (B).

The complete complexes formation of PEI (10 kDa)/pEGFP, PEI (1.8 kDa)/pEGFP and PEI (0.6 kDa)/pEGFP complexes was also determined by agarose gel retardation. The complexes were prepared at weight ratio of 0.1, 0.25, 0.5, 0.75 and 1. The result showed the complete complex formation at weight ratio of 0.5 and the higher for all molecular weight of PEI (Figure 4.17). For PEI 0.6 kDa, it could complex with pEGFP and retained in the wells at the first weight ratio of 0.5 and the result was relevant to that received from dye adsorption method. However, the zeta potential analysis indicated that the surface charge of complexes was positive at weight ratio of 2. It might be possible that even PEI 0.6 kDa was able to complex with pEGFP, the association was loose and could not result in sufficiently high positive charge on the surface.

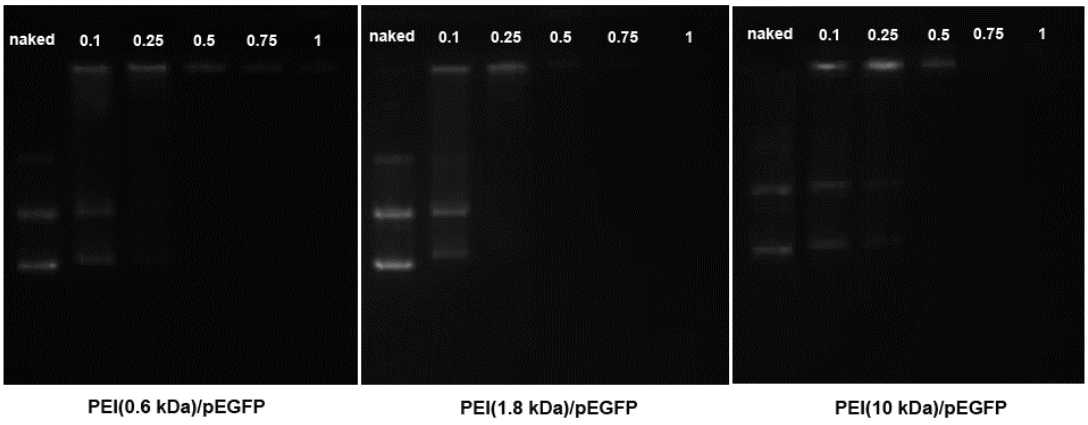

Figure 4.17 Agarose gel retardation of PEI (10 kDa)/pEGFP, PEI (1.8 kDa)/pEGFP and PEI(0.6 kDa)/pEGFP complexes.

For agarose gel retardation of PEI (25 kDa)/siRNA complexes, the complete complex formation occurred at the weight ratio of 0.5 (Figure 4.18). This was slightly different from that obtained from dye adsorption method and zeta potential analysis. Since the migration of nucleic acid on gel depended on charge to mass ratio [216], it suggested that gel electrophoresis determined the neutralization of negative charge of siRNA. Thus at the low PEI (25 kDa)/siRNA weight ratio, PEI bound to siRNA and only changed the electrophoretic behavior but the PEI amount might not be enough to form the discrete particles [9]. On the other hand, the dye adsorption method and zeta potential analysis could detect the charge on the surface of discrete particles.

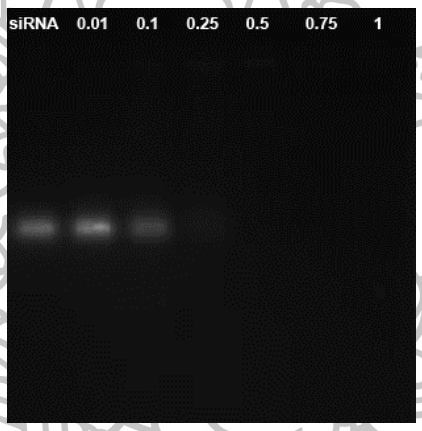

Figure 4.18 Agarose gel retardation of PEI (25 kDa)/siRNA complexes

4.1.9 Transfection efficiency of PEI (25 kDa)/pEGFP complex

From the estimation of complete complex formation experiment, it suggested that the complete PEI (25 kDa)/pEGFP complex formation occurred at the weight ratio of 0.5. The transfection efficiency of PEI (25 kDa)/pEGFP complex was then evaluated in HeLa cell to compare the weight ratio which gave the highest transfection with that from the preliminary complete complex formation study. The result showed that EGFP expression occurred in cells were transfected with the complexes which had positive surface charge (weight ratio of 0.5 and higher) and transfection efficiency increased proportional to weight ratio. The highest transfection efficiency was at weight ratio of 1 which was slightly higher than the weight ratio from the preliminary study (Figure 4.19). This might be due to the

properties e.g. compactness and stability of complex at weight ratio of 1 which was more appropriate for delivering pEGFP into cell and nucleus than the first weight ratio of complete complex formation. The additional study of complex size also indicated that the size of complex at weight ratio of 0.5 was larger than complexes at weight ratio of 1. This resulted in low transfection efficiency at weight ratio 0.5 since size of complex affected on transfection efficiency (Figure 4.20).

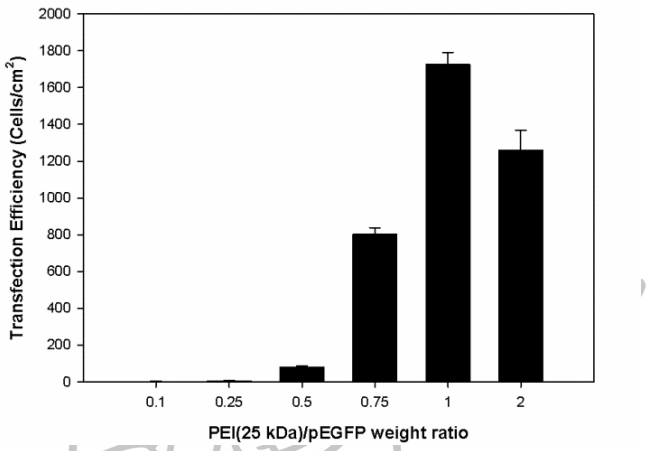

Figure 4.19 Transfection efficiency of PEI (25 kDa)/pEGFP complexes in HeLa cell at different weight ratios detected by direct observing under fluorescent microscope. Each value represented the mean ± SD of triplicate samples.

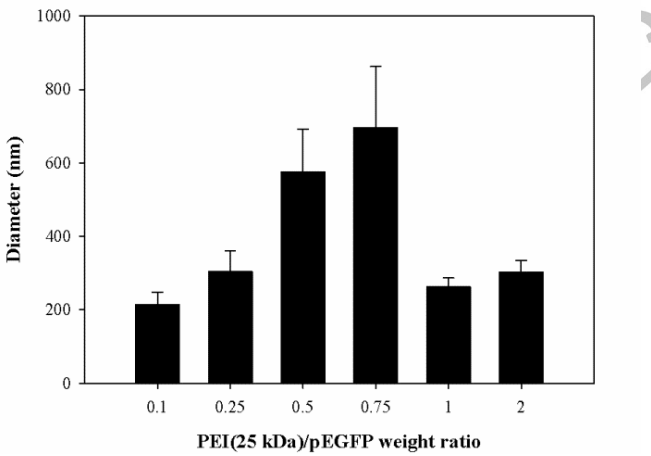

Figure 4.20 Size of PEI (25 kDa)/pEGFP complexes at different weight ratio analyzed by Zeta Nanosizer. Each value represented the mean ± SD of triplicate samples.

4.1.10 Gene silencing efficiency of PEI (25 kDa)/siRNA-EGFP complex

The EGFP gene silencing was studied in HeLa cell stably expressing green fluorescent protein. The specific EGFP gene silencing was determined by normalizing the fluorescence intensity of siRNA-EGFP transfected cells with those transfected with siRNA-mismatch. The result showed the highest gene silencing efficiency was at weight ratio of 2 which was slightly higher than that obtained from preliminary determination of first complete complex formation ratio (Figure 4.21).

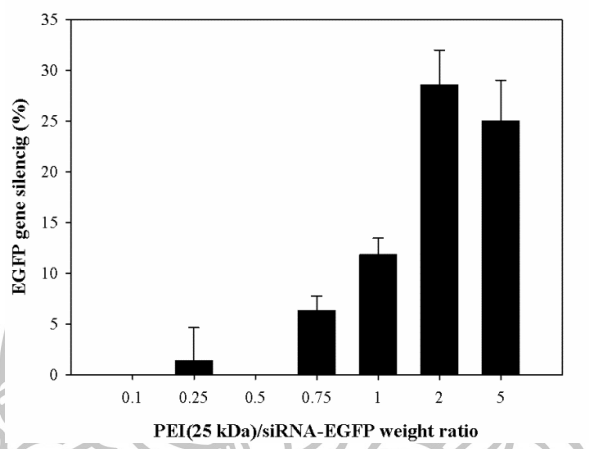

Figure 4.21 Percentage of gene silencing at day 4 of HeLa-EGFP cells after transfected by PEI (25 kDa)/siRNA-EGFP complexes. Each value represented the mean ± SD of triplicate sample.

4.1.11 Summary of dye adsorption method

From all experiments of complete complex formation determination, the developed dye adsorption method was able to apply for preliminary determination of complete complex formation before *in vitro* study. The optimal conditions of dye adsorption method for determining of complete complex formation were illustrated in Table 4.1.

Table 4.1. The optimum conditions of dye adsorption method for determining the complete complex formation

Parameters	Optimum conditions
pDNA amount	Not less than 0.5 µg
siRNA amount	Not less than 1 µg
DCF concentration	0.075 mg/mL
pH	Neutral to weak basic

As mentioned above, the several methods for detection of complete complexes were reported. The comparison of well-known established method was presented in Table 4.2. In addition, detection time and cost per sample was also evaluated.

Table 4.2. The comparison of dye adsorption method and general methods for determining the complete complex formation

Method (Detection method)	LOD	Detected species	Detection time
Dye adsorption (Directly observe)	0.5 µg	Surface charge of particles and excess cationic polymer	~ 15 min
Agarose gel retardation with EtBr (UV transillumination)	~20 ng [217]	Free nucleic acid	~ 1 hr 15 min
Dye exclusion assay (Fluorescence intensity) - EtBr - SYBR green® - Picogreen®	 10 µg/mL [218] 0.25 pg/µl [219] 250 pg/mL [220]	Free nucleic acid	~ 15 min
Zeta potential analysis (Electrophoretic light scattering)	N/A	Surface charge of particles	~ 20 min/sample

However, there were some limitations of this method. Thus, the advantages and limitation of dye adsorption method was concluded in Table 4.3.

Table 4.3. Advantages and limitations of dye adsorption method

Advantages	**Limitations**
1. Low cost 2. Sophisticated instrument was not required 3. Hazardous reagents were eliminated 4. Fast and easy 5. Accurate when using the optimal nucleic acid amount	1. Higher limit of detect than other techniques 2. Detectable for only complexes which have positive surface charge 3. Condition must be neutral to weak basic

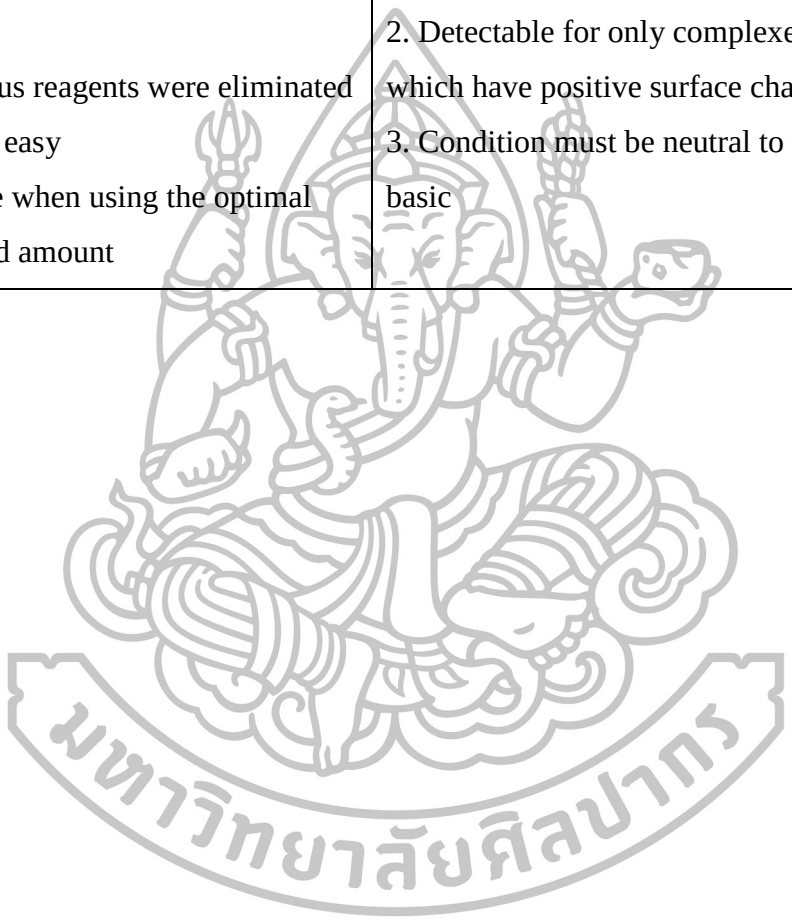

4.2 Chitosan combined with poly L arginine for siRNA delivery

In this study, the natural polymer, chitosan (CS) combined with poly L arginine (PLA) was used as polymeric carrier for siRNA. Since CS has a weak acid property (pKa = 6.4) and can be protonated only at acidic condition, it is not capable to deliver siRNA into cells at physiological pH (7.4). In previous study, it was suggested that the combination of CS (45 kDa) with PLA (> 70 kDa) was efficiently deliver pDNA in HeLa cell and showed low cytotoxicity [221]. Although pDNA and siRNA share the general properties that they are double stand nucleic acids with anionic phosphate backbones, siRNA shows the smaller size and rigid rod which might effect on complexation and transfection efficiency. In addition, cellular location of mechanistic activation was also different. DNA therapy requires delivery of DNA in to nucleus while RNAi by siRNA occures in cytoplasm [214, 215]. Therefore, the same polymeric carrier system, CS combined with PLA, was also tested for delivering siRNA in order to prove that this system was efficient for both pDNA and siRNA delivery.

4.2.1 Agarose gel retardation

The association ability of polymers with siRNA was evaluated by agarose gel retardation assay. The CS/siRNA-mismatch and PLA/siRNA-mismatch complexes containing 0.112 µg siRNA were prepared at different weight ratio. As seen in Figure 4.22, CS could not completely self-assembly formed with siRNA even at highest tested weight ratio of 20. However, the electrophoretic mobility of siRNA was shifted up at weight ratio of 5. This suggested that CS could bind with free-siRNA, like protein did [222] and caused less mobility than free siRNA. For PLA/siRNA complexes, the complete association was occurred at weight ratio of 1 and higher. To prepare CS/PLA/siRNA complexes, the amount of CS thus was fixed at weight ratio of 5 which free-siRNA did not appear on gel while the amount of PLA was increased. The gel retardation of CS/PLA/siRNA complex illustrated the complete complex formation at weight ratio of 5/0.5/1with no siRNA migrated on gel (Figure 4.22 C). Interestingly, it suggested that CS combined with PLA efficiently bound with siRNA and could reduce the amount of each polymer used for self-assembly.

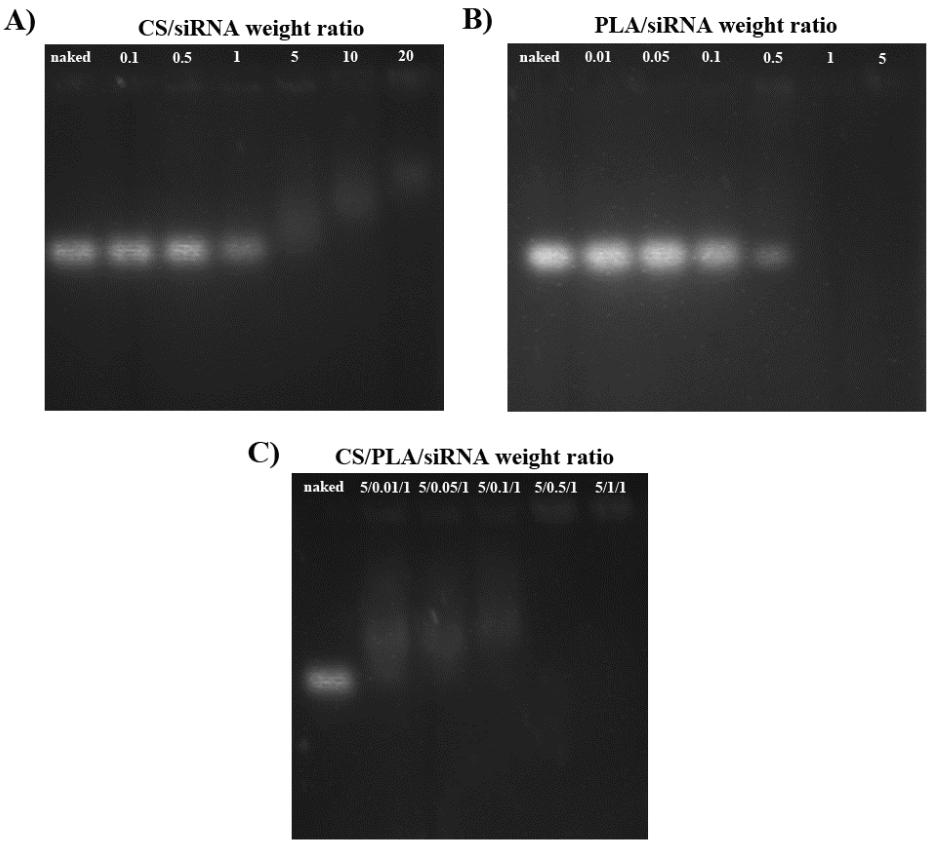

Figure 4.22 Gel retardation assay of CS/siRNA complexes (A) and PLA/siRNA complexes (B) and CS/PLA/siRNA complexes (C).

4.2.2 Zeta potential and size

The zeta potential and hydrodynamic size of CS/siRNA, PLA/siRNA and CS/PLA/siRNA complexes were determined at pH 6.4 and 7.4. The zeta potential of complexes increased with the increasing of polymers amount (Figure 4.23). The surface charge of CS/siRNA complexes turned to positive at weight ratio of 1 and 5 at pH 7.4 and 6.4, respectively. For PLA/siRNA complexes, the surface charge of complexes was positive at weight ratio of 1 in both pH 6.4 and 7.4. Furthermore, the zeta potential at pH 6.4 was higher than at pH 7.4 for all polymers due to the higher protonation at acidic condition. The CS/PLA/siRNA complexes were prepared using the fixed CS weight ratio of 5 which the amount of CS was enough for providing the positive surface complex at both pH 6.4 and 7.4. By combining CS with PLA, the surface charge of complex gradually increased with the increasing of PLA amount

suggesting that PLA did not highly affect the surface charge property of complex however it might assist on other properties such as compactness and stability of complexes.

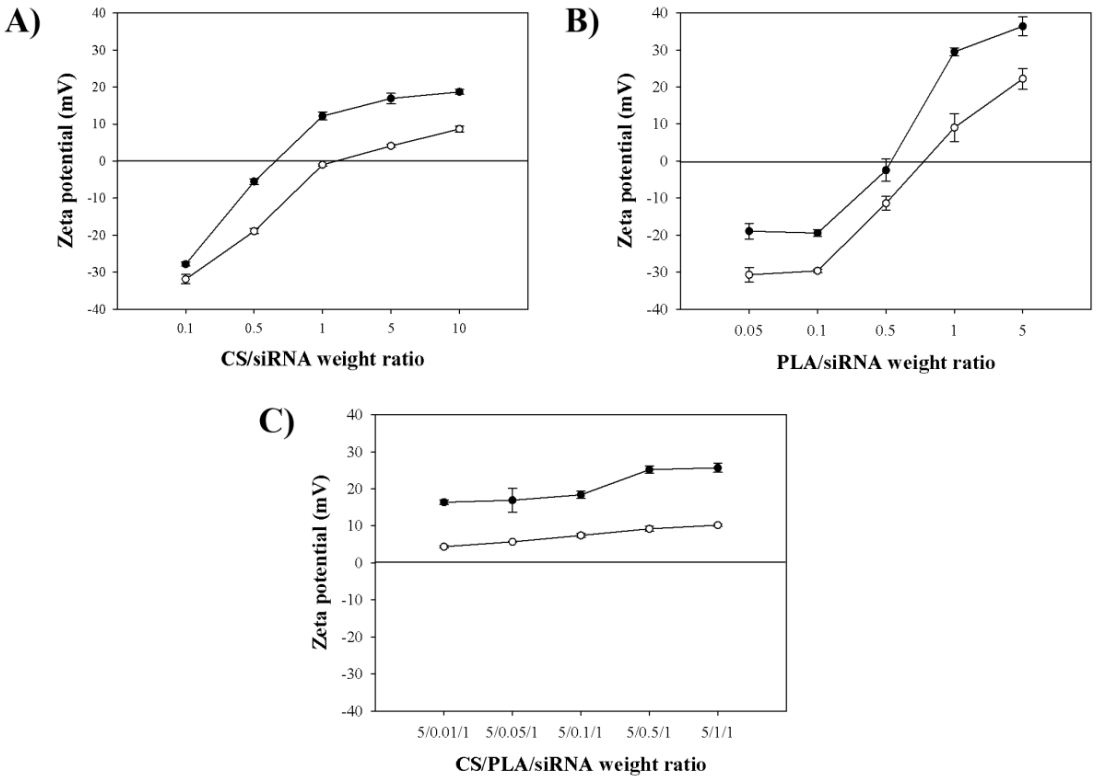

Figure 4.23 Zeta potential of CS/siRNA complexes (A), PLA/siRNA complexes (B) and CS/PLA/siRNA complexes (C) at different weight ratios at pH 6.4 (●) and pH 7.4 (○). Each value represented the mean ± SD of triplicate measurements.

The hydrodynamic size of complexes is illustrated in Figure 4.24. The size of CS/siRNA complexes increased with the increasing of weight ratio from 0.1 to 0.5 and then decreased at weight ratio of 1. This trend also occurred in case of PLA/siRNA complexes which size increased at weight ratio of 0.5 and then decreased. For CS/PLA/siRNA complexes, the size was relatively constant with the range of 300-400 nm. This suggested that the addition of PLA did not change in size property even PLA itself provided the large complexes at weight ratio of 0.5. In addition, the different of pH did not effect on size of complexes.

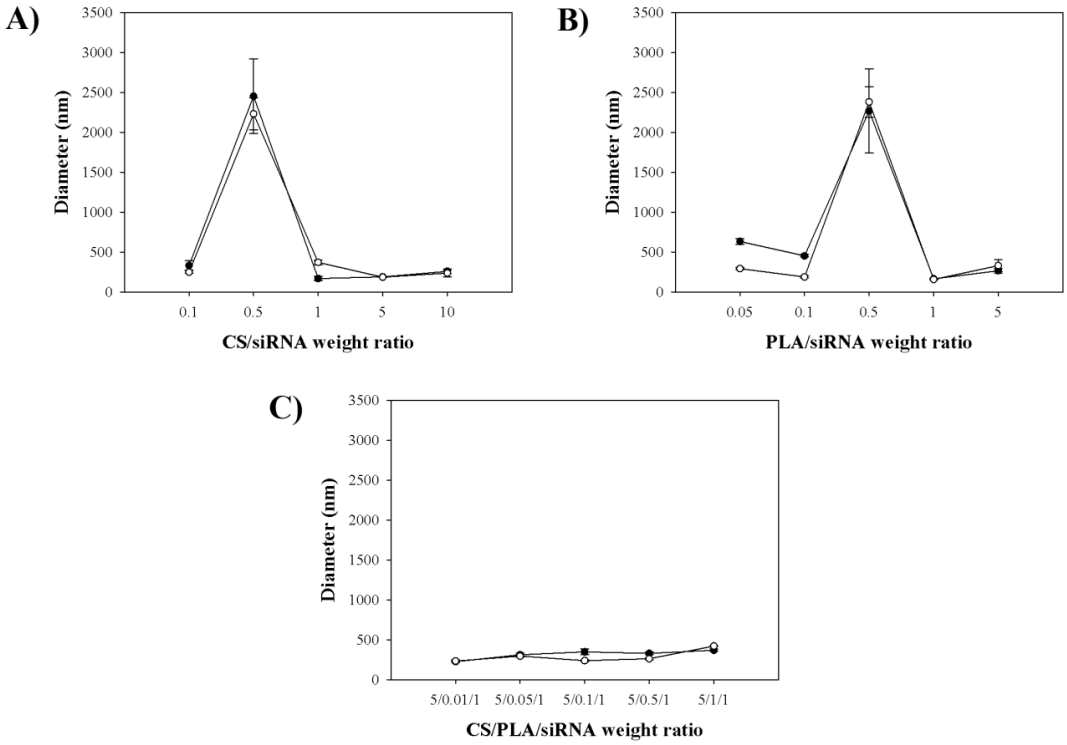

Figure 4.24 Size of CS/siRNA complexes (A), PLA/siRNA complexes (B) and CS/PLA/siRNA complexes (C) at different weight ratios at pH 6.4 (●) and pH 7.4 (○). Each value represented the mean ± SD of triplicate measurements.

4.2.3 *In vitro* gene silencing efficiency

The transfection efficiency of complexes was determined as EGFP gene silencing in HeLa-EGFP cells at pH 6.4 and 7.4. Cells were transfected with CS/siRNA, PLA/siRNA and CS/PLA/siRNA complexes in serum free media and the fluorescence intensity was measured using fluorescence microplate reader. The gene silencing efficiency was determined as the decreasing of fluorescence intensity in EGFP-specific siRNA treated group compared with mismatch siRNA treated group. The naked siRNA treated group showed negligible EGFP gene silencing effect. The PEI (25 kDa)/siRNA complexes was used as the positive control at the optimal weight ratio of 2. The percent gene silencing of this complex was 21.66 ± 2.90% and 26.24 ± 3.40% at pH 7.4 and 6.4, respectively. For CS/siRNA complexes, the result showed effectively EGFP gene silencing of about 28% at weight ratio of 1 and higher in pH 6.4 whereas the gene silencing efficiency of these complexes in physiological pH

(7.4) was drastically decreased (Figure 4.25A). This was due to the amine groups on CS were higher protonated in pH 6.4 than pH 7.4 resulting in less positive charge and loss of ability to stabilize the complexes during delivered siRNA into cells. Thus, CS did not efficiently delivered siRNA into cells at physiological pH. The PLA/siRNA complexes showed low gene silencing efficiency at both pH as compared to CS/siRNA at pH 6.4. The highest gene silencing was obtained at weight ratio of 5 (11.78 ± 1.32%) and decreased with increasing PLA/siRNA weight ratio. This suggested that the decreasing of gene silencing might be due to the cytotoxicity of high PLA amount (Figure 4.28B).

According to the limitation of each polymer for siRNA delivery, the combination of CS and PLA was performed to overcome this problem. The complexes were prepared by adding PLA solution to siRNA solution at the different weight ratio of 0.1 to 1. The CS at fixed weight ratio of 5 was then added to the PLA/siRNA complexes and incubated for 30 min. As seen in Figure 4.25 C, the gene silencing efficiency at pH 6.4 was not significantly different by adding the various amount of PLA and also was not different from CS/siRNA complex at weight ratio of 5. This suggested that PLA did not promote the transfection efficiency of CS at pH 6.4 which CS efficiently delivered siRNA by itself at this pH. While the expression of EGFP was inhibited in cells were transfected with CS/PLA/siRNA complexes and the percent gene silencing increased with the increasing of PLA amount. The highest gene silencing was obtained at CS/PLA/siRNA weight ratio of 5/0.5/1 with 25.04 ± 1.84 % gene silencing and was comparable to PEI (25 kDa)/siRNA complexes. Figure 4.26 illustrated the reduction of EGFP expression in HeLa-EGFP cell which was transfected with CS/PLA/siRNA-EGFP complex at weight ratio of 5/0.5/1 under fluorescent microscope compared with non-transfected cells. These results indicated that although CS did not show ability to deliver siRNA at pH 7.4 and PLA was not an efficient carrier, the combination of CS with PLA exhibited the efficient carrier for siRNA delivery at physiological pH. It was possible due to PLA provided the positive charge of complexes during delivered siRNA into cell and generated the stable complexes which suitable for siRNA delivery.

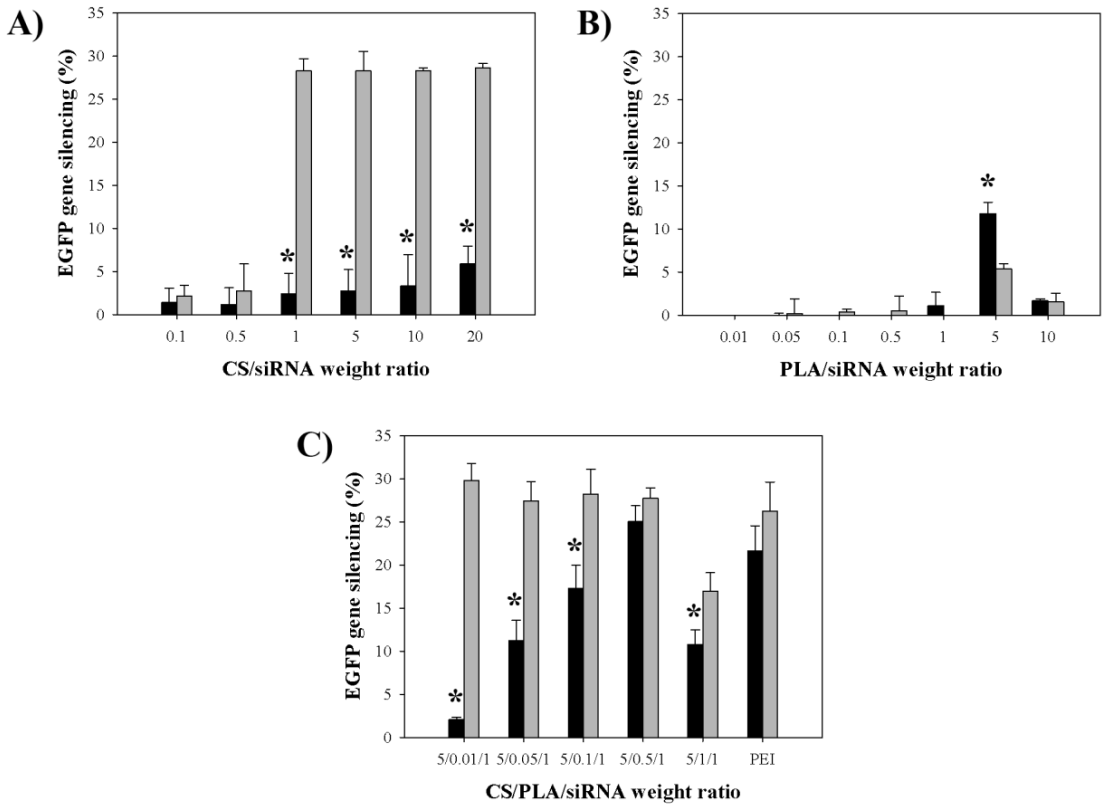

Figure 4.25 Percentage of EGFP gene silencing of (A) CS/siRNA-EGFP, (B) PLA/siRNA-EGFP and (C) CS/PLA/siRNA-EGFP complexes at different weight ratio after 4 days of transfection in HeLa-EGFP cell at pH 6.4 (gray bars) and pH 7.4 (black bars). PEI (25 kDa)/siRNA-EGFP complex at weight ratio of 2 was used as a positive control. Each value presented in mean ± SD of triplicate samples.

* Significantly different from the group(s) treated with the same weight ratio at pH 6.4 ($p < 0.05$).

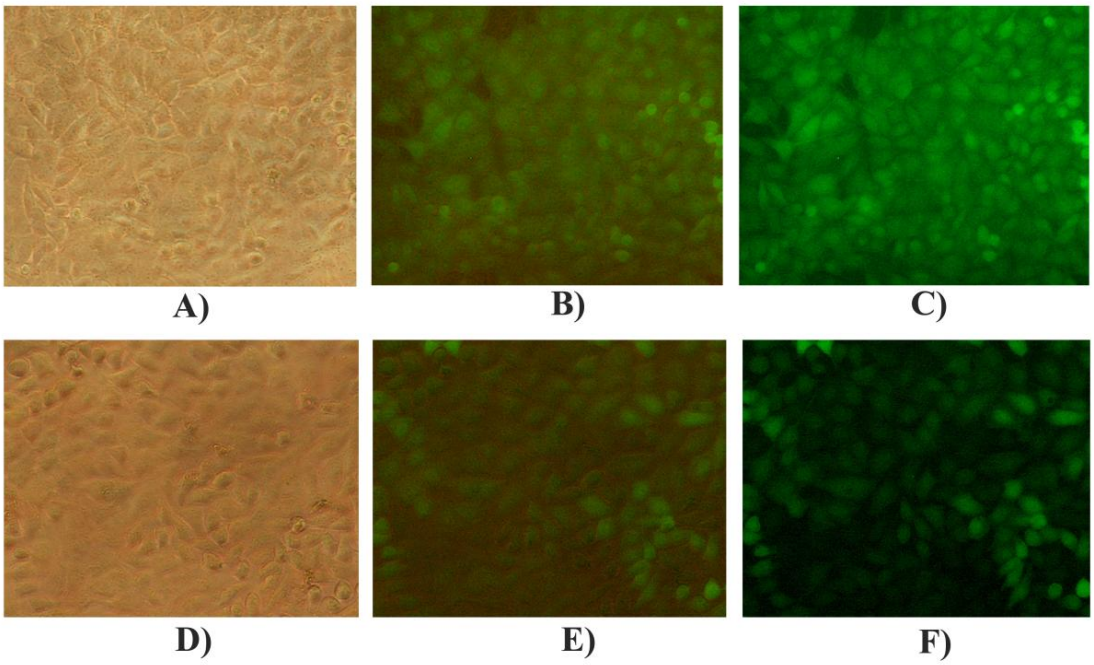

Figure 4.26 Fluorescence microscopic picture of non-transfected HeLa-EGFP cell (A-C) and cells transfected with CS/PLA/siRNA-EGFP complex (D-F) at weight ratio of 5/0.5/1 after 3 days of transfection. The images were observed under bright field (A and D), merge field (B and E), and fluorescence field (C and F) microscopy at the magnification of 100x.

4.2.4 Effect of serum on transfection efficiency

Since the composition in serum might effect on transfection efficiency of polymers/siRNA complexes, the transfection efficiency of CS/PLA/siRNA-EGFP complexes in the present of serum (10% FBS) was determined. As seen in Figure 4.27, the CS combined with PLA was able to deliver siRNA-EGFP into HeLa-EGFP cell even in the presence of serum and the percent EGFP gene silencing was equivalent to those in the absence of serum. There were the published studies which reported that the transfection efficiency of CS/DNA complexes did not decrease in the presence of serum [223, 224]. In contrast, the transfection efficiency of PEI (25 kDa)/siRNA-EGFP complexes was negligible in the presence of serum. This suggested that the serum composition might interfere the property of PEI (25 kDa)/siRNA complex and transfection efficiency. This was relevant to other studies demonstrated that the transfection efficiency decreased in the presence of serum by

using PEI 25 kDa as a polymeric carrier [225, 226]. These results suggested that the new carrier system, CS combined with PLA was possible for further use *in vivo* study.

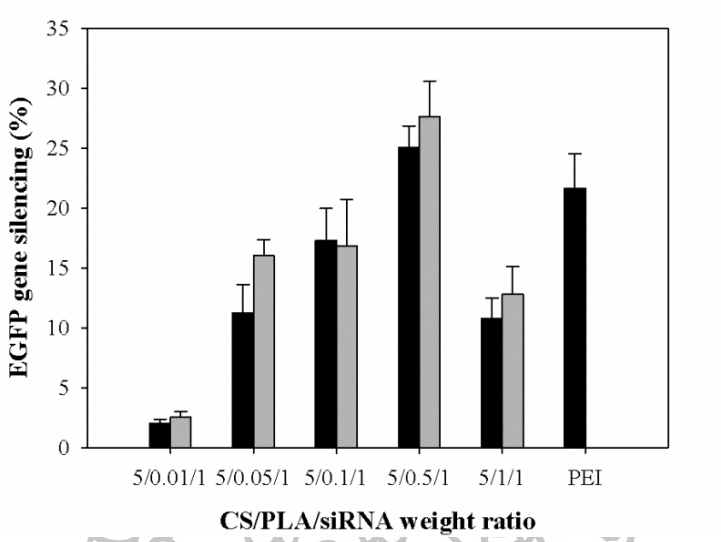

Figure 4.27 Comparison of percent EGFP gene silencing of CS/PLA/siRNA-EGFP complexes at different weight ratio in HeLa-EGFP cell after 4 days of transfection at pH 7.4 between in the absence of serum (black bars) and in the presence of serum (gray bars). PEI (25 kDa)/siRNA-EGFP complex at weight ratio of 2 was a control. Each value presented in mean ± SD of triplicate samples.

4.2.5 Cytotoxicity of complexes

Apart from the efficiency of polymers for delivering siRNA, cytotoxicity was also an important issue for siRNA delivery. To determine the cytotoxicity of complexes, cells were transfected with CS/siRNA, PLA/siRNA and CS/PLA/siRNA complexes at different weight ratios. As seen in Figure 4.28, the viability of cells which were transfected with CS/siRNA complexes was about 70% at weight ratio ranging from 0.5 to 10. While the cell viability decreased by transfecting with PLA/siRNA complexes at higher weight ratio. In addition, the cell viability of PLA/siRNA complexes was lower than CS/siRNA by comparing at the same weight ratio of 5. This suggested that the CS/siRNA complexes were safer than PLA/siRNA complexes at high weight ratio. As mentioned in EGFP gene silencing efficiency, the maximum EGFP gene silencing of PLA/siRNA-EGFP complexes was at weight ratio of 5 (11.78 ± 1.32%). PLA was not suitable for delivering siRNA owing to high

cytotoxicity at this weight ratio. For CS/PLA/siRNA complexes, the cell viability decreased with the increasing of weight ratio and less than 80% at weight ratio of 5/1/1. This result suggested that the EGFP gene silencing efficiency of CS/PLA/siRNA-EGFP complexes decreased at high weight ratio due to the increasing of cytotoxicity of complexes.

Figure 4.29 illustrates the comparing of the cell viability of complexes at the weight ratio which provided the highest gene silencing. The viability of cells transfected with CS/PLA/siRNA complex at weight ratio of 5/0.5/1 (75.08 ± 4.72%) was not significantly different from cells treated with naked siRNA (85.73 ± 7.49%) and CS/siRNA complex at weight ratio of 5 (73.40 ± 2.13%). Whereas, the viability of cells transfected with PEI (25 kDa)/siRNA complexes at weight ratio of 2 and PLA/siRNA complexes at weight ratio of 5 was 66.30 ± 3.75% and 29.72 ± 0.94%, respectively, which was significantly lower than cells treated with naked siRNA. Moreover, the result demonstrated that the combination of CS and PLA could reduce the amount of PLA for siRNA delivery with lower cytotoxicity.

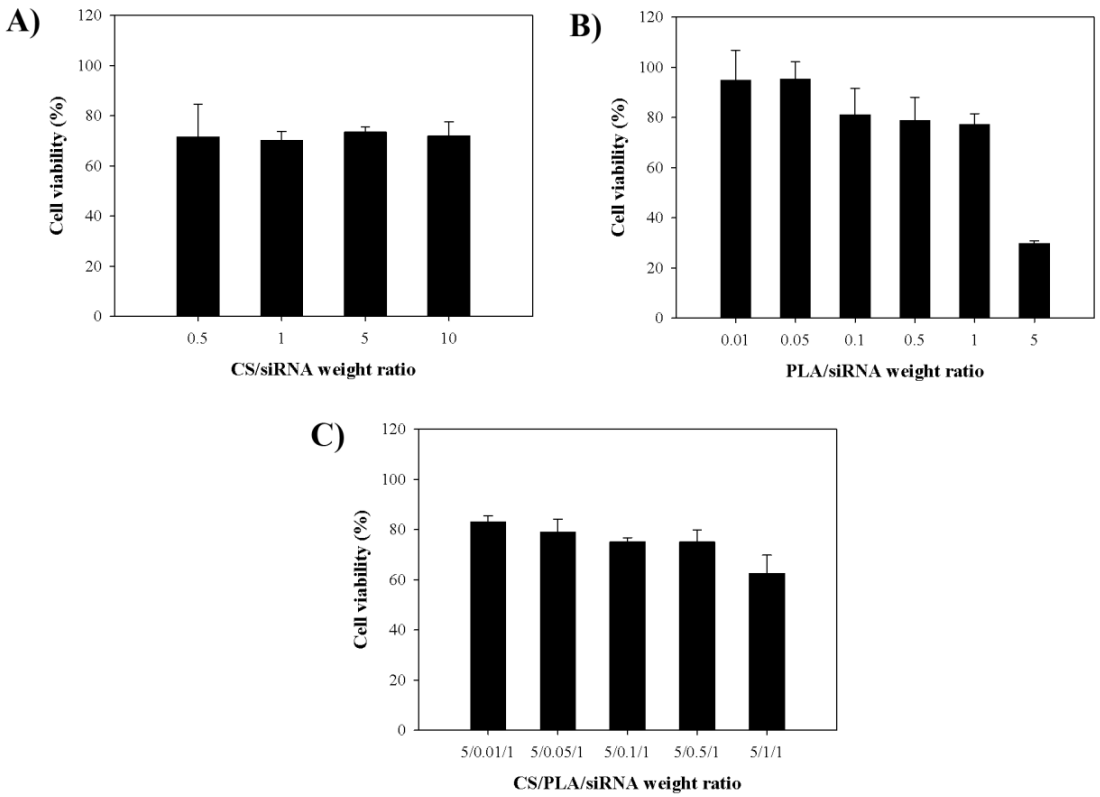

Figure 4.28 Cell viability of HeLa-EGFP cells after transfected with CS/siRNA complexes (A), PLA/siRNA complexes (B) and CS/PLA/siRNA complexes (C) at pH 7.4. Each value presented in mean ± SD of triplicate samples.

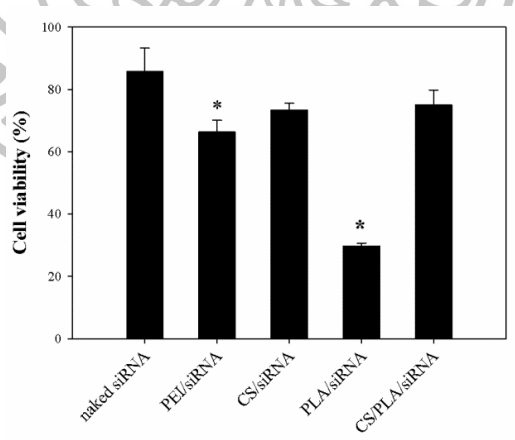

Figure 4.29 Cell viability of PEI (25 kDa)/siRNA, CS/siRNA, PLA/siRNA and CS/PLA/siRNA complexes at weight ratio of 2, 5, 5 and 5/0.5/1, respectively. Each value presented in mean ± SD of triplicate samples. * Significantly different from naked siRNA treated group ($p < 0.05$).

4.2.6 RNase protection ability of CS/PLA

The enzymatic degradation of siRNA is one of the important barriers for siRNA delivery resulting in reduction of therapeutic efficiency [227, 228]. To investigate the protection ability of CS combined with PLA from enzymatic degradation, the CS/PLA/siRNA complex was prepared at weight ratio of 5/0.5/1 which showed the maximum gene silencing. The complexes were incubated with RNase in different time points at 37 ˚C. As seen in Figure 4.30, CS combined with PLA could protect siRNA from RNase degradation and remained an intact siRNA at least 6 hr. In contrast, naked siRNA was totally degraded by contacting with RNase for 10 min. This result suggested CS combined with PLA was able to protect siRNA from RNase degradation during delivered siRNA and possible transferred for further *in vivo* study.

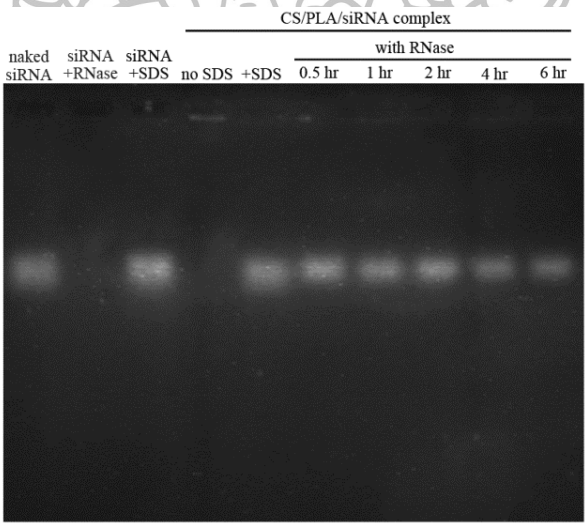

Figure 4.30 RNase protection ability of CS combined with PLA by incubating the complexes with RNase A at 37 ˚C at different time points. RNase A was inactivated by heating at 70 ˚C and the remaining siRNA was released by SDS. Naked siRNA was incubated with RNase A for 10 min and used as a control.

4.2.7 Cellular uptake pathway of polymers/siRNA-EGFP complexes

The uptake pathway study of complex is also important for understanding the intracellular route of complex which affects transfection efficiency. There are evidences that the internalization of particles via caveolae-mediated endocytosis could bypass lysosome system [229, 230]. Therefore, it will be more advantage to look for

the carriers that can deliver siRNA though non-endosome/lysosome pathway. In this study, the cellular uptake pathway of CS/siRNA-EGFP and CS/PLA/siRNA-EGFP was investigated using specific inhibitors in endocytosis pathway i.e.

a Chlorpromazine as an inhibitor for clathrin-mediated endocytosis (CME)
b Genistein, filipin and methyl-β-cyclodextrin as the inhibitors for caveolae-mediated endocytosis
c Nocodazole as an inhibitor for polymerization of microtubules
d Wortmannin as an inhibitor for macropinocytosis
e Ammonium chloride as an inhibitor for endosomal and lysosomal acidification

Before investigating the cellular uptake pathway of CS/PLA/siRNA and CS/siRNA complexes, the optimal concentration of inhibitors which did not affect cell viability was determined in HeLa-EGFP cell by MTT assay. The concentration of each inhibitor was showed in Table 4.4.

Table 4.4 The optimal concentration of inhibitors used in this study

Inhibitors	**Concentration**
Chlorpromazine	100 µM
Genistein	100 µM
Filipin	10 µM
Methyl- β-cyclodextrin	1 mM
Nocodazole	10 nM
Wortmannin	50 nM
Ammonium chloride	10 mM

After pre-incubated with inhibitors for 30 min, cells were transfected with CS/siRNA and CS/PLA/siRNA complex at weight ratio of 5 and 5/0.5/1, respectively, and further incubated for 6 hr. The percentage of EGFP gene silencing in the cells treated with inhibitors and non-treated cells was compared. For CS/siRNA complex,

the experiment was done at pH 6.4. Figure 4.31A, it illustrates that CS/siRNA complex was taken up though caveolae-mediated endocytosis as seen by the decrease of gene silencing in cells treated with genistein (2.48 ± 10.44 % of control). This result was agreed with the previous studies which suggested that CS/DNA complex was also taken up via caveolae-mediated endycytosis [231, 232].

For CS/PLA/siRNA complex uptake pathways, the result showed the decrease of EGFP gene silencing in cells treated with chlorpromazine (55.07 ± 13.43 % of control), genistein (35.75 ± 6.73 % of control) and ammonium chloride (64.03 ± 13.98 % of control) (Figure 4.31B). These results suggested that CS/PLA/siRNA complex was internalized into cells though clathrin-mediated endocytosis, caveolae-mediated endocytosis and enhanced transfection efficiency by facilitating acidification of endosome-lysosome system, respectively. There was also evidence that the uptake pathway of arginine-based polymeric carrier involved in both clathrin-mediated endocytosis and caveolae-mediated endocytosis [233]. This was probably the same phenomenon by combining CS with PLA for delivering siRNA. In addition, amine groups on PLA might also play role in proton sponge effect. Thus, the combination of CS and PLA assisted the delivery of siRNA into cells via more than one mechanism and could enhance transfection efficiency.

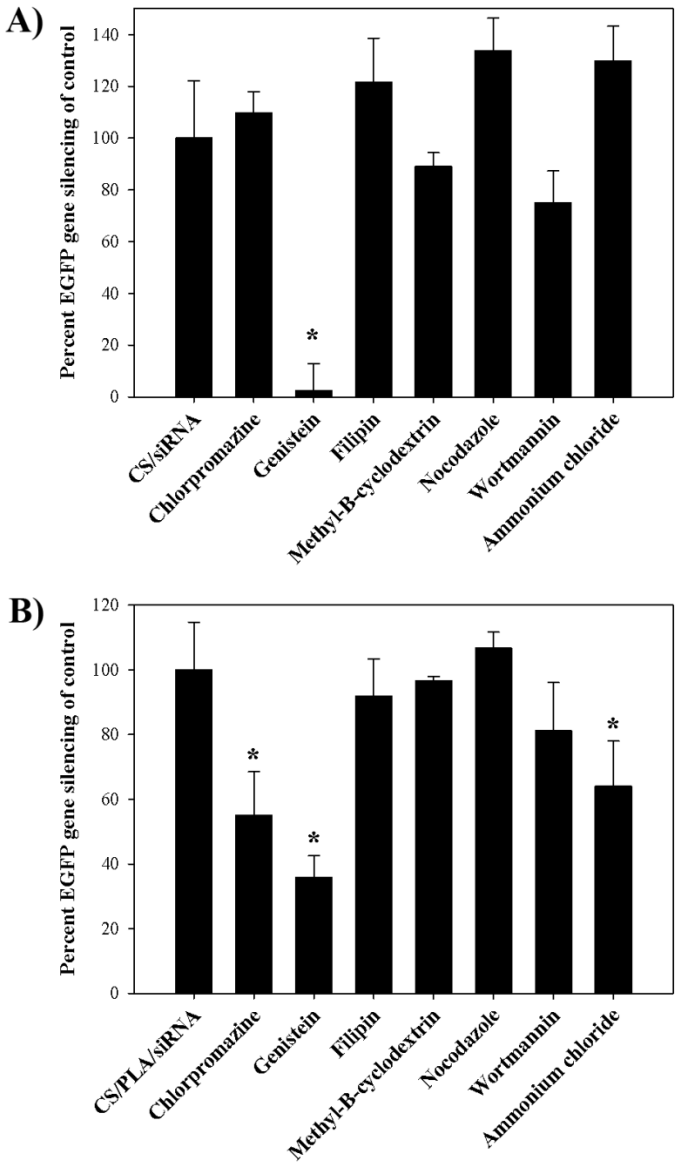

Figure 4.31 Effect of inhibitors on the percent EGFP gene silencing of CS/siRNA complex (A) and CS/PLA/siRNA complex (B) by taken the percent gene silencing of no-inhibitors treated group as 100% (control group). Each value presented in mean ± SD of triplicate samples. * Significantly different from control group ($p < 0.05$).

CHAPTER 5

CONCLUSION

In this study, the cationic polymers were used as carriers for gene delivery. The study involved in the development of dye adsorption method for determining the complete complex formation and also the investigation of efficiency of CS combined with PLA for siRNA delivery in HeLa cell stably expressing green fluorescence protein.

5.1 Dye adsorption method for determination of complete complex formation

Dichlorofluorescein, a dye adsorption which were used in Fajan's precipitation titration could successfully apply for estimating the complete complex formation between nucleic acid and cationic polymers prior to *in vitro* study. The weight ratio of complete complex formation which obtained from the developed method was comparable to general method i.e. gel retardation and zeta potential analysis. In addition, the weight ratio of complete complex formation from dye adsorption method was close to the weight ratio that gave the maximum transfection efficiency and gene silencing efficiency for PEI (25 kDa)/pEGFP complex and PEI (25 kDa)/siRNA-EGFP complex, respectively.

By comparing the dye adsorption method with other general method, it suggested that the developed method is fast, simple, safe for operators and environment as well as no sophisticate instruments were required. Although the dye adsorption method has many advantages for estimating the complete complex formation, there are also some limitations of this method. The nucleic acid amount of this method is higher than others since the detection is performed by visualization. The optimum pH for this method is at neutral to weak base for keeping the solubility and anionic charge of DCF ions. However, from the fundamental of dye adsorption method, it is not only a green and low-cost alternative method for routine task in the formulation of polymers and nucleic acids, but also a fast technique useful for the

screening of new polymers e.g. from the combinatorial synthesis prior to *in vitro* and *in vivo* evaluation of gene delivery performance.

5.2 Chitosan combined with poly L arginine for siRNA delivery

The new siRNA delivery system, CS (45 kDa) combined with PLA (> 70 kDa), was able to self-assembly form complex with siRNA into positive surface nanoparticle and efficiently delivered siRNA into HeLa-EGFP cell resulting in decreasing of GFP expression. By combining these two polymers, the limitation of each polymer was eliminated. This CS/PLA/siRNA complex was able to transfect cells at the physiological pH (7.4) and showed the maximum EGFP gene silencing at weight ratio of 5/0.5/1 with low cytotoxicity when compared with PEI 25 kDa (weight ratio of 2). Whereas the EGFP gene silencing effect of CS/siRNA complexes only occurred at pH 6.4 and PLA/siRNA complexes did not show EGFP gene silencing efficiency at both pH. Moreover, the gene silencing efficiency of CS/PLA/siRNA complex did not decrease in the present of serum (10% FBS) and CS/PLA had the RNase protection ability at least 6 hr.

For the internalization pathway of CS/PLA/siRNA complex, it suggested that CS/PLA/siRNA complex was taken up via clathrin-mediated endocytosis and caveolae-mediated endocytosis. After internalization, CS/PLA also showed the proton sponge effect which could enhance the transfection efficiency by endosomal escape. This supported that the CS combined with PLA improved siRNA delivery via more than one mechanism, whereas CS/siRNA was only taken up through caveolae-mediated endocytosis.

Therefore, this study suggested that CS combined with PLA was successfully delivered siRNA *in vitro*. However, the efficiency as well as toxicity of this carrier system *in vivo* still required.

REFERENCES

[1] El-Aneed, A. (2004). "An overview of current delivery systems in cancer gene therapy." **Journal of Controlled Release** 94, 1: 1-14.

[2] Jin, L., et al. (2014). "Current progress in gene delivery technology based on chemical methods and nano-carriers." **Theranostics** 4, 3: 240-255.

[3] Yin, H., et al. "Non-viral vectors for gene-based therapy." **Nature Reviews Genetics** 15, 8: 541-555.

[4] Yousefi, A., et al. "Trends in polymeric delivery of nucleic acids to tumors." **Journal of Controlled Release** 170, 2: 209-218.

[5] Al-Dosari, M. and X. Gao. (2009). "Nonviral Gene Delivery: Principle, Limitations, and Recent Progress." **The AAPS Journal** 11, 4: 671-681.

[6] Park, T.G., J.H. Jeong, and S.W. Kim. (2006). "Current status of polymeric gene delivery systems." **Advanced Drug Delivery Reviews** 58, 4: 467-486.

[7] Lungwitz, U., et al. (2005). "Polyethylenimine-based non-viral gene delivery systems." **European Journal of Pharmaceutics and Biopharmaceutics** 60, 2: 247-266.

[8] Godbey, W.T., K.K. Wu, and A.G. Mikos. (1999). "Poly(ethylenimine) and its role in gene delivery." **Journal of Controlled Release** 60, 2-3 (August): 149-160.

[9] Parker, A.L., et al. (2002). "Methodologies for Monitoring Nanoparticle Formation by Self-Assembly of DNA with Poly(l-lysine)." **Analytical Biochemistry** 302, 1 (January): 75-80.

[10] Lumpkin, O.J., P. Dejardin, and B.H. Zimm. (1985). "Theory of gel electrophoresis of DNA." **Biopolymers** 24, 8 (August): 1573-1593.

[11] Meyers, J.A., et al. (1976). "Simple agarose gel electrophoretic method for the identification and characterization of plasmid deoxyribonucleic acid." **Journal of Bacteriology** 127, 3 (September): 1529-1537.

[12] Singer, V.L., T.E. Lawlor, and S. Yue. (1999). "Comparison of SYBR® Green I nucleic acid gel stain mutagenicity and ethidium bromide mutagenicity in the Salmonella/mammalian microsome reverse mutation assay (Ames test)." **Mutation Research/Genetic Toxicology and Environmental Mutagenesis** 439, 1: 37-47.

[13] Waring, M.J. (1965). "Complex formation between ethidium bromide and nucleic acids." **Journal of molecular biology** 13, 1 (August): 269-282.

[14] 0, F.K.a.H. (1923). "A New method for titration of silver and halogen ions with organic dyestuff indicators." **Z. Elektrochem** 29: 6.

[15] Kolthoff, I.M. (1935). "Adsorption Indicators." **Chemical Reviews** 16, 1 (September): 87-98.

[16] Akinc, A., et al. (2008). "A combinatorial library of lipid-like materials for delivery of RNAi therapeutics." **Nature Biotechnology** 26, 5: 561-569.

[17] Green, J.J., R. Langer, and D.G. Anderson. (2008). "A Combinatorial Polymer Library Approach Yields Insight into Nonviral Gene Delivery." **Accounts of Chemical Research** 41, 6 (September): 749-759.

[18] Thomas, M., et al. (2007). "Identification of Novel Superior Polycationic Vectors for Gene Delivery by High-throughput Synthesis and Screening of a Combinatorial Library." **Pharmaceutical Research** 24, 8: 1564-1571.

[19] de Fougerolles, A., et al. (2007). "Interfering with disease: a progress report on siRNA-based therapeutics." **Nature Reviews Drug Discovery** 6, 6: 443-453.

[20] Zhang, S., et al. (2012). "Non-viral vectors for the mediation of RNAi." **Bioorganic Chemistry** 40, 0: 10-18.

[21] Grayson, A.C., A.M. Doody, and D. Putnam. (2006). "Biophysical and structural characterization of polyethylenimine-mediated siRNA delivery in vitro." **Pharmaceutical Research** 23, 8 (August): 1868-1876.

[22] Patil, M.L., et al. (2008). "Surface-modified and internally cationic polyamidoamine dendrimers for efficient siRNA delivery." **Bioconjugate Chemistry** 19, 7 (July): 1396-1403.

[23] Urban-Klein, B., et al. (2005). "RNAi-mediated gene-targeting through systemic application of polyethylenimine (PEI)-complexed siRNA in vivo." **Gene therapy** 12, 5 (March): 461-466.

[24] Zhou, J., et al. (2006). "PAMAM dendrimers for efficient siRNA delivery and potent gene silencing." **Chemical communications (Cambridge, England)** 22 (June): 2362-2364.

[25] Lavertu, M., et al. (2006). "High efficiency gene transfer using chitosan/DNA nanoparticles with specific combinations of molecular weight and

degree of deacetylation." **Biomaterials** 27, 27 (September): 4815-4824.

[26] Sato, T., T. Ishii, and Y. Okahata. (2001). "In vitro gene delivery mediated by chitosan. effect of pH, serum, and molecular mass of chitosan on the transfection efficiency." **Biomaterials** 22, 15 (August): 2075-2080.

[27] Xu, S., et al. (2007). "Direct force measurements between siRNA and chitosan molecules using force spectroscopy." **Biophysical journal** 93, 3 (August): 952-959.

[28] Martin, M.E. and K.G. Rice. (2007). "Peptide-guided gene delivery." **AAPS Journal** 9, 1: E18-29.

[29] Saccardo, P., A. Villaverde, and N. Gonzalez-Montalban. (2009). "Peptide-mediated DNA condensation for non-viral gene therapy." **Biotechnology advances** 27, 4 (July-August): 432-438.

[30] Yamagata, M., et al. (2007). "Structural advantage of dendritic poly(L-lysine) for gene delivery into cells." **Bioorganic & medicinal chemistry** 15, 1 (January): 526-532.

[31] Shahana, S., C. Kampf, and G.M. Roomans. (2002). "Effects of the cationic protein poly-L-arginine on airway epithelial cells in vitro." **Mediators of inflammation** 11, 3 (June): 141-148.

[32] Kim, E.J., et al. (2009). "Hyaluronic acid complexed to biodegradable poly L-arginine for targeted delivery of siRNAs." **Journal of Gene Medicine** 11, 9 (September): 791-803.

[33] Noh, S.M., et al. (2010). "Pegylated poly-l-arginine derivatives of chitosan for effective delivery of siRNA." **Journal of Controlled Release** 145, 2 (July): 159-164.

[34] Opanasopit, P., et al. (2011). "Chitosan enhances transfection efficiency of cationic polypeptides/DNA complexes." **Int J Pharm** 410, 1-2 (May 30): 161-168.

[35] Vercauteren, D., et al. "The Use of Inhibitors to Study Endocytic Pathways of Gene Carriers: Optimization and Pitfalls." **Molecular Therapy** 18, 3: 561-569.

[36] Khalil, I.A., et al. (2006). "Uptake pathways and subsequent intracellular trafficking in nonviral gene delivery." **Pharmacological Reviews** 58, 1 (March): 32-45.

[37] Wirth, T., N. Parker, and S. Ylä-Herttuala. (2013). "History of gene therapy." **Gene** 525, 2: 162-169.

[38] Wang, D. and G. Gao. (2014). "STATE-OF-THE-ART HUMAN GENE THERAPY: PART II. GENE THERAPY STRATEGIES AND APPLICATIONS." **Discovery medicine** 18, 98: 151-161.

[39] Cotrim, A.P. and B.J. Baum. (2008). "Gene Therapy: Some History, Applications, Problems, and Prospects." **Toxicologic Pathology** 36, 1 (January): 97-103.

[40] Mhashilkar, A., et al. (2001). "Gene therapy: Therapeutic approaches and implications." **Biotechnology Advances** 19, 4: 279-297.

[41] Resnik, D.B. and P.J. Langer. (2001). "Human Germline Gene Therapy Reconsidered." **Human Gene Therapy** 12, 11 (July): 1449-1458.

[42] Anderson, W.F. (1985). "Human Gene Therapy: Scientific and Ethical Considerations." **Journal of Medicine and Philosophy** 10, 3 (August): 275-292.

[43] Ibraheem, D., A. Elaissari, and H. Fessi. (2014). "Gene therapy and DNA delivery systems." **International Journal of Pharmaceutics** 459, 1–2: 70-83.

[44] Stribley, J.M., et al. (2002). "Gene therapy and reproductive medicine." **Fertility and Sterility** 77, 4: 645-657.

[45] Hacein-Bey-Abina , S., et al. (2002). "Sustained Correction of X-Linked Severe Combined Immunodeficiency by ex Vivo Gene Therapy." **New England Journal of Medicine** 346, 16: 1185-1193.

[46] Soofiyani, S.R., et al. (2013). "Gene therapy, early promises, subsequent problems, and recent breakthroughs." **Advanced pharmaceutical bulletin** 3, 2: 249.

[47] Nayerossadat, N., T. Maedeh, and P.A. Ali. (2012). "Viral and nonviral delivery systems for gene delivery." **Advanced biomedical research** 1, 1: 27.

[48] Nam, H.Y., et al. (2009). "Lipid-based emulsion system as non-viral gene carriers." **Archives of Pharmacal Research** 32, 5: 639-646.

[49] Soutschek, J., et al. (2004). "Therapeutic silencing of an endogenous gene by systemic administration of modified siRNAs." **Nature** 432, 7014: 173-178.

[50] Kawabata, K., Y. Takakura, and M. Hashida. (1995). "The fate of plasmid DNA after intravenous injection in mice: involvement of scavenger receptors in its hepatic uptake." **Pharmaceutical Research** 12, 6 (June): 825-830.

[51] Nagasaki, T. and S. Shinkai. (2007). "The concept of molecular machinery is useful for design of stimuli-responsive gene delivery systems in the mammalian cell." **Journal of Inclusion Phenomena and Macrocyclic Chemistry** 58, 3: 205-219.

[52] Wiethoff, C.M. and C.R. Middaugh. (2003). "Barriers to Nonviral Gene Delivery." **Journal of Pharmaceutical Sciences** 92, 2: 203-217.

[53] Somia, N. and I.M. Verma. (2000). "Gene therapy: trials and tribulations." **Nature Reviews Genetics** 1, 2: 91-99.

[54] Kay, M.A., J.C. Glorioso, and L. Naldini. (2001). "Viral vectors for gene therapy: the art of turning infectious agents into vehicles of therapeutics." **Nature Medicine** 7, 1: 33-40.

[55] Bouard, D., N. Alazard-Dany, and F.L. Cosset. (2009). "Viral vectors: from virology to transgene expression." **British Journal of Pharmacology** 157, 2: 153-165.

[56] Lowenstein, P.R., et al. (2007). "Immune responses to adenovirus and adeno-associated vectors used for gene therapy of brain diseases: the role of immunological synapses in understanding the cell biology of neuroimmune interactions." **Current Gene Therapy** 7, 5 (October): 347-360.

[57] Bushman, F.D. (2007). "Retroviral integration and human gene therapy." **Journal of Clinical Investigation** 117, 8: 2083-2086.

[58] Hacein-Bey-Abina, S., et al. (2003). "LMO2-associated clonal T cell proliferation in two patients after gene therapy for SCID-X1." **Science** 302, 5644 (October): 415-419.

[59] Nair, V. (2008). "Retrovirus-induced oncogenesis and safety of retroviral vectors." **Current opinion in molecular therapeutics** 10, 5 (October): 431-438.

[60] Vorburger, S.A. and K.K. Hunt. (2002). "Adenoviral Gene Therapy." **The Oncologist** 7, 1 (February): 46-59.

[61] Giacca, M. and S. Zacchigna. (2012). "Virus-mediated gene delivery for human gene therapy." **Journal of Controlled Release** 161, 2: 377-388.

[62] Lai, C.M., Y.K. Lai, and P.E. Rakoczy. (2002). "Adenovirus and adeno-associated virus vectors." **DNA Cell Biology** 21, 12 (December): 895-913.

[63] Flotte, T., et al. (1996). "A phase I study of an adeno-associated virus-CFTR gene vector in adult CF patients with mild lung disease." **Human Gene Therapy** 7, 9 (June): 1145-1159.

[64] Nathwani , A.C., et al. (2011). "Adenovirus-Associated Virus Vector–Mediated Gene Transfer in Hemophilia B." **New England Journal of Medicine** 365, 25: 2357-2365.

[65] Wang, B., J. Li, and X. Xiao. (2000). "Adeno-associated virus vector carrying human minidystrophin genes effectively ameliorates muscular dystrophy in mdx mouse model." **Proceedings of the National Academy of Sciences** 97, 25 (December): 13714-13719.

[66] Hauswirth, W.W., et al. (2008). "Treatment of Leber Congenital Amaurosis Due to RPE65 Mutations by Ocular Subretinal Injection of Adeno-Associated Virus Gene Vector: Short-Term Results of a Phase I Trial." **Human Gene Therapy** 19, 10 (October): 979-990.

[67] Maguire-Zeiss, K.A., W.J. Bowers, and H.J. Federoff. (2001). "HSV vector-mediated gene delivery to the central nervous system." **Current opinion in molecular therapeutics** 3, 5 (October): 482-490.

[68] Marconi, P., R. Manservigi, and A.L. Epstein. (2010). "HSV-1-derived helper-independent defective vectors, replicating vectors and amplicon vectors, for the treatment of brain diseases." **Current opinion in drug discovery & development** 13, 2 (March): 169-183.

[69] Latchman, D.S. (2002). "Herpes Simplex Virus Vectors for Gene Delivery to a Variety of Different Cell Types." **Current Gene Therapy** 2, 4: 415-426.

[70] Wolfe, D., M. Mata, and D.J. Fink. (2009). "A human trial of HSV-mediated gene transfer for the treatment of chronic pain." **Gene therapy** 16, 4: 455-460.

[71] Shen, Y. and J. Nemunaitis. (2006). "Herpes simplex virus 1 (HSV-1) for cancer treatment." **Cancer Gene Therapy** 13, 11: 975-992.

[72] Cockrell, A.S. and T. Kafri. (2007). "Gene delivery by lentivirus vectors." **Molecular Biotechnology** 36, 3: 184-204.

[73] Wong, L.-F., et al. (2006). "Lentivirus-mediated gene transfer to the central nervous system: therapeutic and research applications." **Human gene therapy** 17, 1: 1-9.

[74] Gao, X., K.-S. Kim, and D. Liu. "Nonviral gene delivery: What we know and what is next." **The AAPS Journal** 9, 1: E92-E104.

[75] Capecchi, M.R. (1980). "High efficiency transformation by direct microinjection of DNA into cultured mammalian cells." **Cell** 22, 2 Pt 2 (November): 479-488.

[76] Mehier-Humbert, S. and R.H. Guy. (2005). "Physical methods for gene transfer: Improving the kinetics of gene delivery into cells." **Advanced Drug Delivery Reviews** 57, 5: 733-753.

[77] O'Brien, J. and S.C. Lummis. (2002). "An improved method of preparing microcarriers for biolistic transfection." **Brain Research Protocols** 10, 1 (August): 12-15.

[78] Heller, L.C., K. Ugen, and R. Heller. (2005). "Electroporation for targeted gene transfer." **Expert Opin Drug Deliv** 2, 2 (March): 255-268.

[79] Hofmann, G.A., et al. (1999). "Electroporation therapy of solid tumors." **Critical reviews in therapeutic drug carrier systems** 16, 6: 523-569.

[80] Miao, C.H., X. Ye, and A.R. Thompson. (2003). "High-level factor VIII gene expression in vivo achieved by nonviral liver-specific gene therapy vectors." **Human Gene Therapy** 14, 14 (September): 1297-1305.

[81] Herweijer, H. and J.A. Wolff. (2007). "Gene therapy progress and prospects: hydrodynamic gene delivery." **Gene Therapy** 14, 2 (January): 99-107.

[82] Jiang, J., E. Yamato, and J. Miyazaki. (2001). "Intravenous delivery of naked plasmid DNA for in vivo cytokine expression." **Biochemical and Biophysical Research Communications** 289, 5 (December): 1088-1092.

[83] Maruyama, H., et al. (2004). "Rat liver-targeted naked plasmid DNA transfer by tail vein injection." **Molecular Biotechnology** 26, 2 (Febuary): 165-172.

[84] Wells, D.J. (2004). "Gene therapy progress and prospects: electroporation and other physical methods." **Gene therapy** 11, 18 (September): 1363-1369.

[85] Gupta, P.K. and C.T. Hung. (1989). "Magnetically controlled targeted micro-carrier systems." **Life Science** 44, 3: 175-186.

[86] Scherer, F., et al. (2002). "Magnetofection: enhancing and targeting gene delivery by magnetic force in vitro and in vivo." **Gene therapy** 9, 2 (January): 102-109.

[87] Fraley, R., et al. (1980). "Introduction of liposome-encapsulated SV40 DNA into cells." **Journal of Biological Chemistry** 255, 21 (November): 10431-10435.

[88] Al-Dosari, M.S. and X. Gao. (2009). "Nonviral Gene Delivery: Principle, Limitations, and Recent Progress." **The AAPS Journal** 11, 4 :671-681.

[89] Farhood, H., N. Serbina, and L. Huang. (1995). "The role of dioleoyl phosphatidylethanolamine in cationic liposome mediated gene transfer." **Biochim Biophys Acta** 1235, 2 (May): 289-295.

[90] Tros de Ilarduya, C., Y. Sun, and N. Duzgunes. (2010). "Gene delivery by lipoplexes and polyplexes." **European journal of pharmaceutical sciences** 40, 3 (June): 159-170.

[91] Kwoh, D.Y., et al. (1999). "Stabilization of poly-L-lysine/DNA polyplexes for in vivo gene delivery to the liver." **Biochimica et Biophysica Acta (BBA) - Biomembranes** 1444, 2 (Febuary): 171-190.

[92] Ogris, M., et al. (1999). "PEGylated DNA/transferrin-PEI complexes: reduced interaction with blood components, extended circulation in blood and potential for systemic gene delivery." **Gene Therapy** 6, 4 (April): 595-605.

[93] Nishikawa, M., et al. (1998). "Targeted delivery of plasmid DNA to hepatocytes in vivo: optimization of the pharmacokinetics of plasmid DNA/galactosylated poly(L-lysine) complexes by controlling their physicochemical properties." **Journal of Pharmacology and Experimental Therapeutics** 287, 1 (October): 408-415.

[94] Nah, J.W., et al. (2002). "Artery wall binding peptide-poly(ethylene glycol)-grafted-poly(L-lysine)-based gene delivery to artery wall cells." **Journal of Controlled Release** 78, 1-3 (January): 273-284.

[95] Suh, W., et al. (2001). "Anti-JL1 antibody-conjugated poly (L-lysine) for targeted gene delivery to leukemia T cells." **Journal of Controlled Release** 72, 1-3 (May): 171-178.

[96] Boussif, O., et al. (1995). "A versatile vector for gene and oligonucleotide transfer into cells in culture and in vivo: polyethylenimine." **Proceedings of the National Academy of Sciences of the United States of America** 92, 16 (August): 7297-7301.

[97] Godbey, W.T., K.K. Wu, and A.G. Mikos. (1999). "Size matters: molecular weight affects the efficiency of poly(ethylenimine) as a gene delivery vehicle." **Journal of Biomedical Materials Research** 45, 3 (June): 268-275.

[98] Neu, M., D. Fischer, and T. Kissel. (2005). "Recent advances in rational gene transfer vector design based on poly(ethylene imine) and its derivatives." **Journal of Gene Medicine** 7, 8 (August): 992-1009.

[99] Dunlap, D.D., et al. (1997). "Nanoscopic structure of DNA condensed for gene delivery." **Nucleic Acids Research** 25, 15: 3095-3101.

[100] Lee, H., J.H. Jeong, and T.G. Park. (2001). "A new gene delivery formulation of polyethylenimine/DNA complexes coated with PEG conjugated fusogenic peptide." **Journal of Controlled Release** 76, 1-2 (September): 183-192.

[101] Suh, W., et al. (2002). "An angiogenic, endothelial-cell-targeted polymeric gene carrier." **Molecular Therapy** 6, 5: 664-672.

[102] Chiu, S.J., N.T. Ueno, and R.J. Lee. (2004). "Tumor-targeted gene delivery via anti-HER2 antibody (trastuzumab, Herceptin) conjugated polyethylenimine." **Journal of Controlled Release** 97, 2 (Junuary): 357-369.

[103] Benns, J.M., et al. (2001). "Folate-PEG-folate-graft-polyethylenimine-based gene delivery." **Journal of Drug Targeting** 9, 2 (April): 123-139.

[104] Lim, Y.B., et al. (2000). "Biodegradable polyester, poly[alpha-(4-aminobutyl)-L-glycolic acid], as a non-toxic gene carrier." **Pharmaceutical Research** 17, 7 (July): 811-816.

[105] Lynn, D.M. and R. Langer. (2000). "Degradable Poly(β-amino esters): Synthesis, Characterization, and Self-Assembly with Plasmid DNA." **Journal of the American Chemical Society** 122, 44 (November): 10761-10768.

[106] Gonzalez, H., S.J. Hwang, and M.E. Davis. (1999). "New Class of Polymers for the Delivery of Macromolecular Therapeutics." **Bioconjugate Chemistry** 10, 6 (November): 1068-1074.

[107] Gonzalez, H., S.J. Hwang, and M.E. Davis. (1999). "New class of polymers for the delivery of macromolecular therapeutics." **Bioconjugate Chemistry** 10, 6 (November-December): 1068-1074.

[108] Borchard, G. (2001). "Chitosans for gene delivery." **Advance Drug Delivery Review** 52, 2 (November): 145-150.

[109] Ishii, T., Y. Okahata, and T. Sato. (2001). "Mechanism of cell transfection with plasmid/chitosan complexes." **Biochimica et Biophysica Acta (BBA) - Biomembranes** 1514, 1: 51-64.

[110] Kean, T., S. Roth, and M. Thanou. (2005). "Trimethylated chitosans as non-viral gene delivery vectors: cytotoxicity and transfection efficiency." **Journal of Controlled Release** 103, 3 (April): 643-653.

[111] Germershaus, O., et al. (2008). "Gene delivery using chitosan, trimethyl chitosan or polyethylenglycol-graft-trimethyl chitosan block copolymers: establishment of structure-activity relationships in vitro." **Journal of Controlled Release** 125, 2 (January): 145-154.

[112] Yu, H., et al. (2007). "Poly(L-lysine)-graft-chitosan copolymers: synthesis, characterization, and gene transfection effect." **Biomacromolecules** 8, 5 (May): 1425-1435.

[113] Chan, P., et al. (2007). "Synthesis and characterization of chitosan-g-poly(ethylene glycol)-folate as a non-viral carrier for tumor-targeted gene delivery." **Biomaterials** 28, 3 (January): 540-549.

[114] Hill, A.B., et al. (2016). "Overcoming Gene-Delivery Hurdles: Physiological Considerations for Nonviral Vectors." **Trends in Biotechnology** 34, 2: 91-105.

[115] Pouton, C.W. and L.W. Seymour. (2001). "Key issues in non-viral gene delivery1." **Advanced Drug Delivery Reviews** 46, 1–3: 187-203.

[116] Zhang, S., et al. (2009). "Size-Dependent Endocytosis of Nanoparticles." **Advanced materials (Deerfield Beach, Fla.)** 21: 419-424.

[117] Zhou, X. and L. Huang. (1994). "DNA transfection mediated by cationic liposomes containing lipopolylysine: characterization and mechanism of action." **Biochimica et Biophysica Acta (BBA) - Biomembranes** 1189, 2: 195-203.

[118] Nishikawa, M. and L. Huang. (2001). "Nonviral Vectors in the New Millennium: Delivery Barriers in Gene Transfer." **Human Gene Therapy** 12, 8 (May): 861-870.

[119] Yang, J.P. and L. Huang. (1997). "Overcoming the inhibitory effect of serum on lipofection by increasing the charge ratio of cationic liposome to DNA." **Gene therapy** 4, 9 (September): 950-960.

[120] Collard, W.T., et al. (2000). "Biodistribution, metabolism, and in vivo gene expression of low molecular weight glycopeptide polyethylene glycol peptide DNA co-condensates." **Journal of Pharmaceutical Sciences** 89, 4 (April): 499-512.

[121] Zhang, J.S., F. Liu, and L. Huang. (2005). "Implications of pharmacokinetic behavior of lipoplex for its inflammatory toxicity." **Advanced drug delivery reviews** 57, 5 (April): 689-698.

[122] Wang, T., J.R. Upponi, and V.P. Torchilin. (2012). "Design of multifunctional non-viral gene vectors to overcome physiological barriers: dilemmas and strategies." **International journal of pharmaceutics** 427, 1 (May): 3-20.

[123] Rejman, J., A. Bragonzi, and M. Conese. (2005). "Role of clathrin- and caveolae-mediated endocytosis in gene transfer mediated by lipo- and polyplexes." **Molecular Therapy** 12, 3 (September): 468-474.

[124] Payne, C.K., et al. (2007). "Internalization and trafficking of cell surface proteoglycans and proteoglycan-binding ligands." **Traffic** 8, 4 (April): 389-401.

[125] Jones, C.H., et al. (2013). "Overcoming Nonviral Gene Delivery Barriers: Perspective and Future." **Molecular Pharmaceutics** 10, 11 (November): 4082-4098.

[126] Rejman, J., et al. (2004). "Size-dependent internalization of particles via the pathways of clathrin- and caveolae-mediated endocytosis." **Biochemical journal** 377, Pt 1 (January): 159-169.

[127] Dauty, E. and A.S. Verkman. (2005). "Actin Cytoskeleton as the Principal Determinant of Size-dependent DNA Mobility in Cytoplasm: A NEW BARRIER FOR NON-VIRAL GENE DELIVERY." **Journal of Biological Chemistry** 280, 9 (March): 7823-7828.

[128] Gruenberg, J. and F.G. van der Goot. (2006). "Mechanisms of pathogen entry through the endosomal compartments." **Nature Reviews Molecular Cell Biology** 7, 7: 495-504.

[129] Lian Jin, X.Z., Ming Liu, Yan Deng, Nongyue He. (2014). "Current Progress in Gene Delivery Technology Based on Chemical Methods and Nano-carriers." **Theranostics** 4, 3: 240-255.

[130] Lechardeur, D., et al. (1999). "Metabolic instability of plasmid DNA in the cytosol: a potential barrier to gene transfer." **Gene Therapy** 6, 4 (April): 482-497.

[131] ur Rehman, Z., D. Hoekstra, and I.S. Zuhorn. (2013). "Mechanism of polyplex- and lipoplex-mediated delivery of nucleic acids: real-time visualization of transient membrane destabilization without endosomal lysis." **ACS Nano** 7, 5 (May): 3767-3777.

[132] van der Aa, M.A., et al. (2006). "The nuclear pore complex: the gateway to successful nonviral gene delivery." **Pharmaceutical research** 23, 3 (March): 447-459.

[133] Branden, L.J., A.J. Mohamed, and C.I. Smith. (1999). "A peptide nucleic acid-nuclear localization signal fusion that mediates nuclear transport of DNA." **Nature Biotechnology** 17, 8 (August): 784-787.

[134] Xiang, S., et al. (2012). "Uptake mechanisms of non-viral gene delivery." **Journal of controlled release** 158, 3 (March): 371-378.

[135] Hillaireau, H. and P. Couvreur. (2009). "Nanocarriers' entry into the cell: relevance to drug delivery." **Cellular and Molecular Life Sciences** 66, 17 (September): 2873-2896.

[136] Aderem, A. and D.M. Underhill. (1999). "Mechanisms of phagocytosis in macrophages." **Annual Review of Immunology** 17: 593-623.

[137] Pearse, B.M. (1976). "Clathrin: a unique protein associated with intracellular transfer of membrane by coated vesicles." **Proceedings of the National Academy of Sciences of the United States of America** 73, 4: 1255-1259.

[138] Brodsky, F.M., et al. (2001). "Biological basket weaving: formation and function of clathrin-coated vesicles." **Annual Review of Cell and Developmental Biology** 17, (November): 517-568.

[139] Subtil, A., et al. (1999). "Acute cholesterol depletion inhibits clathrin-coated pit budding." **Proceedings of the National Academy of Sciences of the United States of America** 96, 12 (June): 6775-6780.

[140] Luzio, J.P., et al. (2009). "The delivery of endocytosed cargo to lysosomes." **Biochemical Society Transactions** 37, Pt 5 (October): 1019-1021.

[141] van der Aa, M.A.E.M., et al. (2007). "Cellular Uptake of Cationic Polymer-DNA Complexes Via Caveolae Plays a Pivotal Role in Gene Transfection in COS-7 Cells." **Pharmaceutical Research** 24, 8: 1590-1598.

[142] Wang, Z., et al. (2009). "Size and dynamics of caveolae studied using nanoparticles in living endothelial cells." **ACS Nano** 3, 12 (December): 4110-4116.

[143] Bengali, Z., J.C. Rea, and L.D. Shea. (2007). "Gene expression and internalization following vector adsorption to immobilized proteins: dependence on protein identity and density." **Journal of Gene Medicine** 9, 8 (August): 668-678.

[144] Matveev, S., et al. (2001). "The role of caveolae and caveolin in vesicle-dependent and vesicle-independent trafficking." **Advanced Drug Delivery Reviews** 49, 3 (July): 237-250.

[145] Swanson, J.A. and C. Watts. (1995). "Macropinocytosis." **Trends in cell biology** 5, 11 (November): 424-428.

[146] Hewlett, L.J., A.R. Prescott, and C. Watts. (1994). "The coated pit and macropinocytic pathways serve distinct endosome populations." **Journal of Cell Biology** 124, 5 (March): 689-703.

[147] Kaplan, I.M., J.S. Wadia, and S.F. Dowdy. (2005). "Cationic TAT peptide transduction domain enters cells by macropinocytosis." **Journal of Controlled Release** 102, 1 (January): 247-253.

[148] Zuhorn, I.S., R. Kalicharan, and D. Hoekstra. (2002). "Lipoplex-mediated transfection of mammalian cells occurs through the cholesterol-dependent clathrin-mediated pathway of endocytosis." **The Journal of biological chemistry** 277, 20 (May): 18021-18028.

[149] Parton, R.G., B. Joggerst, and K. Simons. (1994). "Regulated internalization of caveolae." **The Journal of cell biology** 127, 5: 1199-1215.

[150] Ivanov, A.I. (2008). "Pharmacological inhibition of endocytic pathways: is it specific enough to be useful?" **Exocytosis and Endocytosis**: 15-33.

[151] Tartakoff, A.M. (1983). "Perturbation of vesicular traffic with the carboxylic ionophore monensin." **Cell** 32, 4: 1026-1028.

[152] Wattiaux, R., et al. (2000). "Endosomes, lysosomes: their implication in gene transfer." **Advanced drug delivery reviews** 41, 2: 201-208.

[153] Duchardt, F., et al. (2007). "A comprehensive model for the cellular uptake of cationic cell-penetrating peptides." **Traffic** 8, 7: 848-866.

[154] Furuta, K., et al. (1999). "Differential expression of the lysosome-associated membrane proteins in normal human tissues." **Archives of biochemistry and biophysics** 365, 1: 75-82.

[155] Duclos, S., R. Corsini, and M. Desjardins. (2003). "Remodeling of endosomes during lysosome biogenesis involveskiss and run'fusion events regulated by rab5." **Journal of Cell Science** 116, 5: 907-918.

[156] Fire, A., et al. (1998). "Potent and specific genetic interference by double-stranded RNA in Caenorhabditis elegans." **nature** 391, 6669: 806-811.

[157] Bartel, D.P. (2004). "MicroRNAs: genomics, biogenesis, mechanism, and function." **cell** 116, 2: 281-297.

[158] Takeshita, F. and T. Ochiya. (2006). "Therapeutic potential of RNA interference against cancer." **Cancer science** 97, 8: 689-696.

[159] Elbashir, S.M., et al. (2001). "Duplexes of 21-nucleotide RNAs mediate RNA interference in cultured mammalian cells." **nature** 411, 6836: 494-498.

[160] Hickerson, R.P., et al. (2008). "Stability study of unmodified siRNA and relevance to clinical use." **Oligonucleotides** 18, 4: 345-354.

[161] Gavrilov, K. and W.M. Saltzman. (2012). "Therapeutic siRNA: principles, challenges, and strategies." **Yale journal of biology and medicine** 85, 2: 187-200.

[162] Birmingham, A., et al. (2006). "3′ UTR seed matches, but not overall identity, are associated with RNAi off-targets." **Nature methods** 3, 3: 199-204.

[163] Hornung, V., et al. (2005). "Sequence-specific potent induction of IFN-α by short interfering RNA in plasmacytoid dendritic cells through TLR7." **Nature medicine** 11, 3: 263-270.

[164] McLeod, H.L. (2013). "Cancer pharmacogenomics: early promise, but concerted effort needed." **Science** 339, 6127: 1563-1566.

[165] Miele, E., et al. (2012). "Nanoparticle-based delivery of small interfering RNA: challenges for cancer therapy." **International Journal of Nanomedicine** 7: 3637-3657.

[166] Ramachandran, P.V. and S. Ignacimuthu. (2012). "RNA interference as a plausible anticancer therapeutic tool." **Asian Pacific Journal of Cancer Prevention** 13, 6: 2445-2452.

[167] Tomek, M., T. Akiyama, and C.R. Dass. (2012). "Role of Bcl-2 in tumour cell survival and implications for pharmacotherapy." **Journal of Pharmacy and Pharmacology** 64, 12: 1695-1702.

[168] Fu, G.-F., et al. (2005). "RNA interference remarkably suppresses bcl-2 gene expression in cancer cells in vitro and in vivo." **Cancer biology & therapy** 4, 8: 822-829.

[169] Fakih, M. (2013). "The evolving role of VEGF-targeted therapies in the treatment of metastatic colorectal cancer." **Expert review of anticancer therapy** 13, 4: 427-438.

[170] Shi, Y., et al. (2013). "VEGF-C ShRNA inhibits pancreatic cancer growth and lymphangiogenesis in an orthotopic fluorescent nude mouse model." **Anticancer research** 33, 2: 409-417.

[171] Yan, C., et al. (2013). "RNA interference-mediated silencing of VEGF and bFGF suppresses endostatin secretion in pancreatic carcinoma cells." **Oncology letters** 5, 3: 1031-1035.

[172] Zhang, Q. and F. Li. (2013). "Combating P-glycoprotein-mediated multidrug resistance using therapeutic nanoparticles." **Current pharmaceutical design** 19, 37: 6655-6666.

[173] Chen, Y., et al. (2010). "Multifunctional nanoparticles delivering small interfering RNA and doxorubicin overcome drug resistance in cancer." **Journal of Biological Chemistry** 285, 29: 22639-22650.

[174] Lu, P., et al. (2012). "Effect of GPE-AGT nanoparticle shRNA transfection system mediated RNAi on early atherosclerotic lesion." **International journal of clinical and experimental pathology** 5, 7: 698-706.

[175] Xue, B., et al. (2012). "PVN adenovirus-siRNA injections silencing either NOX2 or NOX4 attenuate aldosterone/NaCl-induced hypertension in mice." **American Journal of Physiology-Heart and Circulatory Physiology** 302, 3: H733-H741.

[176] Salta, E. and B. De Strooper. (2012). "Non-coding RNAs with essential roles in neurodegenerative disorders." **The Lancet Neurology** 11, 2: 189-200.

[177] Harper, S.Q., et al. (2005). "RNA interference improves motor and neuropathological abnormalities in a Huntington's disease mouse model." **Proceedings of the National Academy of Sciences of the United States of America** 102, 16: 5820-5825.

[178] Peng, K.A. and E. Masliah. (2010). "Lentivirus-expressed siRNA vectors against Alzheimer disease." **Lentivirus Gene Engineering Protocols: Second Edition**: 215-224.

[179] Hong, C., et al. (2006). "Herpes simplex virus RNAi and neprilysin gene transfer vectors reduce accumulation of Alzheimer's disease-related amyloid-β peptide in vivo." **Gene therapy** 13, 14: 1068-1079.

[180] Sapru, M.K., et al. (2006). "Silencing of human α-synuclein in vitro and in rat brain using lentiviral-mediated RNAi." **Experimental neurology** 198, 2: 382-390.

[181] Lee, N.S., et al. (2002). "Expression of small interfering RNAs targeted against HIV-1 rev transcripts in human cells." **Nature biotechnology** 20, 5: 500-505.

[182] Novina, C.D., et al. (2002). "siRNA-directed inhibition of HIV-1 infection." **Nature medicine** 8, 7: 681-686.

[183] Martínez, M.A., et al. (2002). "Suppression of chemokine receptor expression by RNA interference allows for inhibition of HIV-1 replication." **Aids** 16, 18: 2385-2390.

[184] Krönke, J., et al. (2004). "Alternative approaches for efficient inhibition of hepatitis C virus RNA replication by small interfering RNAs." **Journal of virology** 78, 7: 3436-3446.

[185] Czech, M.P., M. Aouadi, and G.J. Tesz. (2011). "RNAi-based therapeutic strategies for metabolic disease." **Nature Reviews Endocrinology** 7, 8: 473-484.

[186] Chang, J.-H., et al. (2012). "Corneal neovascularization: an anti-VEGF therapy review." **Survey of ophthalmology** 57, 5: 415-429.

[187] Campochiaro, P. (2006). "Potential applications for RNAi to probe pathogenesis and develop new treatments for ocular disorders." **Gene therapy** 13, 6: 559-562.

[188] Parker, A.L., et al. (2002). "Methodologies for monitoring nanoparticle formation by self-assembly of DNA with poly (L-lysine)." **Analytical biochemistry** 302, 1: 75-80.

[189] Muhittin Yılmaz, C.O.a.İ.G. *Principles of Nucleic Acid Separation by Agarose Gel Electrophoresis, Gel Electrophoresis - Principles and Basics*. 2012 [cited 2016 April]; Available from: http://www.intechopen.com/books/gel-electrophoresis-principles-and-basics/principles-of-nucleic-acid-separation-by-agarose-gel-electrophoresis.

[190] Armstrong, J.A. and J.R. Schulz, *Agarose Gel Electrophoresis*, in *Current Protocols Essential Laboratory Techniques*. 2008, John Wiley & Sons, Inc.

[191] Miura, Y., H. Wake, and T. Kato. (1999). "TBE, OR NOT TBE ; THAT IS THE QUESTION : Beneficial Usage of Tris-Borate for Obtaining a Higher Resolution of Small DNA Fragments by Agarose Gel Electrophoresis." **Nagoya medical journal** 43, 1 (July): 1-6.

[192] Ogden, R.C. and D.A. Adams. (1987). "[8] Electrophoresis in agarose and acrylamide gels." **Methods in enzymology** 152: 61-87.

[193] Waring, M. (1965). "Complex formation between ethidium bromide and nucleic acids." **Journal of molecular biology** 13, 1: 269-282.

[194] Jin, X., et al. *Sybr Green (Tm)-1-a new fluorescent dye optimized for detection of picogram amounts of DNA in gels*. in *Biophysical Journal*. 1994. BIOPHYSICAL SOCIETY 9650 ROCKVILLE PIKE, BETHESDA, MD 20814-3998.

[195] Sharp, P.A., B. Sugden, and J. Sambrook. (1973). "Detection of two restriction endonuclease activities in Haemophilus parainfluenzae using analytical

agarose-ethidium bromide electrophoresis." **Biochemistry** 12, 16: 3055-3063.

[196] Zhang, Q.-F., et al. (2015). "Amino Acid-Modified Polyethylenimines with Enhanced Gene Delivery Efficiency and Biocompatibility." **Polymers** 7, 11: 2316-2331.

[197] Rengarajan, K., et al. (2002). "Quantifying DNA concentrations using fluorometry: a comparison of fluorophores." **Molecular Vision** 8: 416-421.

[198] Ahn, S.J., J. Costa, and J.R. Emanuel. (1996). "PicoGreen quantitation of DNA: effective evaluation of samples pre-or psost-PCR." **Nucleic acids research** 24, 13: 2623-2625.

[199] Xu, Y. and F.C. Szoka. (1996). "Mechanism of DNA release from cationic liposome/DNA complexes used in cell transfection." **Biochemistry** 35, 18: 5616-5623.

[200] Le Pecq, J.-B. and C. Paoletti. (1966). "A new fluorometric method for RNA and DNA determination." **Analytical biochemistry** 17, 1: 100-107.

[201] McCann, J., et al. (1975). "Detection of carcinogens as mutagens in the Salmonella/microsome test: assay of 300 chemicals." **Proceedings of the National Academy of Sciences** 72, 12: 5135-5139.

[202] Karlsen, F., H.B. Steen, and J.M. Nesland. (1995). "SYBR green I DNA staining increases the detection sensitivity of viruses by polymerase chain reaction." **Journal of virological methods** 55, 1: 153-156.

[203] Leggate, J., et al. (2006). "Microplate fluorescence assay for the quantification of double stranded DNA using SYBR Green I dye." **Biotechnology Letters** 28, 19: 1587-1594.

[204] Clogston, J.D. and A.K. Patri, *Zeta Potential Measurement*, in *Characterization of Nanoparticles Intended for Drug Delivery*, E.S. McNeil, Editor. 2011, Humana Press: Totowa, NJ. p. 63-70.

[205] Xu, R., C. Wu, and H. Xu. (2007). "Particle size and zeta potential of carbon black in liquid media." **Carbon** 45, 14: 2806-2809.

[206] Mehrotra, R. and K. Tandon. (1964). "Adsorption indicators in precipitation titrations." **Talanta** 11, 8: 1093-1111.

[207] Kolthoff, I., W. Lauer, and C. Sunde. (1929). "The Use of Dichlorofluorescein as an Adsorption Indicator for the Argentometric Titration of Chlorides." **Journal of the American Chemical Society** 51, 11: 3273-3277.

[208] Wrona, M., K. Patel, and P. Wardman. (2005). "Reactivity of 2′,7′-dichlorodihydrofluorescein and dihydrorhodamine 123 and their oxidized forms toward carbonate, nitrogen dioxide, and hydroxyl radicals." **Free Radical Biology and Medicine** 38, 2: 262-270.

[209] Bardez, E., et al. (1990). "Counterion control of reactivity in anionic reverse micellar aggregates." **Chemical Physics Letters** 171, 4 (August): 362-368.

[210] Mchedlov-Petrossyan, N.O., et al. (2006). "A dibasic acid with reversed order of the stepwise ionization constants: 2, 7-dichlorofluorescein in the ternary solvent mixture benzene–ethanol–water." **Journal of physical organic chemistry** 19, 6: 365-375.

[211] Techaarpornkul, S., et al. (2010). "Chitosan-Mediated siRNA Delivery In Vitro: Effect of Polymer Molecular Weight, Concentration and Salt Forms." **AAPS PharmSciTech** 11, 1: 64-72.

[212] Godbey, W.T., K.K. Wu, and A.G. Mikos. (1999). "Size matters: Molecular weight affects the efficiency of poly(ethylenimine) as a gene delivery vehicle." **Journal of Biomedical Materials Research** 45, 3: 268-275.

[213] Baker, A., et al. (1997). "Polyethylenimine (PEI) is a simple, inexpensive and effective reagent for condensing and linking plasmid DNA to adenovirus for gene delivery." **Gene therapy** 4, 8: 773-782.

[214] Scholz, C. and E. Wagner. (2012). "Therapeutic plasmid DNA versus siRNA delivery: Common and different tasks for synthetic carriers." **Journal of Controlled Release** 161, 2: 554-565.

[215] Gary, D.J., N. Puri, and Y.-Y. Won. (2007). "Polymer-based siRNA delivery: Perspectives on the fundamental and phenomenological distinctions from polymer-based DNA delivery." **Journal of Controlled Release** 121, 1–2: 64-73.

[216] Smith, D.R., *Gel Electrophoresis of DNA*, in *Molecular Biomethods Handbook*, R. Rapley and J.M. Walker, Editors. 1998, Humana Press: Totowa, NJ. p. 17-33.

[217] Williams, D.R. and R. Rapley, *Agarose Gel Electrophoresis of Nucleic Acids*, in *The Nucleic Acid Protocols Handbook*, R. Rapley, Editor. 2000, Humana Press: Totowa, NJ. p. 67-70.

[218] Dutton, M.D., R.J. Varhol, and D.G. Dixon. (1995). "Technical Considerations for the Use of Ethidium Bromide in the Quantitative Analysis of Nucleic Acids." **Analytical Biochemistry** 230, 2: 353-355.

[219] Vitzthum, F., et al. (1999). "A Quantitative Fluorescence-Based Microplate Assay for the Determination of Double-Stranded DNA Using SYBR Green I and a Standard Ultraviolet Transilluminator Gel Imaging System." **Analytical Biochemistry** 276, 1: 59-64.

[220] Singer, V.L., et al. (1997). "Characterization of PicoGreen Reagent and Development of a Fluorescence-Based Solution Assay for Double-Stranded DNA Quantitation." **Analytical Biochemistry** 249, 2: 228-238.

[221] Opanasopit, P., et al. (2011). "Chitosan enhances transfection efficiency of cationic polypeptides/DNA complexes." **International Journal of Pharmaceutics** 410, 1–2: 161-168.

[222] Hellman, L.M. and M.G. Fried. (2007). "Electrophoretic Mobility Shift Assay (EMSA) for Detecting Protein-Nucleic Acid Interactions." **Nature protocols** 2, 8: 1849-1861.

[223] Sato, T., T. Ishii, and Y. Okahata. (2001). "In vitro gene delivery mediated by chitosan. Effect of pH, serum, and molecular mass of chitosan on the transfection efficiency." **Biomaterials** 22, 15: 2075-2080.

[224] Erbacher, P., et al. "Chitosan-Based Vector/DNA Complexes for Gene Delivery: Biophysical Characteristics and Transfection Ability." **Pharmaceutical Research** 15, 9: 1332-1339.

[225] Lin, C., et al. (2008). "Bioreducible poly(amido amine)s with oligoamine side chains: Synthesis, characterization, and structural effects on gene delivery." **Journal of Controlled Release** 126, 2: 166-174.

[226] Kim, T.-i., et al. (2009). "Arginine-grafted bioreducible poly(disulfide amine) for gene delivery systems." **Biomaterials** 30, 4: 658-664.

[227] Kim, J., et al. (2009). "Intracellular small interfering RNA delivery using genetically engineered double-stranded RNA binding protein domain." **The Journal of Gene Medicine** 11, 9: 804-812.

[228] Mao, S., et al. (2006). "Influence of Polyethylene Glycol Chain Length on the Physicochemical and Biological Properties of Poly(ethylene imine)-graft-Poly(ethylene glycol) Block Copolymer/SiRNA Polyplexes." **Bioconjugate Chemistry** 17, 5 (September): 1209-1218.

[229] Thomsen, P., et al. (2002). "Caveolae Are Highly Immobile Plasma Membrane Microdomains, Which Are not Involved in Constitutive Endocytic Trafficking." **Molecular Biology of the Cell** 13, 1 (January): 238-250.

[230] Doherty, G.J. and H.T. McMahon. (2009). "Mechanisms of Endocytosis." **Annual Review of Biochemistry** 78, 1: 857-902.

[231] Peng, S.-F., et al. (2011). "Mechanisms of cellular uptake and intracellular trafficking with chitosan/DNA/poly(γ-glutamic acid) complexes as a gene delivery vector." **Biomaterials** 32, 1: 239-248.

[232] Garaiova, Z., et al. (2012). "Cellular uptake of DNA–chitosan nanoparticles: The role of clathrin- and caveolae-mediated pathways." **International Journal of Biological Macromolecules** 51, 5: 1043-1051.

[233] Kim, T.-i., et al. (2007). "Synthesis and Characterization of a Novel Arginine-Grafted Dendritic Block Copolymer for Gene Delivery and Study of Its Cellular Uptake Pathway Leading to Transfection." **Bioconjugate Chemistry** 18, 2 (March): 309-317.

APPENDIX

APPENDIX A

Absorbance spectrum of 2',7' dichlorofluorescein solution

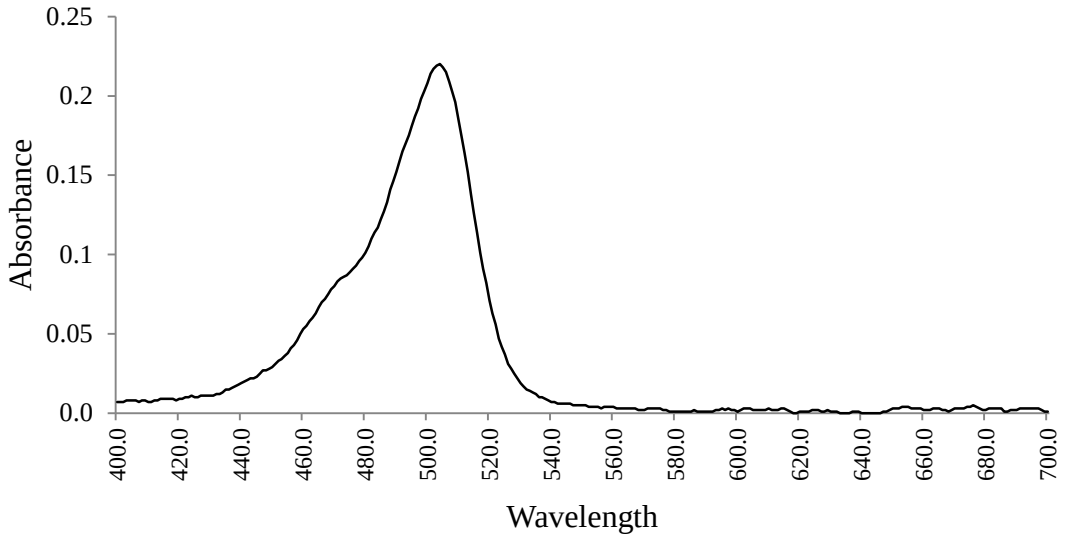

Figure A1 Absorbance spectrum of 2',7' dichlorofluorescein solution (0.15 mg/ml in TAE buffer, pH 8) scanned by NanoVue™ spectrophotometer.

Size of PEI(25 kDa)/siRNA-EGFP complexes

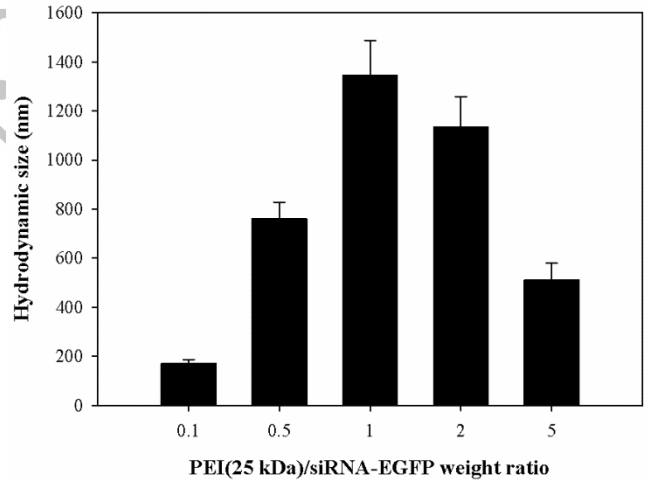

Figure A2 Size of PEI(25 kDa)/siRNA-EGFP complexes at different weight ratio analyzed by Zeta Nanosizer. Each value represented the mean ± SD of triplicate samples.

EGFP gene silencing efficiency of PEI(25 kDa)/siRNA-EGFP at different time

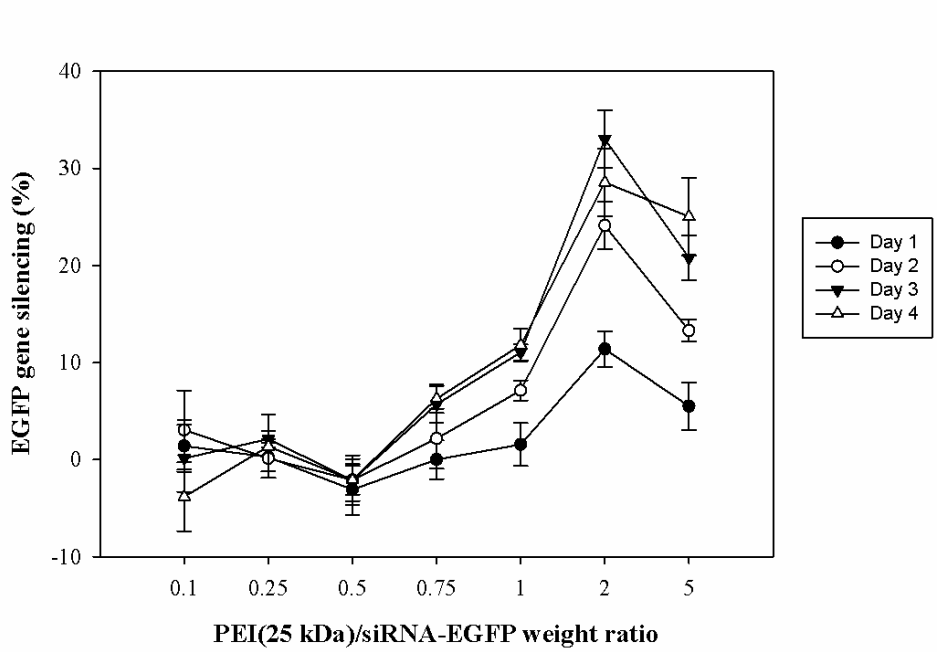

Figure A3 Percentage of gene silencing at different time in HeLa-EGFP cells after transfected with PEI(25 kDa)/siRNA-EGFP complexes. Each value represented the mean ± SD of triplicate sample.

Estimation of PEI(25 kDa)/pEGFP complex formation using pEGFP 2.5 µg

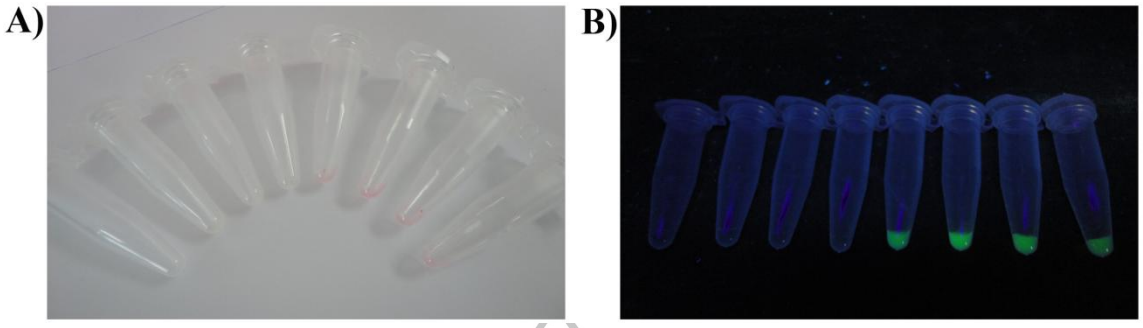

Figure A4 Estimation of complete PEI(25 kDa)/pEGFP complex formation using 2.5 µg pEGFP by dye adsorption method. The pink pellets under visible light (A) or green fluorescence under UV light at 366 nm (B). The complexes were prepared at weight ratio of 0, 0.01, 0.1, 0.25, 0.5, 0.75, 1 and 2 (from left to right).

Estimation of PEI(25 kDa)/pEGFP complex formation using pEGFP 1 µg

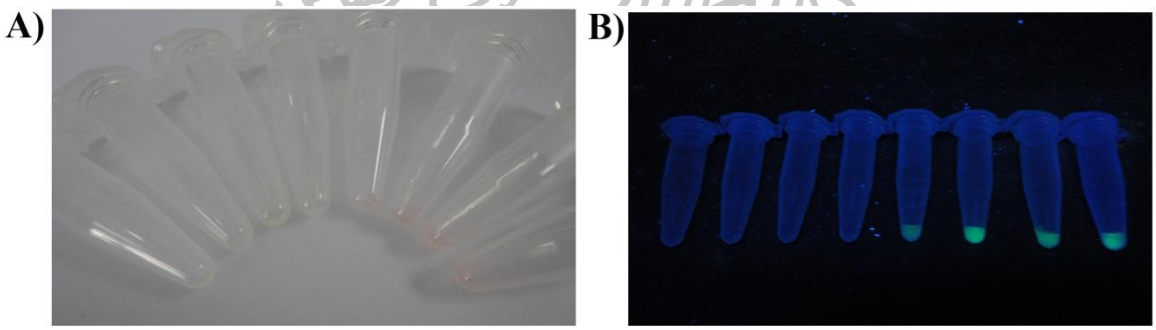

Figure A5 Estimation of complete PEI(25 kDa)/pEGFP complex formation using 1 µg pEGFP by dye adsorption method. The pink pellets under visible light (A) or green fluorescence under UV light at 366 nm (B). The complexes were prepared at weight ratio of 0, 0.01, 0.1, 0.25, 0.5, 0.75, 1 and 2 (from left to right).

Estimation of PEI(25 kDa)/pEGFP complex formation using pEGFP 0.5 µg

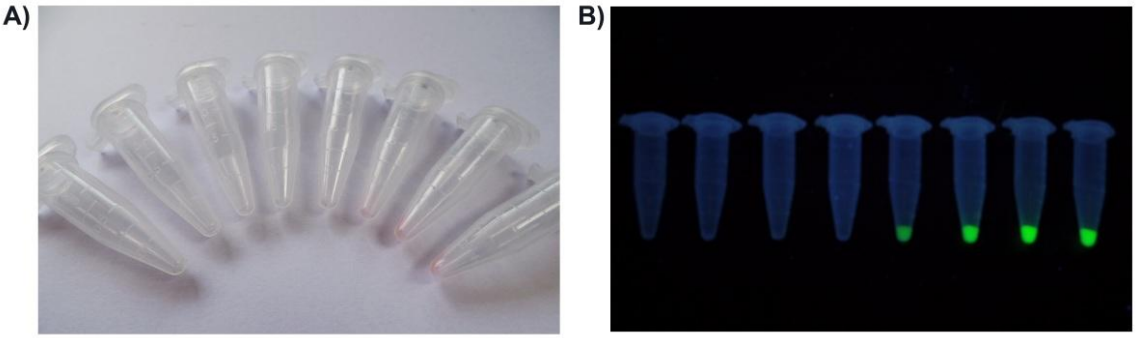

Figure A6 Estimation of complete PEI(25 kDa)/pEGFP complex formation using 0.5 µg pEGFP by dye adsorption method. The pink pellets under visible light (A) or green fluorescence under UV light at 366 nm (B). The complexes were prepared at weight ratio of 0, 0.01, 0.1, 0.25, 0.5, 0.75, 1 and 2 (from left to right).

Estimation of PEI(25 kDa)/pEGFP complex formation using DCF 0.075 mg/mL

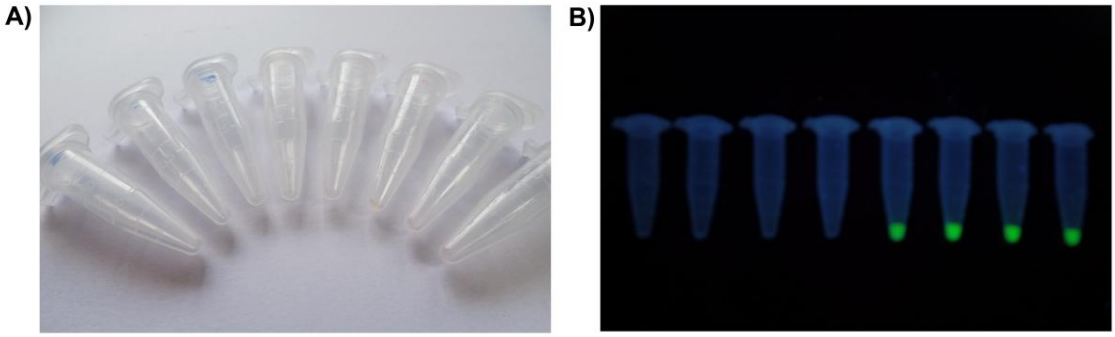

Figure A7 Estimation of complete PEI(25 kDa)/pEGFP complex formation using DCF 0.075 mg/mL by dye adsorption method. The pink pellets under visible light (A) or green fluorescence under UV light at 366 nm (B). The complexes were prepared at weight ratio of 0, 0.01, 0.1, 0.25, 0.5, 0.75, 1 and 2 (from left to right).

APPENDIX B

EGFP gene silencing efficiency of CS/siRNA-EGFP at different time

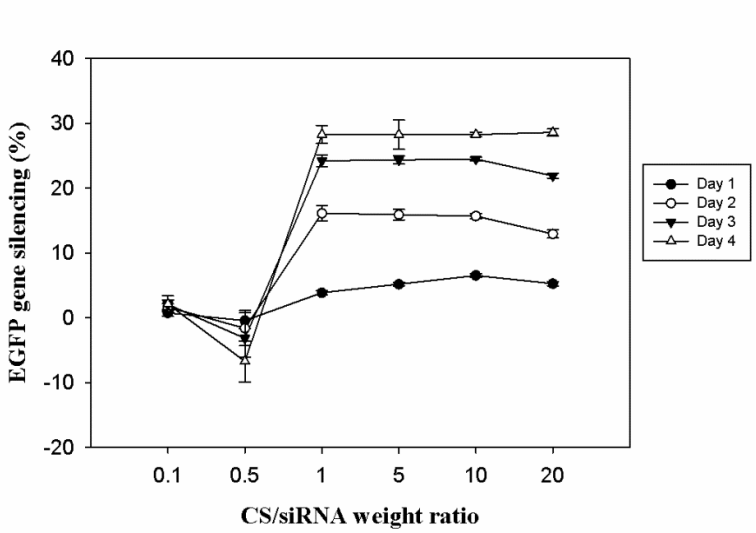

Figure B1 Percentage of gene silencing at different time in HeLa-EGFP cells after transfected with CS/siRNA-EGFP complexes at pH 6.4. Each value represented the mean ± SD of triplicate sample.

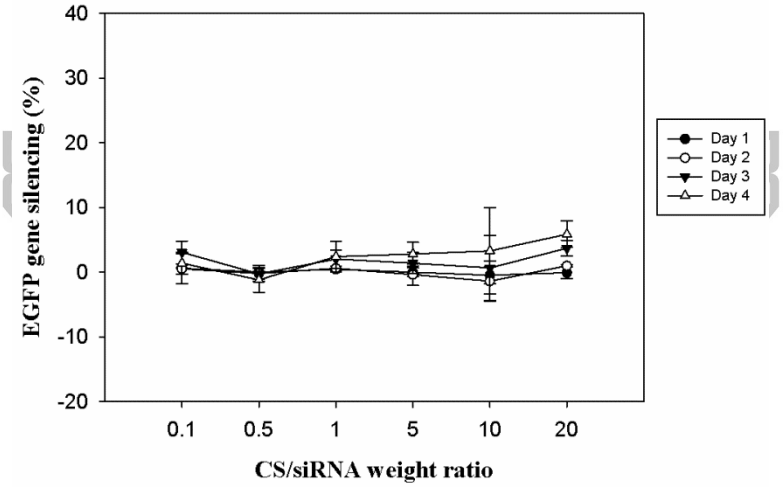

Figure B2 Percentage of gene silencing at different time in HeLa-EGFP cells after transfected with CS/siRNA-EGFP complexes at pH 7.4. Each value represented the mean ± SD of triplicate sample.

EGFP gene silencing efficiency of PLA/siRNA-EGFP at different time

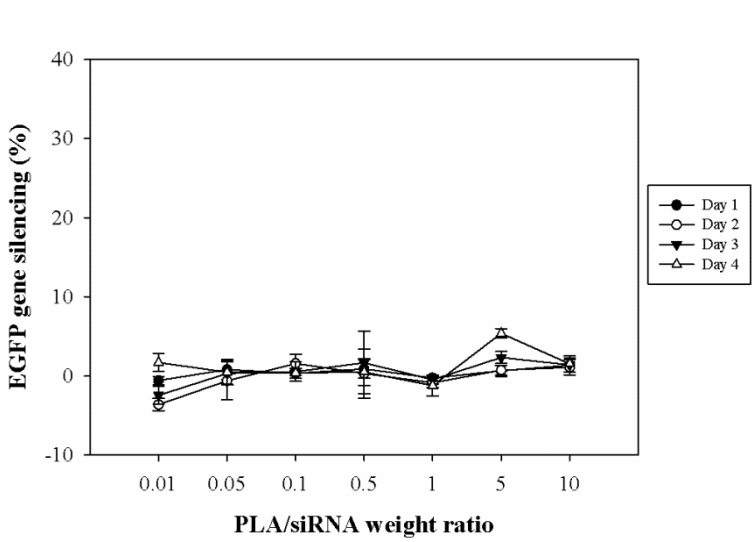

Figure B3 Percentage of gene silencing at different time in HeLa-EGFP cells after transfected with PLA/siRNA-EGFP complexes at pH 6.4. Each value represented the mean ± SD of triplicate sample.

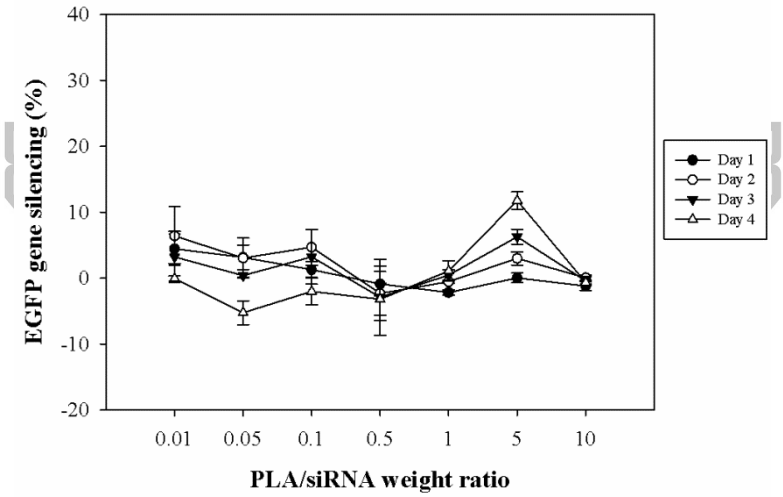

Figure B4 Percentage of gene silencing at different time in HeLa-EGFP cells after transfected with PLA/siRNA-EGFP complexes at pH 7.4. Each value represented the mean ± SD of triplicate sample.

EGFP gene silencing efficiency of CS/PLA/siRNA-EGFP at different time

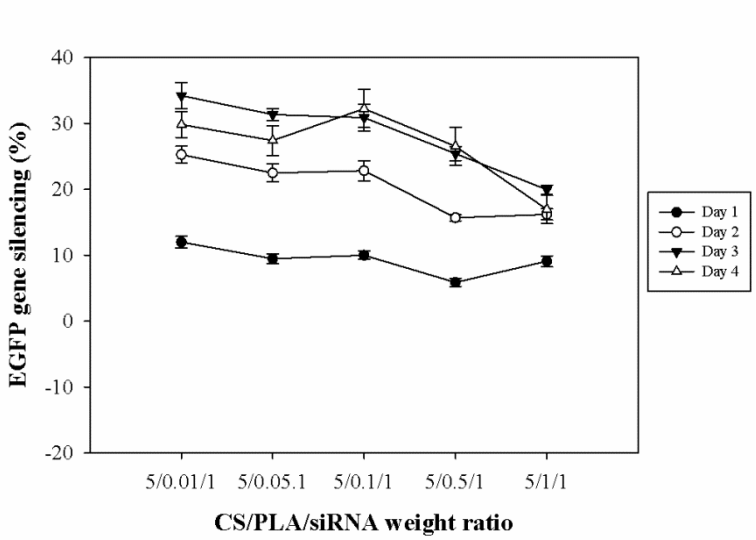

Figure B5 Percentage of gene silencing at different time in HeLa-EGFP cells after transfected with CS/PLA/siRNA-EGFP complexes at pH 6.4. Each value represented the mean ± SD of triplicate sample.

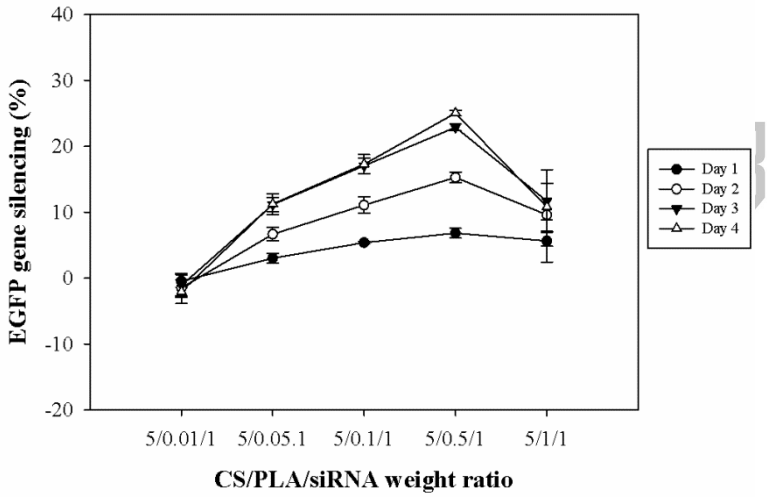

Figure B6 Percentage of gene silencing at different time in HeLa-EGFP cells after transfected with CS/PLA/siRNA-EGFP complexes at pH 7.4. Each value represented the mean ± SD of triplicate sample.

EGFP gene silencing efficiency of CS/PLA/siRNA-EGFP in the different of order of mixing at different time

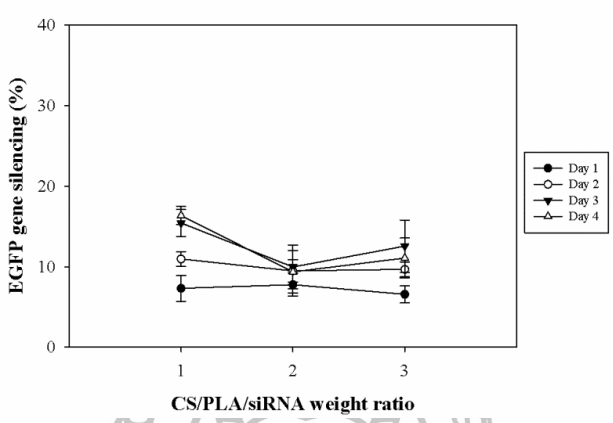

Figure B7 Percentage of EGFP gene silencing after transfected HeLa-EGFP cell with the complexes which were prepared by the order of CS/PLA/siRNA-EGFP at pH 7.4. The weight ratios of PLA were varied at 0.5, 1 and 2 which the x axis was labeled in 1, 2 and 3, respectively while CS was fixed at 5. Each value presented in mean ± SD of triplicate samples.

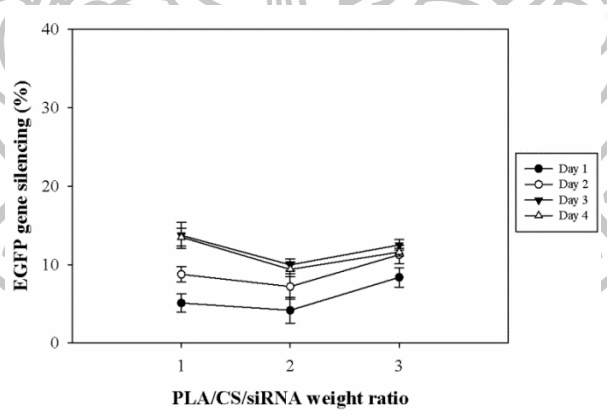

Figure B8 Percentage of EGFP gene silencing after transfected HeLa-EGFP cell with the complexes which were prepared by the order of PLA/CS/siRNA-EGFP at pH 7.4. The weight ratios of PLA were varied at 0.5, 1 and 2 which the x axis was labeled in 1, 2 and 3, respectively while CS was fixed at 5. Each value presented in mean ± SD of triplicate samples.

Effect of serum on EGFP gene silencing efficiency of CS/PLA/siRNA-EGFP at different time

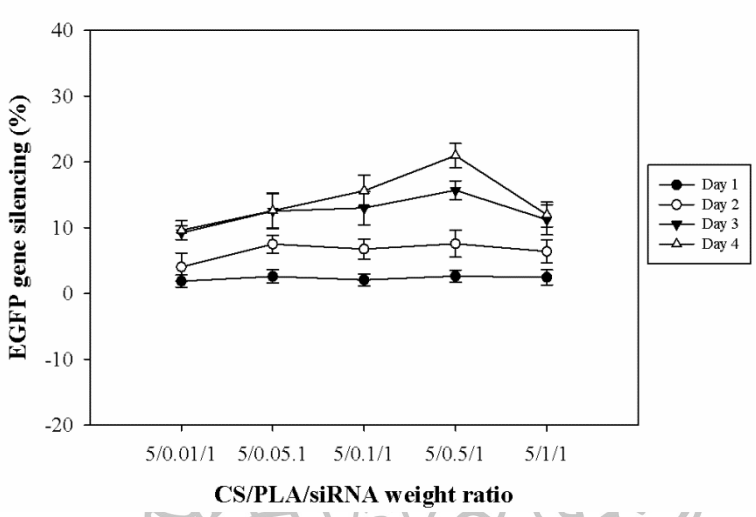

Figure B9 Percentage of gene silencing at different time in HeLa-EGFP cells after transfected with CS/PLA/siRNA-EGFP complexes in the absence of serum at pH 7.4. Each value represented the mean ± SD of triplicate sample.

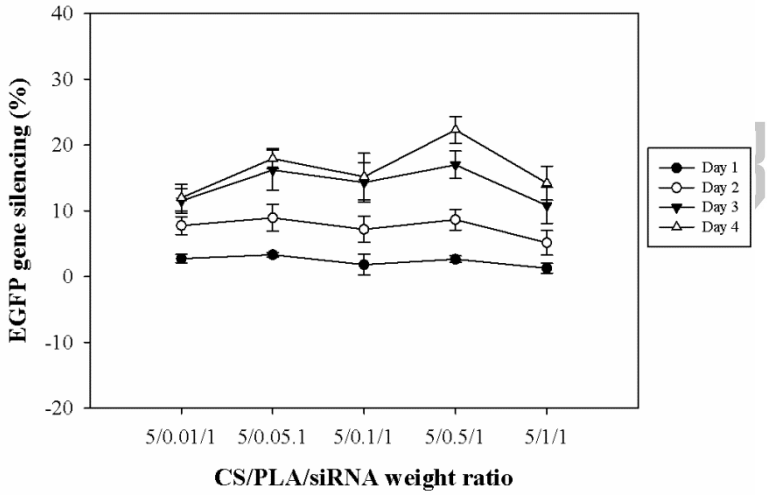

Figure B10 Percentage of gene silencing at different time in HeLa-EGFP cells after transfected with CS/PLA/siRNA-EGFP complexes in the presence of serum (10% FBS) at pH 7.4. Each value represented the mean ± SD of triplicate sample.

Optimum amount of RNase A and sodium dodecyl sulfate (SDS) for RNase protection ability study

1. RNase A amount

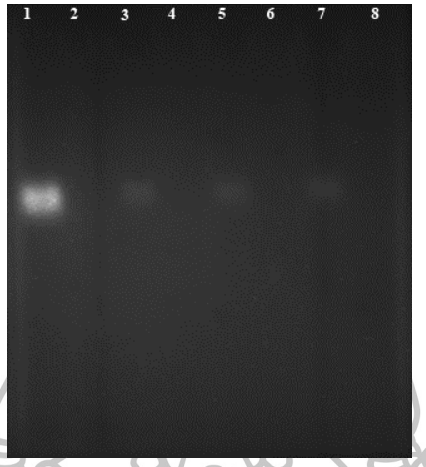

Figure B11 Effect of RNase A amount on siRNA degradation of naked siRNA (lane 1, 3, 5 and 7) and CS/PLA/siRNA complex at weight ratio of 5/0.5/1 (lane 2, 4, 6 and 8). RNase A amount was varied at 2 mU/µg siRNA (lane 3 and 4), 2.5 mU/µg siRNA (lane 5 and 6) and 3 mU/µg siRNA. The naked siRNA and CS/PLA/siRNA complex were incubated with RNase A at 30 ˚C for 30 min. Naked siRNA and CS/PLA/siRNA complex which were not incubated with RNase A as controls.

2. SDS amount

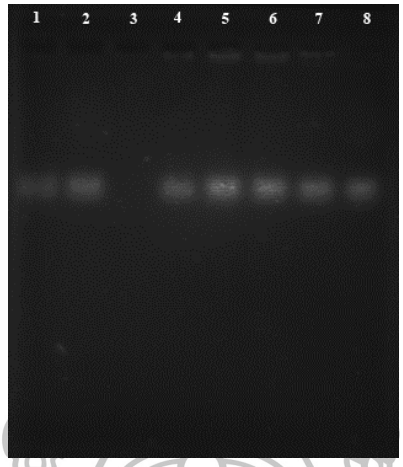

Figure B12 Effect of SDS amount on siRNA releasing from complex. The CS/PLA/siRNA complex was prepared at weight ratio of 5 and siRNA was repelled from complex by adding 1 µL of 16 mM SDS (lane 4), 1.5 µL of 16 mM SDS (lane 5), 2 µL of 16 mM SDS (lane 6), 2.5 µL of 16 mM SDS and 3 µL of 16 mM SDS. Naked siRNA (lane 1), naked siRNA with SDS (lane 2) and CS/PLA/siRNA complex (lane 3) were the controls.

Cytotoxicity of inhibitor in endocytosis pathways

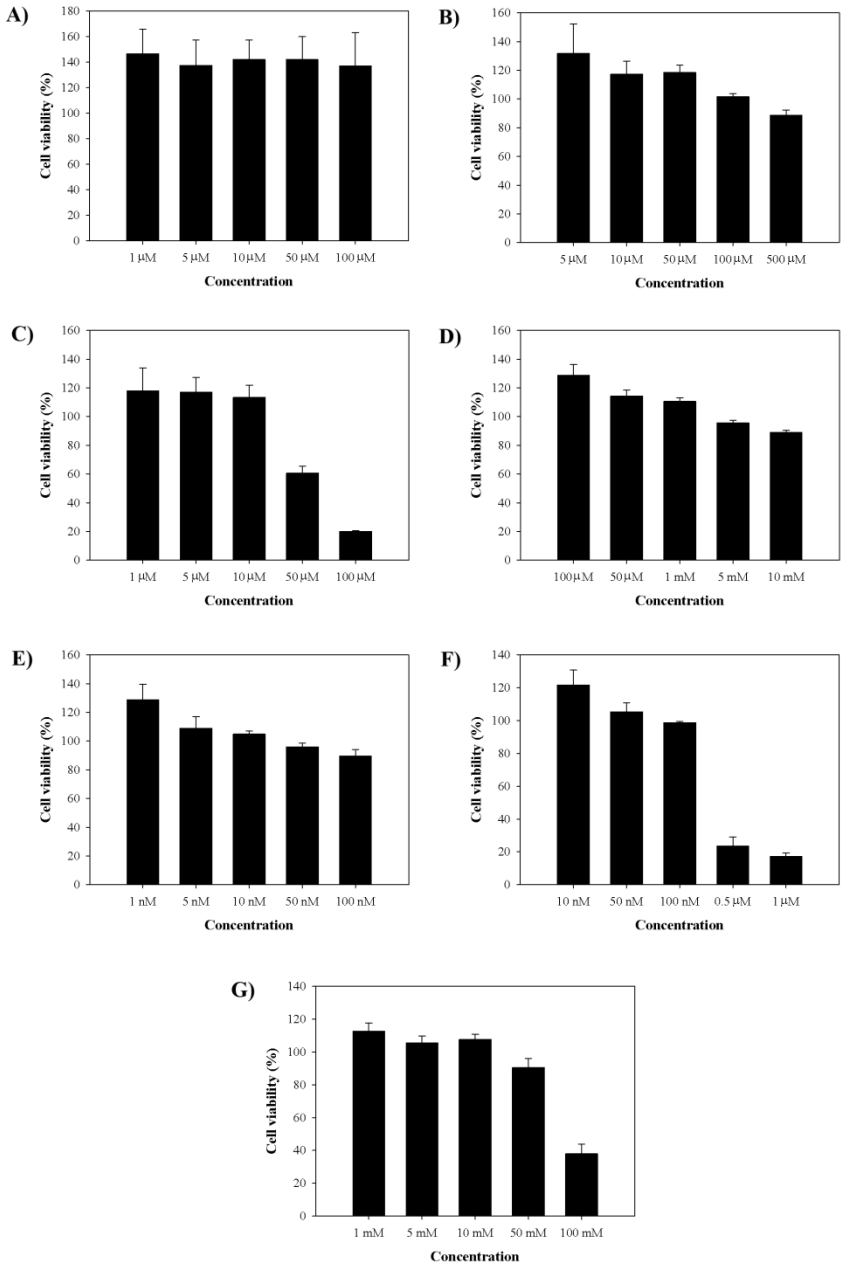

Figure B13 Cytotoxicity of inhibitors in HeLa-EGFP cell. Cell viability was performed by MTT assay after incubating cells with chlorpromazine (A), genistein (B), filipin (C), methyl- β-cyclodextrin (D), nocodazole (E), wortmannin (F) and ammonium chloride (G).

BIOGRAPHY

Name Samarwadee Plianwong, Ms.

Date of Birth May 03, 1988

Place of Birth Ratchaburi, Thailand

Present Address Ph.D. student in Department of Pharmaceutical Chemistry and Natural Products, Faculty of Pharmacy, Silpakorn University, Nakhon pathom 73000, Thailand

E-mail address P.Samarwadee@gmail.com

Education

2006 - 2010: Bachelor of Pharmacy (The 1st class honors, gold medal), Pharmaceutical Science, Faculty of Pharmacy, Silpakorn University, Thailand.

2011 - Present: Pharmaceutical Chemistry and Natural Products PhD. Program, Faculty of Pharmacy, Silpakorn University, Thailand.

2015: Visiting student, Department of Chemical and Materials Engineering, University of Alberta, Edmonton, AB, Canada.

Scholarship Thailand Research Funds through the Royal Golden Jubilee Ph.D. Program.

Publications

1. Theerasak Rojanarata, Junlathip Tankul, Chayanee Woranaipinich, Paweena Potawanich,

   Samarwadee Plianwong, Sirinart Sakulma and Choedchai Saehuan. Stability of Fortified Cefazolin Ophthalmic Solutions Prepared in Artificial Tears Containing Surfactant-Based Versus Oxidant-Based Preservatives. J Ocul Pharmacol Ther. 2010; 26: 485-490.
2. **Samarwadee Plianwong**, Areerut Sripattanaporn, Kwanrutai Waewsa-nga, Parin Buacheen, Praneet Opanasopit, Tanasait Ngawhirunpat, Theerasak Rojanarata. Operator care and eco-concerned development of a fast, facile and

economical assay for basic nitrogenous drugs based on simplified ion-pair mini-scale extraction using safer solvent combined with drop-based spectrophotometry. Talanta. 2012; 98: 220-225.

3. Theerasak Rojanarata, **Samarwadee Plianwong**, Kosit Su-uta, Praneet Opanasopit, Tanasait Ngawhirunpat. Electrospun cellulose acetate nanofibers as thin layer chromatographic media for eco-friendly screening of steroids adulterated in traditional medicine and nutraceutical products. Talanta. 2013; 115: 208‑213.
4. **Samarwadee Plianwong**, Praneet Opanasopit, Tanasait Ngawhirunpat, Theerasak Rojanarata. Fast, facile and ethidium bromide-free assay based on the use of adsorption indicator for the estimation of polyethylenimine to nucleic acid ratio of complete polyplex assembly for gene delivery. Talanta. 2013; 115: 241-245.
5. **Samarwadee Plianwong**, Praneet Opanasopit, Tanasait Ngawhirunpat, Theerasak Rojanarata. Chitosan Combined with Poly-L-arginine as Efficient, Safe, and Serum-Insensitive Vehicle with RNase Protection Ability for siRNA Delivery. BioMed Research International. 2013.
6. Breanne Landry, Hilal Gül-Uludağ, **Samarwadee Plianwong**, Cezary Kucharski, Zoulika Zak, Manoj B. Parmar, Olaf Kutsch, Hongxing Jiang, Joseph Brandwein, Hasan Uludağ. Targeting CXCR4/SDF-1 axis by lipopolymer complexes of siRNA in acute myeloid leukemia. J Control Release. 2016; 224: 8-21.

Oral Presentations

1. **Samarwadee Plianwong**, Areerut Sripattanaporn, Kwanrutai Waewsa-nga, Parin Buacheen, Praneet Opanasopit, Tanasait Ngawhirunpat, Theerasak Rojanarata. Incorporation of “6-R” approach into the design of green pharmaceutical analysis: mini-scale extraction with drop-based spectrophotometry for the assay of chlorpheniramine maleate in syrup. The 2nd Current Drug Development International Conference, 2nd -4th May 2012, Phuket, Thailand.

2. **Samarwadee Plianwong**, Kosit Su-uta, Theerasak Rojanarata. Electrospun Cellulose Acetate Nanofiber Mat as Analytical Device for Consumer Protection. The 10th National Kasetsart University Kamphaeng Saen Conference, 6th -7th December 2013, Kasetsart University, Nakhon pathom, Thailand.
3. **Samarwadee Plianwong**, Praneet Opanasopit, Tanasait Ngawhirunpat, Theerasak Rojanarata. Estimation of Polyethylenimine to Nucleic Acid Ratio for Complete Polyplex Formation Based on Non-toxic Adsorption Indicator for Gene Delivery. The 3rd Current Drug Development (CDD 2014), 1st -3rd May 2014, The Pavillion Queen's Bay Krabi, Ao Nang, Krabi, Thailand.
4. **Samarwadee Plianwong**, Praneet Opanasopit, Tanasait Ngawhirunpat, Theerasak Rojanarata. Application of Adsorption Dye for the Estimation of Complete Polyplex Formation for Gene Delivery. The 100th RGJ Seminar Series C "Second Generation of RGJ-Ph.D. Advisors", 12th September 2014, The Sukosol, Bangkok, Thailand.

Poster Presentations

1. **Samarwadee Plianwong**, Kosit Su-utha1, Praneet Opanasopit1, Tanasait Ngawhirunpat, Theerasak Rojanarata. Factors Influencing the Morphology of Cellulose Acetate Electrospun Fiber Mats. Chiang Mai International Conference on Biomaterials & Applications, CMICBA 2011, 9th – 10th August 2011, Chiang Mai, Thailand.
2. **Samarwadee Plianwong**, Praneet Opanasopit, Tanasait Ngawhirunpat, Theerasak Rojanarata. Chitosan Combinated with Poly-L-Arginine as Effective Carrier for siRNA delivery. The 15th Asian Chemical Congress (ACC), 19th - 23th August 2013, Resorts World Sentosa, Singapore.
3. **Samarwadee Plianwong**, Praneet Opanasopit, Tanasait Ngawhirunpat, Theerasak Rojanarata. The Estimation of Chitosan and Chitosan Pyridine to pDNA Ratio for Complex Polyplex Formation Based on Adsorption Indicator Method. The 30th Annual Research Conference in Pharmaceutical Sciences, 10th – 12th January 2014, Chulalongkorn University, Bangkok, Thailand.

4. **Samarwadee Plianwong**, Praneet Opanasopit, Tanasait Ngawhirunpat, Theerasak Rojanarata. DNA Polyplex Formation and Gene Delivery Ability of Chitosan Salts Prepared by Using Different Hydroxy Acids. The JSPS-NRCT Follow-Up Seminar 2015 and 31st International Annual Meeting in Pharmaceutical Sciences, 22nd – 23rd January 2015, Faculty of Pharmaceutical Sciences, Chulalongkorn University, Bangkok, Thailand.

Awards

1. **The best oral presentation awards**. Samarwadee Plianwong, Praneet Opanasopit, Tanasait Ngawhirunpat, Theerasak Rojanarata. Estimation of Polyethylenimine to Nucleic Acid Ratio for Complete Polyplex Formation Based on Non-toxic Adsorption Indicator for Gene Delivery. The 3rd Current Drug Development (CDD 2014), 1st -3rd May 2014, The Pavillion Queen's Bay Krabi, Ao Nang, Krabi, Thailand.

2. **Kawaguchi awards** and **Honorable mention award for quality research.** Samarwadee Plianwong, Kosit Su-uta, Theerasak Rojanarata. Electrospun Cellulose Acetate Nanofiber Mat as Analytical Device for Consumer Protection. The 10th National Kasetsart University Kamphaeng Saen Conference, 6th -7th December 2013, Kasetsart University, Nakhon pathom, Thailand.